Cusps and shocks in the renormalized potential of glassy random manifolds: How functional renormalization group and replica symmetry breaking fit together

Pierre Le Doussal, Markus Müller, and Kay Jörg Wiese
CNRS-Laboratoire de Physique Théorique de l'Ecole Normale Supérieure, 24 rue Lhomond, 75231 Cedex 05, Paris, France and Department of Physics, Harvard University, Lyman Laboratory, Cambridge, Massachusetts 02138, USA
(Received 29 November 2007; published 21 February 2008)

We compute the functional renormalization group (FRG) disorder-correlator function $R(v)$ for d-dimensional elastic manifolds pinned by a random potential in the limit of infinite embedding space dimension N. It measures the equilibrium response of the manifold in a quadratic potential well as the center of the well is varied from 0 to v. We find two distinct scaling regimes: (i) a "single shock" regime, $v^2 \sim L^{-d}$, where L^d is the system volume, and (ii) a "thermodynamic" regime, $v^2 \sim N$. In regime (i), all the equivalent replica symmetry breaking (RSB) saddle points within the Gaussian variational approximation contribute, while in regime (ii), the effect of RSB enters only through a single anomaly. When the RSB is continuous (e.g., for short-range disorder, in dimension $2 \leq d \leq 4$), we prove that regime (ii) yields the large-N FRG function obtained previously. In that case, the disorder correlator exhibits a cusp in both regimes, though with different amplitudes and of different physical origin. When the RSB solution is one step and nonmarginal (e.g., $d<2$ for short-range disorder), the correlator $R(v)$ in regime (ii) is considerably reduced and exhibits no cusp. Solutions of the FRG flow corresponding to nonequilibrium states are discussed as well. In all cases, regime (i) exhibits a cusp nonanalyticity at $T=0$, whose form and thermal rounding at finite T are obtained exactly and interpreted in terms of shocks. The results are compared with previous work, and consequences for manifolds at finite N as well as extensions to spin glasses and related models are discussed.

DOI: 10.1103/PhysRevB.77.064203 PACS number(s): 05.10.Cc

I. INTRODUCTION

A major difficulty in devising analytical methods to handle glassy systems, such as systems with quenched disorder, is to describe accurately the many metastable states which play a role both in the statics (equilibrium) and in the dynamics, as well as the barriers separating these states. Two main general methods have been developed. The first is a mean-field theory, based on the Gaussian variational method (GVM), which, in the statics, captures the many states by a multitude of saddle points exhibiting spontaneous replica symmetry breaking (RSB).[1] Being highly versatile, the GVM has been applied to numerous problems, notably in spin glasses, and has later been extended to the dynamics.[2,3] The second method is the functional renormalization group (FRG) which has been applied successfully to disordered elastic systems and random-field spin models, both in the statics[4–28] and for the driven dynamics.[29–36] Although its range of applications is at present smaller, it is a powerful and promising method which allows to compute fluctuations not captured by mean-field theory. The (relevant) coupling constant in FRG is the disorder correlator $R(u)$. In contrast to standard field theories, it is not a number but a *function* of the field u, defined for the microscopic model in Eq. (6). Since the two methods GVM and FRG are rather different in spirit, and historically have developed along separate tracks, it is important to compare them whenever possible. A further goal is to understand whether and how they may be extended to a broader range of models.

In this paper, we focus on disordered elastic systems, where both methods have been applied. As we discuss, some of the conclusions and ideas may extend to other models with quenched disorder. Besides being of direct interest for experiments, including vortex lattices, magnetic systems, and density waves,[5,37–42] models of manifolds in a random potential provide the simplest example of a glass phase where numerous metastable states occur beyond the so-called Larkin scale. As for random-field systems, the so-called dimensional reduction phenomenon occurs, which renders conventional zero-temperature perturbation theory trivial,[43–45] indicating the failure of the latter to capture the complexity of the energy landscape. A big success of both methods, GVM and FRG, has been to circumvent this problem. However, they achieve this in seemingly rather different ways: The GVM approximates the Gibbs measure by a hierarchical superposition of Gaussians, encoded in the Mézard-Parisi ansatz.[1,46] In the FRG, the existence of a cusp [in the coupling function $R''(u)$] beyond the Larkin scale is related to the existence of many metastable states. This was nicely illustrated in an early paper by Balents *et al.*[47] The idea that coarse graining leads to shocks in the force landscape, and the similarity of the pinning problem to the Burgers equation, was introduced using a toy renormalization group (RG) model with two degrees of freedom. However, the function $R(u)$ defined in that work does not coincide with the one usually studied in field theory, making a precise comparison difficult.

In this paper, we want to make this comparison quantitative. Let us denote $u(x)$, $x \in R^d$, the N-component displacement (or "height") field which parametrizes the position of a manifold of internal dimension d in the N-dimensional embedding space. The GVM was applied to the problem by Mézard and Parisi (MP),[46] introducing replicated fields $u_a(x)$. For long-range disorder, or for short-range disorder and internal dimensions above $d=2$, they found a solution with continuous replica symmetry breaking (RSB) with a roughness exponent for the manifold $u(x) \sim x^{\zeta}$ given by the Flory estimate. (The FRG allows one to go beyond this result and to compute deviations from Flory for $N < \infty$.) For short-range disorder, with $d < 2$, they found a one-step RSB solution, analogous to the one in infinite range p-spin models.[2,3]

In the infinite-N limit, the GVM becomes formally exact and, hence, can be compared with the FRG. Two of us[11,13] obtained a self-consistent equation for the coupling function of the FRG, $R(u)$. It was defined from the effective action of the replicated field theory [for a uniform mode $u(x)=u$], a standard field theory definition, and computed in the large-N limit, performing the usual rescaling $R(u)=N\tilde{B}(u^2/N)$. Although the resulting self-consistent equation for $\tilde{B}(x)$ is formally valid only below the Larkin scale, the corresponding FRG equation could be continued "naturally" to scales beyond the Larkin scale (with a cusp present at $u=0$), extending the flow all the way to the RG fixed point. For $2 \leqslant d \leqslant 4$, where the RSB is continuous, this FRG flow recovered[11,13] the MP result for small overlap, i.e., it yielded only, even though exactly, the (nontrivial) contribution of the most distant states to the correlation function. However, quite surprisingly, varying the IR cutoff m in the confining potential well finally allows for the reconstruction of the complete self-energy function obtained in the GVM, without ever referring to ultrametric matrices.[11,13]

Despite this quantitative progress in understanding the connection between FRG and GVM, several questions remained. It is natural that the FRG recovers the contribution of distant states, since it introduces an external field which explicitly breaks replica symmetry and, hence, splits all the replicas: $u_a - u_b \neq 0$. However, one would hope FRG to describe all states, not just the ones with smallest overlap. Further, no thermal rounding of the cusp was found, which is physically surprising in view of results relating finite-temperature droplets and FRG.[22,48,49] Finally, one would like to describe better the situation where the GVM yields a *non-marginal* one-step RSB solution, namely, the case $d < 2$ with short-range disorder, which includes, in particular, the Kardar-Parisi-Zhang (KPZ) problem with $d=1$.[50–54]

The first aim of this paper is to compute the FRG functions from first principles in the large-N limit. We take advantage of the recently obtained direct relation between the field theoretic definition of the FRG function $R(u)$ and directly observable quantities.[48,49] This has allowed for a numerical determination of $R(u)$ or the force correlator

$$\Delta(u) = -R''(u) \tag{1}$$

for $N=1$ interfaces at $T=0$ in dimensions $d=0$, 1, 2, and 3 in Ref. 55 as well as for the depinning problem in Refs. 56 and 57. It was found that the numerics compares remarkably well with the $\epsilon=4-d$ expansion, to one loop, and even better to two-loop order. The idea, also implemented here, is to subject the manifold, in addition to the random potential, to an external quadratic potential well $\frac{m^2}{2}\int d^dx[u(x)-v]^2$, centered at v. The "mass" m acts as an infrared cutoff limiting the interface fluctuations. By measuring the free energy $\hat{V}(v)$ of the system as a function of v, one obtains a random landscape whose second cumulant is the function $R(v)$. More generally, if $v \to v(x)$, the whole second cumulant functional $R[v]$ is retrieved.

Here, we compute this functional exactly. We find *two* distinct scaling regimes with nontrivial infinite-N limits, the first one where $v^2 \sim N^0 L^{-d}$, the second for $v^2 \sim N$. The reason for this peculiar property is that at $v=0$ there is spontaneous RSB, which implies the contribution of many saddle points which are equivalent under replica permutations. If the "applied field" v remains "small" (first regime), the spontaneous RSB saddle point is not significantly modified and all saddle points contribute to a given observable (though, now, not all of them equivalently). This can be handled by a method introduced in Ref. 47, and will be applied here with some improvements. In the second regime, which corresponds to the more conventional scaling at large N, the applied field is stronger and the saddle point is modified. We explicitly compute the v dependence, and show how, for large v, a nontrivial FRG function emerges. Specifically, in the case of a uniform field $v(x)=v$, we obtain

$$R(v) - R(0) = \begin{cases} L^{-d}\tilde{r}(v^2L^d) & \text{for } v^2 \sim L^{-d} \quad (2a)\\ Nr(v^2/N) & \text{for } v^2 \sim N, \quad (2a) \end{cases}$$

with two different scaling functions which we compute. We check that the two regimes match, i.e., $\tilde{r}(z) \sim Az$ at large z and $r(z) \sim Az$ at small z. In the case where the RSB is continuous (e.g., for $2 \leqslant d \leqslant 4$), we prove that regime (2b) yields the large-N FRG function obtained in our previous study.[11,13] Hence, the natural continuation (using the FRG flow equation) performed there is correct, and one of the main results of the present paper is to show this rigorously. Remarkably, RSB enters in this regime only through a single number, an anomaly. In the case of continuous RSB (including the marginal one-step solution in $d=2$), we find that both regimes (2a) and (2b) exhibit a cusp in $R''(v)$ at the origin, though of different nature. Specifically, one finds $\tilde{r}(z) = Bz + \tilde{C}z^{3/2}$ at small z (at $T=0$) and $r(z) \sim Az + Cz^{3/2}$ at small z (for all T in the glass phase). These cusps are caused by jump discontinuities in $\hat{V}'(v)$, called shocks, as the center of the well v is moved. In regime (2a), the scaling function describes a fluctuation of the energy, as measured by the connected correlator

$$\overline{[\hat{V}(v) - \hat{V}(0)]^2} = 2L^d[R(v) - R(0)] \tag{3}$$

of order unity as v is moved by a very small amount $\sim L^{-d/2}$. Hence, we call this regime "single shock regime." By contrast, in regime (2b), the variance of the energy fluctuations scales with volume and N. Hence, we call this regime "thermodynamic," since the scaling function $r(z)$ encodes the average properties of many shocks. The two regimes also exhibit different properties with respect to temperature. In regime (2b), as was found in Refs. 11 and 13, the temperature dependence is weak and the cusp survives even for $T > 0$. Regime (2a) exhibits a thermal rounding of the cusp, whose form is obtained in an exact closed form. We compare its form with the predictions for the thermal boundary layer of the FRG obtained previously[48,49] in cases where it can be obtained using droplet arguments (i.e., at finite N). For sufficiently short-ranged disorder in $d<2$, the equilibrium one-step RSB solution yields a considerably reduced regime (2b) with no nonanalyticity. A nonanalyticity in this regime would indicate the criticality of the system toward clustering of the states into an ultrametric superstructure (higher-step RSB). This kind of criticality is not present in typical samples in $d<2$, and only arise in exponentially rare disorder realizations, as we confirm by studying the configurational entropy of nonequilibrium states. Possible consequences of our results for manifolds at finite N are discussed, as well as extensions to spin glasses and related models.

The outline of the paper is as follows. In Sec. II, we define the model and the observable to be studied. In Sec. III, we analyze regime (2a) for both continuous and one-step RSB, discussing various subtleties of the phase diagram in the one-step case. We study, in particular, the nonanalytic cusp arising in the force correlator at $T=0$ and its thermal rounding. Taking the limit of large $v\gg 1$, we establish the matching with the regime $v^2\sim N$, which is analyzed in detail in Sec. IV. We rigorously show how to compute the FRG function $R(v)$ exactly by introducing two replica groups and derive from it the correct FRG flow equations in all cases, including the anomaly arising from RSB. The physical significance of the presence or absence of a cusp in this regime is discussed. The results are summarized in Sec. V, and possible applications are discussed.

II. MODEL, OBSERVABLES, AND PREVIOUS RESULTS

A. Model

We consider an elastic manifold parametrized by an N-component displacement field $u(x)$, also denoted u_x, where x belongs to the internal d-dimensional space. The manifold is exposed to a random potential, $V(x,u)$, which lives in a $(D=d+N)$-dimensional space. Indices of the field u_x^i, $i=1,\ldots,N$, are shown only when strictly needed, and we use the notation $u\cdot v=\sum_{i=1}^N u^i v^i$. We study the (classical) equilibrium statistical mechanics defined by the canonical partition sum $Z_V=\mathrm{Tr}\, e^{-\beta H_V}$ at temperature T, and denote thermal averages by $\langle F[u]\rangle_V$ (or, sometimes, simply $\langle F[u]\rangle$) in a given realization of the random potential. The model is defined by the total energy:

$$H_V[u]=\frac{1}{2}\int_k g_k^{-1}u_k\cdot u_{-k}+\int_x V(x,u_x), \tag{4}$$

where $u_k=\int_x u_x e^{ikx}$, $\int_x=\int d^dx$ and $u_x=\int_k u_k e^{-ikx}$, $\int_k=\int\frac{d^dk}{(2\pi)^d}$. To fix the average center-of-mass position $\overline{u_{\rm cm}}:=\overline{u_{k=0}}/L^d$, we choose a nonzero value for $g_{k=0}^{-1}=cm^2$, which takes the role of a mass, c being the elastic constant. The mass provides a quadratic well for the manifold and, thus, serves as an IR cutoff to limit the displacement fluctuations. One is often interested in the scale invariant limit, $m\to 0$. A UV cutoff $\sim\Lambda^{-1}$ in x space (e.g., due to a lattice) is implicit everywhere. For specific applications, we consider[58]

$$g_k=\frac{1}{c(k^2+m^2)}, \tag{5}$$

even though most results apply to more general forms of g_k. The quenched disorder is chosen to possess statistical translational invariance, with second cumulant

$$\overline{V(x,u)V(x',u')}=\delta^{(d)}(x-x')R_0(u-u'). \tag{6}$$

This property entails a useful symmetry (see below), usually referred to as statistical tilt symmetry (STS). We always assume $O(N)$ symmetry of the disorder, choosing the bare correlator to be[59]

$$R_0(u)=NB(u^2/N). \tag{7}$$

This scaling with N yields a nontrivial large-N limit. Among the variety of models parametrized by the function $B(z)$, one distinguishes short-range (SR) disorder; one often studied example being

$$B(z)=B_0e^{-z/r_f^2}, \tag{8}$$

and long-range (LR) disorder, often represented by the family of power law force correlator:[60]

$$B'(z)=-\frac{B_0}{r_f^2\left(1+\frac{z}{\gamma r_f^2}\right)^{\gamma}}. \tag{9}$$

Here, the parametrization of model (9) is chosen[61] such that the limit $\gamma\to\infty$ corresponds to model (8), and that the limits $\gamma\to 1$ and $\gamma\to 0$ are meaningful. These two models possess a special scale-invariance property at infinite N: As discussed below in Sec. IV, they arrive at their FRG fixed point after a finite renormalization time.[62]

It is well known[37] that the effect of disorder in model (4) for any N becomes nonlinear, and metastability appears when the mass is decreased beyond some characteristic scale. As easily seen from dimensional analysis, the natural unit is the so-called Larkin scale:[63]

$$\mu_c\equiv\frac{1}{L_c}:=\left(\frac{B_0}{c^2r_f^4}\right)^{1/\epsilon}, \tag{10}$$

where $\epsilon=4-d$. In finite dimensions $d>0$, $L_c=1/\mu_c$ has the loose interpretation of the smallest typical size of domains which may be trapped in different metastable states and, thus, exhibit glassiness at low temperature. The energy of such domains is naturally expressed in the unit of energy

$$E_c:=c\mu_c^{-d}(r_f\mu_c)^2, \tag{11}$$

while r_f and $L_c=1/\mu_c$ are the natural scales for embedding space and internal space (i.e., inverse mass) lengths in the problem. We are free to choose units in which $E_c=L_c=r_f=1$, or, equivalently, $c=B_0=r_f=1$, which we adopt throughout the paper. For completeness, we give the dimensions of all observables used in the present paper in Appendix A, which allows us to restore the full dependence on these parameters.

In order to study model (4), one introduces replicated fields $u^a(x)$, $a=1,\ldots,n$. Using standard methods, all disorder-averaged correlation functions of the $u(x)$ field can be expressed as correlation functions of the replicated fields $u^a(x)$ in the theory with partition sum $\overline{Z_V^n}=\mathrm{Tr}\, e^{-S[u]}$ and action $S[u]$:

$$S[u]=\frac{1}{T}\sum_a\int_k g_k^{-1}u_k^a\cdot u_{-k}^a-\frac{1}{2T^2}\sum_{ab}\int_x R_0(u_x^a-u_x^b). \quad (12)$$

B. Summary of previous studies

1. Gaussian variational method

Before defining the observable computed in the present work, let us briefly review the quantities studied in previous publications,[11,13,46] and the main results obtained there (details are skipped and can be found in these original publications). Model (12) was studied in Ref. 46 using the GVM, which becomes exact in the limit $N=\infty$. The central observable calculated there is the two point correlation function of the replicated field:

$$\langle u_k^{ai}u_{k'}^{bj}\rangle_S=G_{ab}(k)\delta_{ij}(2\pi)^d\delta^{(d)}(k+k'). \quad (13)$$

Here, we denote by $\langle .\rangle_S$ averages over the replicated action (we later drop the subscript S when not strictly needed). Correlation (13) encodes[64] the averages $\overline{\langle u_k^i u_{k'}^j\rangle}=G_{aa}(k)\delta_{ij}(2\pi)^d\delta^{(d)}(k+k')$ (diagonal part) and $\overline{\langle u_k^i u_{k'}^j\rangle^c}=\Sigma_b G_{ab}(k)\delta_{ij}(2\pi)^d\delta^{(d)}(k+k')$ (connected thermal average). The large distance behavior of the first one defines the roughness exponent ζ of the manifold, i.e., $\overline{\langle(u_x-u_{x'}')^2\rangle}\sim|x-x'|^{2\zeta}$, equivalently $G_{aa}(k)\sim k^{-(d+2\zeta)}$ at small k. These hold at fixed scale in the limit $m\to 0$, or at small but fixed m for scales smaller than the IR cutoff, $k\gg 1/m$. Another important exponent characterizes how the fluctuations of the ground state energy (or of the free energy) scale with system size, $\Delta E\sim L^{\theta}$. Here, thanks to the statistical tilt symmetry, one has the relation $\theta=d-2+2\zeta$.

Quite generally, Eq. (13) takes the form

$$TG_{ab}^{-1}(k)=\delta_{ab}g_k^{-1}-\sigma_{ab}(k), \quad (14)$$

and, within the GVM, the self-energy is taken to be k independent, $\sigma_{ab}(k)\equiv\sigma_{ab}$. It obeys a self-consistent equation which arises as a large-N saddle-point equation, reading

$$\sigma_{ab}=-\frac{2}{T}B'\left(2\int_k[G_{aa}(k)-G_{ab}(k)]\right). \quad (15)$$

There are two types of saddle points: Either they respect the replica symmetry of action (12), $\sigma_{a\neq b}=\sigma$, which happens in the high-temperature phase [where the roughness exponent assumes its thermal value, $\zeta=\zeta_{\mathrm{th}}=\max(0,(2-d)/2)$], or the saddle points spontaneously break the symmetry (RSB), $\sigma_{ab}\to\sigma(\mathsf{u})$, where $\mathsf{u}\in[0,1]$ labels the distance of replicas in an ultrametric Parisi scheme describing the glassy, pinned phase.

Let us summarize the results for $N=\infty$ and $g_k^{-1}=k^2+m^2$, for which the dependence on the mass is worked out in Ref. 13. We start with the case where the glass phase is described

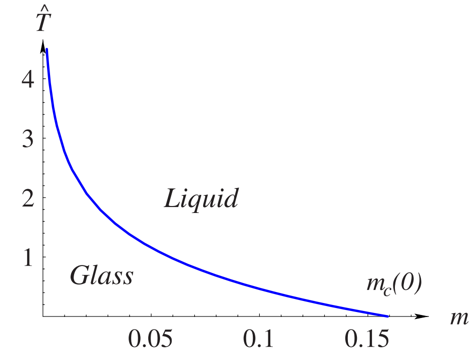

FIG. 1. (Color online) Phase diagram for model (16a) in $d=3$ for $\Lambda/m_c\gg 1$. The phase transition as given by Eq. (17) is everywhere continuous, and the glass phase exhibits continuous RSB. The transition temperature $\hat{T}_c$ diverges as $m\to 0$. An unconstrained system ($m=0$) is, therefore, always glassy. A similar phase diagram applies to $d>2$ for both models (16a) and (16b), and to $d<2$ for model (16b) with sufficiently long-ranged correlators, $\gamma<\gamma_c$ [the temperature scale being set, for $d<2$, by $I_1(m_c(T=0))$].

by continuous RSB (also called infinite-step or full RSB). Within such a RSB scheme, it is found that the roughness exponent equals its "Flory" value:

$$\zeta=\zeta_F=\begin{cases}0 & (16a)\\ (4-d)/[2(1+\gamma)] & (16b)\end{cases}$$

and the continuous RSB solution is self-consistent if the corresponding energy exponent is positive, $\theta=\theta_F=d-2+2\zeta_F>0$. This occurs in dimensions $4\geq d\geq 2$ for both models and any γ, as well as in dimensions $d<2$ for sufficiently long-ranged disorder in model (16b) [$\gamma<\gamma_c(d)=2/(2-d)$], including model (16a) in $d=2$.

The replica symmetry is broken for small IR cutoff $m<m_c$, where $m_c=m_c(T)$ is the temperature dependent Larkin mass, which is determined by the instability of the replica-symmetric (RS) solution:

$$1=4B''(2TI_1(m_c))I_2(m_c), \quad (17)$$

$$I_n(m)=\int_k\frac{1}{(k^2+m^2)^n}, \quad (18)$$

and decreases as a function of T from $m_c(T=0)=O(1)$ to zero as $T\to\infty$. Hence, in that case, an unconstrained system ($m=0$) is always glassy, while a strong confinement $m>m_c(T)$ leads to an ergodic (replica symmetric) high-temperature phase. This is illustrated in Fig. 1 where we plot the phase diagram for model (16a) in $d=3$. Since the temperature always enters in the combination $2TI_1$, where I_1 is dominated by the UV cutoff for $d>2$, we have introduced the rescaled temperature:

$$\hat{T}=2TI_1(m=0)=\frac{4T\Lambda^{d-2}}{(4\pi)^{d/2}(d-2)\Gamma(d/2)} \quad (19)$$

for a circular UV cutoff in k space.

The self-energy function $\sigma(\mathsf{u})$ of a continuous RSB solution generally interpolates continuously between two plateaux at small and large u. For both models (16a) and (16b) (with $\gamma<\gamma_c$ in $d\leqslant 2$), $\sigma(\mathsf{u})$ takes the form[65]

$$\sigma(\mathsf{u}) = \frac{2}{2-\theta}\frac{m_c^2}{\mathsf{u}_c}\times\begin{cases}(m/m_c)^{2-\theta} & \mathsf{u}<\mathsf{u}_m\\ (\mathsf{u}/\mathsf{u}_c)^{(2/\theta)-1}, & \mathsf{u}_m<\mathsf{u}<\mathsf{u}_c\\ 1, & \mathsf{u}_c<\mathsf{u}<1.\end{cases} \tag{20}$$

Here, $m_c=m_c(T)$ and[66]

$$\mathsf{u}_c = ATm_c^\theta, \tag{21}$$

$$\mathsf{u}_m = ATm^\theta, \tag{22}$$

where, with I_n defined in Eq. (18),

$$A = \frac{I_2(m_c)^2}{m_c^{d-2}I_3(m_c)} = \frac{4A_d}{\epsilon^2}, \tag{23}$$

$$A = \frac{4A_d}{\epsilon^2}\left(1+\frac{1}{\gamma}\right)\left(\frac{\epsilon}{4A_d}\right)^{1/(1+\gamma)}, \tag{24}$$

and $A_d := \epsilon\int_k (1+k^2)^{-2} = 2\Gamma(3-d/2)/(4\pi)^{d/2}$.

In the sequel, the value of $\sigma(0)$ will play a central role, and we give an explicit expression for later reference:

$$\sigma(0) = \sigma(\mathsf{u}_m) = \frac{2}{2-\theta}\frac{m^{2-\theta}}{AT}. \tag{25}$$

In the case of sufficiently short-ranged disorder in $d\leqslant 2$ [model (23) or model (24) with $\gamma>\gamma_c(d)$], the glass phase is described by a one-step RSB solution which is fully characterized by three numbers: the breakpoint u_c and the self-energy parameters

$$\sigma_0 \equiv \sigma(\mathsf{u}<\mathsf{u}_c) = \sigma(0),$$

$$\sigma_1 \equiv \sigma(\mathsf{u}>\mathsf{u}_c) = \sigma(1). \tag{26}$$

The borderline between one-step and full RSB is characterized by $\theta=\theta_F=0$: $\gamma=\gamma_c$ for model (24) in $d<2$, or model (23) in $d=2$. In this case, the one-step solution can equivalently be obtained as the limit of a continuous RSB solution, which entails that the one-step scheme is only marginally stable. In this limiting case of continuous RSB, $m_c(T)$ remains a decreasing function of T, however, it vanishes at a finite $T=T_c$, signalling a continuous glass transition for the unconstrained system ($m=0$) at T_c. The phase diagram for the marginal case of SR disorder in $d=2$ is shown in Fig. 2.

Away from the borderline in the (d,γ) plane, the one-step solution is genuinely stable. This includes, in particular, the case of the directed polymer and the KPZ problem ($d=1$). The phase diagram in the (T,m) plane is more complicated (cf. Fig. 4) and will be discussed together with the one-step solution within the GVM in Sec. III D 3. The essential difference with the cases discussed above is the nature of the temperature-driven glass transition at small mass, which becomes a discontinuous random first-order transition. Similar to ordinary first-order transitions, two locally stable solutions coexist at least close enough to the transition: Here, these are the RS solution and the one-step solution. The roughness exponent of all one-step solutions equals the thermal exponent, $\zeta=\zeta_{\mathrm{th}}=(2-d)/2$.

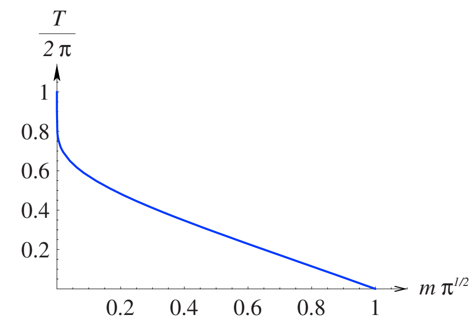

FIG. 2. (Color online) Phase diagram for model (23) in $d=2$ (with a UV cutoff $\Lambda=10$). The phase transition is everywhere continuous, and the glass phase exhibits continuous one-step RSB. The transition temperature has a finite limit $T_c\to 2\pi$ as $m\to 0$. A similar phase diagram applies to model (24) with critical long-range disorder $\gamma=\gamma_c$ in $d<2$. The transition line has a cusplike behavior as $m\to 0$, $[T_c(0)-T_c(m)]/T_c(0)\sim m^{2-d}$ [and $\sim 1/\log(1/m)$ in $d=2$].

2. Effective action and functional renormalization group

In an effort to connect the results described above to the functional RG approach, two of us performed a calculation of the effective action $\Gamma[u]$ for model (4) (cf. Refs. 11 and 13). One starts by defining the standard generating functional $W[j]$ for connected correlations in the replica theory with, in general, $j=(j^1(x),\ldots,j^n(x))$:

$$e^{W[j]} = Z[j] = \overline{\prod_{a=1}^{n} Z_V[j^a]}, \tag{27}$$

$$Z_V[j^a] = \int \mathcal{D}[u]\exp\left(-\beta H_V[u] + \int_x j_x^a\cdot u_x\right), \tag{28}$$

and the effective action functional is defined via the Legendre transform:

$$\Gamma[u] + W[j] = \sum_a \int_x j_x^a \cdot u_x^a, \quad \frac{\delta W}{\delta j_x^a}[j] = u_x^a. \tag{29}$$

In Refs. 11 and 13, the effective action for a uniform configuration $\Gamma(u)=\frac{1}{L^d}\Gamma[\{u_x^a=u^a\}]$ was studied in the large-N limit. It has a nontrivial limit in the regime

$$u^2 \sim N, \quad \Gamma\sim N. \tag{30}$$

It was further computed in an expansion in the "number of replica sums" (which is effectively a cumulant expansion) as follows:

$$\Gamma(u) = \sum_a \frac{m^2(u^a)^2}{2T} - \frac{1}{2T^2}\sum_{ab} R(u^{ab}) - \frac{1}{6T^3}\sum_{abc} S^{(3)}(u^{abc}) + \cdots \tag{31}$$

up to a constant. Here and below, $u^{ab}=u^a-u^b$ and $u^{abc}=u^a,u^b,u^c$. This defines unambiguously (for any N) the second cumulant of the renormalized disorder potential $R(u) = R_m(u)$, where we will usually keep the m dependence implicit. At large N, it obeys the scaling form

$$R(u) = N\tilde{B}(u^2/N). \tag{32}$$

Remarkably, the scaling function $\tilde{B}(z)$ satisfies a closed equation:

$$\tilde{B}(z) = B'(z + 2TI_1 + 4I_2[\tilde{B}(z) - \tilde{B}(0)]), \tag{33}$$

where $z=u^2/N$, and $I_n = I_n(m)$ was given in Eq. (18). As we will show later, this equation is only valid in the nonglassy regime since it was derived under the implicit assumption that the replica symmetry is not spontaneously broken as $u \to 0$. Taking a derivative with respect to the mass m and introducing a scaled function $\tilde{b}(x) = 4A_d m^{4\zeta-\epsilon}\tilde{B}(xm^{-2\zeta})$, a FRG equation was derived for the renormalized and scaled potential correlator $\tilde{b}(x)$ [denoted $b(x)$ in Refs. 11 and 13]. Remarkably, this FRG equation admits a natural continuation to the glassy regime. In that continuation a linear cusp exists for all $m \leq m_c$. The resulting large-N equation, valid to all orders in $\epsilon = 4-d$, exactly matches the equation previously derived to first order in ϵ (one loop), but for arbitrary N, by Balents and Fisher,[6] by a quite different method. In addition, for all universality classes characterized by (d,γ), such that $\theta > 0$ (ensuring continuous RSB in the GVM), the fixed points $\tilde{b}^*(x)$ could be related to the solution of the GVM. All the above strongly suggested that the derived flow equation was the correct large-N limit of the FRG.

3. Relation between Gaussian variational method and functional renormalization group in the case of continuous replica symmetry breaking

However, establishing a link between the GVM results and the FRG is rather subtle. To a considerable extent, this has been achieved for the case of continuous RSB in Refs. 11 and 13, while the same task for situations exhibiting one-step RSB has remained an open problem, which is addressed in the present paper. In order to review the results for the continuous case, we recall the multiplication formulas for two ultrametric matrices $AB=C$:

$$A^c B^c = C^c, \tag{34}$$

$$(A^c - [A](\mathsf{u}))(B^c - [B](\mathsf{u})) = C^c - [C](\mathsf{u}), \tag{35}$$

$$A(0)B^c + B(0)A^c = C(0), \tag{36}$$

where

$$A^c := A_{aa} - \int_0^1 A(\mathsf{u}')d\mathsf{u}', \tag{37}$$

$$[A](\mathsf{u}) := \mathsf{u}A(\mathsf{u}) - \int_0^{\mathsf{u}} A(\mathsf{u}')d\mathsf{u}'. \tag{38}$$

We also introduce the notation for the diagonal element $\tilde{A} := A_{aa}$.

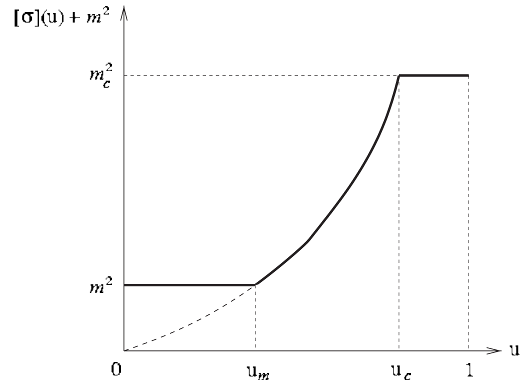

FIG. 3. The MP function $[\sigma](u)+m^2$ for $m>0$. By changing m^2, only the lower plateau will move, while the remainder of the function (for $\mathsf{u} > \mathsf{u}_m$) remains unchanged.

From Eq. (20) above, one finds

$$m^2 + [\sigma](\mathsf{u}) = m_c^2 \times \begin{cases} (m/m_c)^2, & \mathsf{u} < \mathsf{u}_m \\ (\mathsf{u}/\mathsf{u}_c)^{2/\theta}, & \mathsf{u}_m < \mathsf{u} < \mathsf{u}_c \\ 1, & \mathsf{u}_c < \mathsf{u} < 1, \end{cases} \tag{39}$$

and from Eq. (14), we obtain

$$G^c(k) = Tg_k, \tag{40}$$

$$G^c(k) - [G](k,\mathsf{u}) = \frac{T}{g_k^{-1} + [\sigma](\mathsf{u})}, \tag{41}$$

$$G(k,0) = G(k,\mathsf{u}_m) = T\sigma(\mathsf{u}_m)g_k^2. \tag{42}$$

Further, using $\frac{d}{d\mathsf{u}}[\sigma](\mathsf{u}) = \mathsf{u}\frac{d}{d\mathsf{u}}\sigma(\mathsf{u})$, we find

$$G(k,\mathsf{u}) = T\sigma(\mathsf{u}_m)g_k^2 + T\int_{\mathsf{u}_m}^{\mathsf{u}} \frac{\dot{\sigma}(\mathsf{u})d\mathsf{u}}{[g_k^{-1} + [\sigma](\mathsf{u})]^2} \tag{43}$$

(we often denote $\dot{\sigma} \equiv \frac{d}{d\mathsf{u}}\sigma$ here and below), which relates $G(k,\mathsf{u})$ to the self-energy $\sigma(\mathsf{u})$ (Fig. 3), which for $g_k^{-1} = k^2 + m^2$ is given by Eqs. (20) and (39).

In the GVM, the two-point correlation function is, thus, given by contributions from states at all distances u as

$$\frac{\tilde{G}(k)}{T} = g_k + \sigma(\mathsf{u}_m)g_k^2 + g_k\int_{\mathsf{u}_m}^1 \frac{d\mathsf{u}}{\mathsf{u}^2}\frac{[\sigma](\mathsf{u})}{g_k^{-1} + [\sigma](\mathsf{u})}. \tag{44}$$

Using Eq. (39) and integrating over u yield the final result:

$$\tilde{G}(k) \sim Cm^{-(d+2\zeta)}f(k/m), \tag{45}$$

in the limit $m \to 0$, with $f(0)=1$ and $f(z) \sim z^{-(d+2\zeta)}$ with $\zeta = \zeta_F$, exhibiting the anticipated scaling.

On the other hand, the FRG allows one to compute the two-point function using Eq. (31) through the exact relation:

$$(2\pi)^d\delta^{(d)}(k+k')G_{ab}^{-1}(k) = \left.\frac{\delta^2\Gamma[u]}{\delta u_k^a \delta u_{k'}^b}\right|_{u=0}, \tag{46}$$

which, upon matrix inversion, yields the zero-momentum correlation function:

$$\tilde{G}(k=0) = -\frac{2\tilde{B}'(0)}{m^4} + \frac{T}{m^2}. \qquad (47)$$

It turns out that this *does not* yield the full MP result [Eqs. (44) and (45)]. Indeed, the contribution from the integral over u in Eq. (44) is missing. However, Eq. (47) exactly reproduces the first two terms in Eq. (44), i.e., the contribution from the most distant states corresponding to $0<\mathsf{u}<\mathsf{u}_m$, as well as the trivial term T/m^2 describing the connected correlations $G^c(k=0)$. Using the natural continuation to the glassy regime of the RG flow associated with the solution of Eq. (33), it was, indeed, inferred that

$$-2\tilde{B}'(0) = T\sigma(\mathsf{u}_m), \qquad (48)$$

as will be derived rigorously in Sec. IV. This is already a nontrivial result: obtaining it within the GVM does require the RSB ansatz, while the FRG considered in Refs. 11 and 13 does not make reference to ultrametric matrices and their properties.

The fact that the FRG calculation of Refs. 11 and 13 reproduced only the contribution of the most distant states within the Parisi hierarchy was argued to arise because Γ and W were computed by introducing sources which split all replicas, i.e., $u^{ab}\neq 0$ (and of order $\sqrt{N}$) for all $a\neq b$. However, it remained to be understood how the full result (45) can be recovered and how the crossover to spontaneous RSB takes place as $u^{ab}\to 0$.

This is the aim of the present paper. We will show the existence of a regime whose large-N limit is different from Eq. (30):

$$u^2 \sim N^0 L^{-d}, \quad \Gamma \sim N^0, \qquad (49)$$

and where RSB cannot be neglected. This will allow us to recover the complete GVM result, i.e., to correctly perform the (nontrivial) zero-field limit $u_k^a \to 0$ in Eq. (46). We first show, in the following section, that it is equivalent, but physically more transparent, to studying the generating functional W rather than Γ. Further, we will revisit the attempt by Balents *et al.*[47] to connect RSB and FRG. Although we choose a different observable than those authors (so as to connect more directly to the FRG), we employ techniques similar to theirs, at least in the regime $v^2=O(1)$.

C. Observable studied here

The observable studied here is the free energy $\hat{V}[v]$ of the elastic manifold in a quadratic potential well centered at position v_x and defined by[67]

$$e^{-\hat{V}[v]/T} = \int \mathcal{D}[u] e^{-H_V[u;v]/T},$$

$$H_V[u;v] = \frac{1}{2}\int_k g_k^{-1}|u_k - v_k|^2 + \int_x V(x,u_x), \qquad (50)$$

with $g_k=k^2+m^2$. For a uniform $v_x=v$ and $v_k=v(2\pi)^d\delta^{(d)}(k)$, one has[68]

$$H_V[u;v] = H_V[u] - m^2 v\int_x u_x + \frac{1}{2}L^d m^2 v^2. \qquad (51)$$

It is then clear from the definitions (27) and (50) that the statistics of $\hat{V}[v]$ can be obtained from the functional $W[j]$ with

$$j_k = \frac{g_k^{-1}v_k}{T}. \qquad (52)$$

Hence, we denote $\hat{W}[v]=W[j=(g^{-1}v)/T]$, such that

$$e^{\hat{W}[v]} = \exp\left(\frac{1}{2T}\int_k g_k^{-1}\sum_a v_k^a v_{-k}^a\right)\overline{\prod_a e^{-\hat{V}[v_a]/T}}. \qquad (53)$$

It is, thus, clear that the functional can be expanded in a cumulant expansion, i.e., in the number of replica sums:

$$\hat{W}[v] = \frac{1}{2T}\sum_a \int_k g_k^{-1} v_k^a v_{-k}^a + \frac{1}{2T^2}\sum_{ab}\hat{R}[v^{ab}] + \frac{1}{6T^3}\sum_{abc}\hat{S}^{(3)}[v^{abc}] + \cdots, \qquad (54)$$

up to a constant, where again $v_x^{ab}=v_x^a-v_x^b$. Each term in the expansion is a functional, $\hat{R}[v^{ab}]\equiv\hat{R}[\{v_x^{ab}\}]$ with fixed a,b, etc., and represents the free-energy cumulants:

$$\overline{\hat{V}[v]\hat{V}[v']}^c = \hat{R}[v-v'], \qquad (55)$$

and similarly for higher cumulants (the overbar denoting the disorder average over the random potential V). For a uniform configuration $v_x=v$, one has

$$\hat{R}[v] = L^d\hat{R}(v), \qquad (56)$$

which defines $\hat{R}(v)$. Note that with arguments in brackets $[\ldots]$ we denote functionals, while $(\ldots)$ is reserved for functions. When discussing uniform v, we usually switch to the function $R(v)$, separating out the volume factor.

As shown in Refs. 48 and 49 by performing the Legendre transform (29), this observable is directly related to the function $R(u)$ of the FRG:

$$\hat{R}(v) = R(v), \qquad (57)$$

i.e., the two functions are the same, and this holds for the functionals, too. Therefore, by computing $\hat{R}[v]$, which we do here for large N, we simultaneously compute $R[u]$ as defined from the effective action (31). The fact that Eq. (55) defines an observable which is easy to measure has allowed for a numerical determination[55] of $R(u)$ or, more precisely, of the force correlator $\Delta(u)=-R''(u)$, for $N=1$ interfaces at $T=0$.

The derivative of $R(u)$ at $T=0$ contains information about the shocks. Indeed, if one computes the ground state $u(x;v)$ for a fixed well position and defines the center-of-mass displacement $\bar{u}(v):=L^{-d}\int u(x;v)$, one finds that the latter exhibits jumps as v is varied. The statistics of these jumps is encoded in the functions $\hat{R}$, $\hat{S}$, etc., for instance, one has

$$\overline{[\overline{u}^i(v)-v^i][\overline{u}^j(v')-v'^j]} = m^{-4}L^{-d}\Delta_{ij}(v-v'), \qquad (58)$$

and the cusp of $\Delta_{ij}(v)=-\partial_i\partial_j\hat{R}(v)$, i.e., the derivative of Δ at argument 0, is proportional to the second cumulant of the jump sizes.

We now turn to the calculation of this observable in the large-N limit. We will perform separate calculations for the two scaling regimes $v_x^2\sim O(1)$ and $v_x^2\sim O(N)$ in the next sections and check that they match.

III. REGIME OF SMALL v, $v_x^2=O(1)$

We want to compute the generating functional (27) in the form

$$e^{\hat{W}[v]} = \overline{\prod_a Z_V[j^a]}, \quad j_k^a = \frac{g_k^{-1}v_k^a}{T}. \qquad (59)$$

This can be carried out at large N through the saddle-point method as in Ref. 46, introducing the term $i\lambda_{ab}(N\chi_{ab}-u_a u_b)$ and integrating over the field u. This is detailed in the next section, where we study the case where $v_{ab}^2\sim O(N)$, which distorts the saddle point away from Eqs. (14) and (15). In this section, we study $v_{ab}^2=O(1)$ and the above saddle points are unchanged [more precisely, they are shifted only by terms at most of order $O(1/N)$, which are discarded]. Since there is spontaneous RSB, there are, in fact, many saddle points equivalent under replica permutations. Hence, the above average must be written as a sum over all equivalent saddle points:

$$\overline{\prod_a Z_V[j^a]} = C_n\sum_\pi\left\langle \exp\left(\sum_a\int_x j_x^a u_x\right)\right\rangle_\pi, \qquad (60)$$

where $\pi\in S_n$ belongs to the group of permutation of n replica which is used to label the saddle points. Around each saddle point, the measure is Gaussian with correlator $\langle u_x^a u_y^b\rangle_\pi = G_{ab}^\pi(x-y) := G_{\pi(a)\pi(b)}(x-y)$, where $G_{ab}(x)$ is the ultrametric matrix given by Eq. (14). Hence, we obtain

$$e^{\hat{W}[v]-\hat{W}[0]} = \tilde{\sum_\pi}\exp\left[\frac{1}{2T^2}\sum_{ab}\int_k g_k^{-2}G_{ab}^\pi(k)v_{-k}^a\cdot v_k^b\right], \quad (61)$$

where $\tilde{\Sigma}_\pi$ denotes a normalized average over permutations, i.e., $\tilde{\Sigma}_\pi 1=1$. The remainder of this section is devoted to the analysis of this formula.

In principle, by expanding this formula in powers of v to all orders, and regrouping terms, one could check that it is, indeed, possible to put it into the form (54) and to compute all the cumulants (we denote by $\hat{S}^{(n)}$ the nth cumulant). This is a formidable task, however, and we will focus here only on the second cumulant function $\hat{R}$. Before computing it directly, let us give a flavor of the direct expansion in powers of v.

A. Direct expansion in powers of v

The expansion of Eq. (61) in powers of v starts as

$$\hat{W}[v]-\hat{W}[0] = \tilde{\sum_\pi}\frac{1}{2T^2}\sum_{ab}\int_k g_k^{-2}G_{ab}^\pi(k)v_{-k}^a\cdot v_k^b + O(v^4). \qquad (62)$$

Let us recall the structure and parametrization of a hierarchical Parisi matrix. Dropping temporarily the k dependence, one has[69,70]

$$G_{ab} = [\tilde{G}-G(n)]\delta_{ab} + G(n)(\mathbb{1}_n)_{ab} \quad (\text{RS}), \qquad (63)$$

$$G_{ab} = [\tilde{G}-G(1)]\delta_{ab} + [G(1)-G(n)](\mathbb{1}_{\mathsf{u}_c}^{(n)})_{ab} + G(n)\times(1_n)_{ab} \quad (\text{one-step RSB}), \qquad (64)$$

$$G_{ab} = [\tilde{G}-G(1)]\delta_{ab} + \int_n^1 d\mathsf{u}\frac{dG(\mathsf{u})}{d\mathsf{u}}(\mathbb{1}_{\mathsf{u}}^{(n)})_{ab} + G(n)(\mathbb{1}_n)_{ab} \quad (\text{continuous RSB}). \qquad (65)$$

We have defined $\mathbb{1}_m^{(n)}$ as the matrix made of n/m identical blocks along the diagonal, each block being the $m\times m$ matrix with all entries equal to one, and $\mathbb{1}_n^{(n)}=\mathbb{1}_n$. As an example,

$$\mathbb{1}_3^{(12)} = \begin{pmatrix} 1&1&1&0&0&0&0&0&0&0&0&0\\ 1&1&1&0&0&0&0&0&0&0&0&0\\ 1&1&1&0&0&0&0&0&0&0&0&0\\ 0&0&0&1&1&1&0&0&0&0&0&0\\ 0&0&0&1&1&1&0&0&0&0&0&0\\ 0&0&0&1&1&1&0&0&0&0&0&0\\ 0&0&0&0&0&0&1&1&1&0&0&0\\ 0&0&0&0&0&0&1&1&1&0&0&0\\ 0&0&0&0&0&0&1&1&1&0&0&0\\ 0&0&0&0&0&0&0&0&0&1&1&1\\ 0&0&0&0&0&0&0&0&0&1&1&1\\ 0&0&0&0&0&0&0&0&0&1&1&1 \end{pmatrix}. \qquad (66)$$

With these formulas, one easily checks that

$$G^c := \sum_b G_{ab} = \tilde{G} - \int_n^1 G(\mathsf{u})d\mathsf{u} + nG(n) \overset{n\to 0}{=} \tilde{G} - \int_0^1 G(\mathsf{u})d\mathsf{u}. \qquad (67)$$

For symmetry reasons, the permutation average must yield a replica-symmetric matrix

$$\tilde{\sum_\pi} G_{ab}^\pi = \alpha\delta_{ab} + \beta. \qquad (68)$$

Setting $a\neq b$, one finds $\beta=(n-1)^{-1}\Sigma_{b\neq 1}G_{1b}=(G^c-\tilde{G})/(n-1)$, while multiplying with δ_{ab} shows that $\alpha+\beta=\tilde{G}$. Thus, one finds

$$\tilde{\sum_\pi} G^\pi_{ab} = \frac{1}{1-n}[(G^c - n\tilde{G})\delta_{ab} + \tilde{G} - G^c] \overset{n\to 0}{\to} [G^c + n(\tilde{G} - G^c)]\delta_{ab} + \tilde{G} - G^c, \quad (69)$$

which is a replica-symmetric matrix by construction, but with nontrivial entries in the case of RSB. Terms of higher order in n have been neglected, except for the linear term in the replica diagonal part which we retain for later use.

Inserting in Eq. (62), we finally have

$$\hat{W}[v] - \hat{W}[0] = \frac{1}{2T^2}\sum_a \int_k g_k^{-2}[G^c(k) + n(\tilde{G}(k) - G^c(k))]|v_k^a|^2 + \frac{1}{2T^2}\sum_{ab}\int_k g_k^{-2}[\tilde{G}(k) - G^c(k)]v_k^a \cdot v_{-k}^b + O(v^4). \quad (70)$$

On the other hand, expanding Eq. (54), we obtain, for $n=0$,

$$\hat{W}[v] - \hat{W}[0] = \frac{1}{2}\sum_{ab}\int_k \left(\frac{\delta_{ab}}{Tg_k} - \frac{1}{T^2}\hat{R}_k''[0]\right) v_k^a \cdot v_{-k}^b + O(v^4), \quad (71)$$

since the fourth cumulant must start as v^4 and the third as v^6 (as one cannot construct STS invariant combinations of smaller degree; see Appendix B of Ref. 22 for an argument in the case $N=1$). Here and below, we adopt the notation

$$\hat{R}''_{xx'}[v] = \frac{\delta^2 \hat{R}[v]}{\delta v_x^i \delta v_{x'}^i}, \quad (72)$$

$$\int_{xx'} e^{ikx+ik'x'}\hat{R}''_{xx'}[v] = (2\pi)^d \delta(k+k')\hat{R}_k''[v], \quad (73)$$

where the last line uses translational invariance and one has set $v_x = v$ after taking the derivatives. Further, we have assumed $O(N)$ symmetry so that the second derivative of R is diagonal and independent of the $O(N)$ index i in Eq. (72) (where no index summation is assumed).

Identifying Eqs. (70) and (71) shows that for $n=0$:

$$\tilde{G}(k) = Tg_k - g_k^2 \hat{R}_k''[0], \quad G^c(k) = Tg_k, \quad (74)$$

the second identity being a simple consequence of the STS symmetry. Hence, once the functional $\hat{R}=R$ of the FRG is known, the correlation function computed via the GVM can be retrieved as

$$\tilde{\sum_\pi} \langle u_{-k}^a u_k^b \rangle_\pi = \tilde{\sum_\pi} G^\pi_{ab}(k) = Tg_k\delta_{ab} - g_k^2 R_k''[0]. \quad (75)$$

This property of R, here guaranteed by its definition (61) via the effective action, does not hold for the observable defined in Ref. 47 (having a similar form but with $G \to G^{-1}$). This made the comparison of their results with the FRG problematic.

To evaluate the identity (74) at $k=0$, we use that for a uniform v, $d/dv = \int dx \frac{\delta}{\delta v_x}$ and, thus,

$$\hat{R}''_{k=0}[v] = \frac{1}{L^d}\int_{xx'} \hat{R}''_{xx'}[v] = \hat{R}''(v), \quad (76)$$

which yields

$$\tilde{G}(k=0) = \frac{T}{m^2} - \frac{\hat{R}(0)}{m^4}. \quad (77)$$

This relation is exact, and the task is, hence, to evaluate $\hat{R}''(0)$. There is, however, a crucial subtlety in evaluating this derivative at $v\to 0$. If one uses that $\hat{R}(v)=R(v)$, together with the result of Refs. 11 and 13,

$$\hat{R}(v) = N\tilde{B}(v^2/N), \quad v^2 \sim N, \quad (78)$$

a relation also obtained directly in Sec. IV B, one finds that Eq. (77) coincides with formula (47). However, this result is valid only in the region $v^2 \sim N$ and, as pointed out above, it does *not* reproduce the full MP result for $\tilde{G}$. To obtain the latter, as we show below, one needs to be more careful in the $v\to 0$ limit and compute $\hat{R}''(0)$ in the region where $v^2 \sim L^{-d} \ll N$. One could say that the $v\to 0$ and $N\to\infty$ limits do not commute or, more accurately, that to obtain contributions of all ultrametric states (and not just the most distant ones), one must take the limit $v\to 0$ with great care.

The next order $O(v^4)$ is obtained in Appendix B by the direct expansion method and in the next section by a more powerful method which can handle all orders, and to which we now turn.

B. Second cumulant from a two-group analysis

While the results of the previous section were completely general and independent of the RSB scheme, we now focus on a specific choice of external sources. In order to compute the second cumulant function, one best uses two sets of replica, which we denote by $v_x^a = v_x^1$ for $a=1,\ldots,n/2$ and $v_x^a = v_x^2$ for $a=1+n/2,\ldots,n$. Inserting into Eq. (54), we find

$$\hat{W}[v] - \hat{W}[0] = \frac{1}{2T}\frac{n}{2}\int_k g_k^{-1}(v_k^1 \cdot v_{-k}^1 + v_k^2 \cdot v_{-k}^2) + \frac{1}{2T^2}\frac{n^2}{2}(\hat{R}[v^{21}] - \hat{R}[0]) + O(n^3), \quad (79)$$

where

$$v^{21} := v^2 - v^1, \quad (80)$$

since all higher cumulants yield higher powers of n. We compare this with expression (61), slightly rewritten as

$$e^{\hat{W}[v]-\hat{W}[0]} = \tilde{\sum_\pi} \exp\left[\frac{1}{2T^2}\sum_{ab}\int_k g_k^{-2}G_{ab}(k)v_{-k}^{\pi(a)} \cdot v_k^{\pi(b)}\right]. \quad (81)$$

In order to perform the sum over permutations, we introduce Ising spins τ^a as in Ref. 47:

$$v^a = \frac{v^1 + v^2}{2} + \tau^a \frac{v^{21}}{2}, \tag{82}$$

where $\tau^a = -1$ if $\pi(a) \in [1, n/2]$; $\tau^a = +1$, otherwise. Each configuration $\{\tau_a\}$ is left invariant by $[(n/2)!]^2$ permutations, the number of distinct spin configurations being $C_n^{n/2} = n!/[(n/2)!]^2$. They all correspond to vanishing total magnetization, i.e., $\Sigma_{a=1}^n \tau^a = 0$. Inserting Eq. (82) into Eq. (81), the term linear in τ vanishes, and one finds

$$e^{\hat{W}[v]-\hat{W}[0]} = \exp\left[\frac{n}{4T^2}\int_k g_k^{-2} G^c(k)(|v_k^1|^2 + |v_k^2|^2)\right]\frac{1}{C_n^{n/2}} \times \sum_{\{\tau\}}{}' \exp\left[\frac{1}{2T^2}\int_k g_k^{-2}\frac{|v_k^{21}|^2}{4}\sum_{ab}\hat{G}_{ab}(k)\tau^a\tau^b\right],$$

$$\hat{G}_{ab} := G_{ab} - G^c \delta_{ab}. \tag{83}$$

The first factor equals the term proportional to n in Eq. (79), as seen upon using Eq. (74). The prime on the sum indicates that the sum extends over all Ising spin configurations subject to the global constraint $\Sigma_{a=1}^n \tau^a = 0$. Identifying the above expression with Eq. (79), we arrive at the formula

$$\hat{R}[v] - \hat{R}[0] = \lim_{n\to 0}\frac{4T^2}{n^2}\frac{1}{C_n^{n/2}} \times \sum_{\{\tau\}}{}'\left[\exp\left(\int_k \frac{g_k^{-2}}{8T^2}|v_k|^2 \sum_{ab}\hat{G}_{ab}(k)\tau^a\tau^b\right) - 1\right]. \tag{84}$$

Note that we have simplified notations by renaming $v^{21} \to v$. At this stage, we can check the small-v expansion again:

$$\frac{1}{2}\int_k \hat{R}_k''[0]|v_k|^2 = \lim_{n\to 0}\frac{T^2}{2n^2}\int_q \frac{g_k^{-2}}{2T^2}|v_k|^2 \sum_{\{\tau\}}{}' \hat{G}_{ab}(k)\tau^a\tau^b. \tag{85}$$

If we denote the normalized average $A_{ab} := \widetilde{\Sigma}'_{\{\tau\}}\tau_a\tau_b = \frac{1}{C_n^{n/2}}\Sigma'_{\{\tau\}}\tau_a\tau_b$, then one has $A_{aa} = 1$. Further, the identity $0 = \Sigma_b A_{ab} = A_{aa} + (n-1)A_{a\neq b}$ implies $A_{a\neq b} = 1/(1-n)$ and one can, thus, write $A_{ab} = (1 - n\delta_{ab})/(1-n)$ and $\Sigma_{ab}\hat{G}_{ab}A_{ab} = -n^2/(1-n)[\widetilde{G}(k) - G^c(k)]$. Using this in Eq. (85), we recover the result (74) of the previous section. Note that the same result is obtained from the piece $\sim n^2$ in the replica-diagonal part of Eq. (70), while the two-replica sum vanishes.

To evaluate the restricted spin sum in Eq. (84), we use the same method as in Ref. 71, leading to Parisi's nonlinear diffusion equation in the form discussed by Duplantier.[72] We first eliminate the constraint of zero magnetization and rewrite Eq. (84) as

$$\hat{R}[v] - \hat{R}[0] = \lim_{n\to 0}\frac{4T^2}{n^2}\frac{2^{n+1}\Gamma(-n)}{[\Gamma(-n/2)]^2} \times \int_{-\infty}^{\infty} dy \sum_{\{\tau\}}\left[\exp\left(\int_k \frac{g_k^{-2}|v_k|^2}{8T^2} \times \sum_{ab=1}^n \hat{G}_{ab}(k)\tau^a\tau^b + y\sum_{a=1}^n \tau^a\right) - \exp\left(y\sum_{a=1}^n \tau^a\right)\right], \tag{86}$$

which makes use of an identity derived in Ref. 71, valid for $n < 0$ only.

The evaluation of a spin sum such as it appears in Eq. (86) is standard in the mean-field theory of spin glasses. Here, we summarize the main steps following Duplantier.[72] We write the matrix which couples the spins as

$$q_{ab} = \frac{1}{4T^2}\int_k g_k^{-2}|v_k|^2 \hat{G}_{ab}(k),$$

$$q(\mathsf{u}) = \frac{1}{4T^2}\int_k g_k^{-2}|v_k|^2 G(k,\mathsf{u}), \tag{87}$$

with $q^c = \Sigma_b q_{ab} = 0$. Using Eq. (43), this becomes

$$q(\mathsf{u}) = \frac{1}{4T}\int_k |v_k|^2\left[\sigma(\mathsf{u}_m) + \int_{\mathsf{u}_m}^{\mathsf{u}} \frac{\dot{\sigma}(\mathsf{u})d\mathsf{u}}{[g_k^{-1} + [\sigma](\mathsf{u})]^2}\right]. \tag{88}$$

Let us now assume that q_{ab} has a K-step ultrametric structure with breakpoints at

$$n \equiv \mathsf{u}_0 < \mathsf{u}_1 < \cdots < \mathsf{u}_K < \mathsf{u}_{K+1} \equiv 1, \tag{89}$$

and entries parametrized by $q(\mathsf{u})$ with

$$q(\mathsf{u}) = q_\ell \quad \text{for } \mathsf{u}_\ell \leq \mathsf{u} < \mathsf{u}_{\ell+1}. \tag{90}$$

Further, we define $q_{-1} \equiv 0$. Let us introduce the "partial partition sums":

$$g_\ell(y) \equiv e^{\mathsf{u}_\ell \psi_\ell(y)} := \sum_{\{\tau^a\}, a=1,\ldots,\mathsf{u}_\ell} \exp\left[\frac{1}{2}\sum_{a,b=1}^{\mathsf{u}_\ell}\tau^a(q_{ab} - q_{\ell-1})\tau^b + \sum_{a=1}^{\mathsf{u}_\ell}\tau^a y\right], \tag{91}$$

which defines $g_\ell(y)$ and $\psi_\ell(y)$ for $\ell = 0, \ldots, K+1$. Obviously, $g_{K+1}(y) = 2\cosh(y)\exp[\widetilde{q} - q(1)]$.

Expression (86) can then be rewritten as

$$\hat{R}[v] - \hat{R}[0] = \lim_{n\to 0}\frac{-2T^2}{n}\int_{-\infty}^{\infty} dy[g_0(y) - (2\cosh y)^n] = -2T^2\int_{-\infty}^{\infty} dy[\psi_0(y) - \ln(2\cosh y)], \tag{92}$$

where we used that $[\Gamma(-n/2)]^2/\Gamma(-n) = -4/n + O(n^0)$.

As shown in Ref. 72, the functions $g_\ell(y)$ satisfy a recursion relation, the idea being as follows. Consider one of the n/u_ℓ equivalent groups of size u_ℓ, for instance, the first one

$a=1,\ldots,\mathsf{u}_\ell$. It contains $\frac{\mathsf{u}_\ell}{\mathsf{u}_{\ell+1}}$ subgroups of size $\mathsf{u}_{\ell+1}$.[70] The only coupling between the subgroups is through the matrix $\Delta q_\ell 1^n_{\mathsf{u}_\ell}$ with $\Delta q_\ell = q_\ell - q_{\ell-1}$,[73] which couples uniformly all spins in the group. They can be decoupled by a Hubbard-Stratonovich transformation, adding a term $z\sqrt{\Delta q_\ell}\Sigma_{a=1}^{\mathsf{u}_\ell}\tau_a$, where z is a Gaussian random field of variance Δq_ℓ, acting on all spins in the group. This allows us to perform configurational sums independently within each subgroup, and yields the recursion relation

$$g_\ell(y) = \langle g_{\ell+1}(y + z\sqrt{\Delta q_\ell})^{\mathsf{u}_\ell/(\mathsf{u}_{\ell+1})}\rangle_z, \tag{93}$$

where here and below $\langle\ldots\rangle_z := \int_{-\infty}^{\infty}\frac{dz}{2\pi}\ldots e^{-z^2/2}$ denotes the average over a unit Gaussian.

C. Continuous replica symmetry breaking: Second cumulant from an evolution equation

In the case of continuous RSB, we have to take the continuum limit $K\to\infty$ in the above: $\Delta\mathsf{u}_\ell = \mathsf{u}_{\ell+1} - \mathsf{u}_\ell \to 0$, $q(\mathsf{u}_\ell) \equiv q_\ell \to q(\mathsf{u})$, and $\Delta q_\ell \to 0$, while $\Delta q_\ell/\Delta\mathsf{u}_\ell \to dq(\mathsf{u})/d\mathsf{u}$. For the function $\psi(\mathsf{u}_\ell, y) \equiv \psi_\ell(y) \to \psi(\mathsf{u}, y)$, Eq. (93) yields a differential equation:

$$\partial_{\mathsf{u}}\psi = -\frac{1}{2}\frac{dq(\mathsf{u})}{d\mathsf{u}}[\partial_y^2\psi + \mathsf{u}(\partial_y\psi)^2], \tag{94}$$

with initial condition:

$$\psi(\mathsf{u}_c, y) = \psi(1, y) = \frac{\tilde{q} - q(1)}{2} + \ln[2\cosh(y)], \tag{95}$$

where we assume $q(\mathsf{u})$ to be constant for $\mathsf{u}_c < \mathsf{u} < 1$, as is generally the case [cf. Eq. (20)].

Equation (94) must be integrated from u_c to u_m, where $q(\mathsf{u})$ reaches its lower plateau $q_0 = q(\mathsf{u}_m)$. If $q_0 \neq 0$, the recursion (93) for $\ell = 0$ shows that we have to perform a last convolution to obtain

$$\psi(0, y) = \langle\psi(\mathsf{u}_m, y + z\sqrt{q(0)})\rangle_z. \tag{96}$$

The solution of Eq. (94) with initial condition (95) behaves at large $|y|$ like

$$\psi(\mathsf{u}, y) \overset{|y|\to\infty}{\approx} |y| + \frac{1}{2}\left(\tilde{q} - \left[\int_{\mathsf{u}}^{1} d\mathsf{u}' q(\mathsf{u}')\right] - \mathsf{u}q(\mathsf{u})\right), \tag{97}$$

as can be seen by substituting Eq. (97) into Eq. (94). This is also confirmed by noting that for $|y| \gg 1$, the sum in Eq. (86) is dominated by the configuration with all $\tau^a = \mathrm{sign}(y)$, which leads to the simple approximation (97) for $\psi(\mathsf{u}, y)$. This behavior implies $\psi(\mathsf{u}_m, y) \approx |y| + q^c = |y|$, since $q^c = 0$ from the condition $\hat{G}^c = 0$. Hence, the integral (92) converges, the subleading terms of ψ decaying exponentially at large $|y|$.

We can now state the main result of this section. In the regime $v^2 = O(1)$, the second cumulant *functional* can be obtained from the saddle point of the GVM as follows:

$$\hat{R}[v] - \hat{R}[0] = 2T^2\int_{-\infty}^{\infty} dy\, y[M(0, y) - \tanh(y)], \tag{98}$$

where the function $M(\mathsf{u}, y) = \partial_y\psi(\mathsf{u}, y)$ is the solution of

$$\partial_{\mathsf{u}}M = -\frac{1}{2}\frac{dq(\mathsf{u})}{d\mathsf{u}}(\partial_y^2 M + 2\mathsf{u}M\partial_y M), \tag{99}$$

$$M(\mathsf{u}_c, y) = \tanh(y), \tag{100}$$

in the interval $\mathsf{u} \in [\mathsf{u}_m, \mathsf{u}_c]$, and

$$M(0, y) = \langle M(\mathsf{u}_m, y + z\sqrt{q(0)})\rangle_z. \tag{101}$$

Equation (98) follows from Eq. (92) by integration by parts, using that $\lim_{y\to\pm\infty} y\{\psi(0, y) - \ln[2\cosh(y)]\} = 0$ as discussed above.

From the above and Eq. (87), we see that the dependence of the functional $\hat{R}[v]$ on the field v_x occurs only through the combination $q(\mathsf{u}) = \frac{1}{4T^2}\int_{xy} h(x-y, \mathsf{u}) v(x)\cdot v(y)$, where $h(k, \mathsf{u}) = g_k^{-2} G(k, \mathsf{u})$. Hence, for a uniform $v_x = v$, one easily sees that $q(\mathsf{u}) \sim L^d v^2$ and we can expect that Eq. (98) will assume a scaling form with scaling variable $vL^{d/2}$. This dependence on the system size is very different from the one in the regime $v^2 = O(N)$ and will be commented on further below.

The convolution (101) only results in an additive contribution to the potential correlator. This can be seen using the identity:

$$\int_{-\infty}^{\infty} dy\, y[\langle\Phi(y + \sqrt{Q}z)\rangle_z - \Phi(y)] = -\frac{Q}{2}[\Phi(\infty) - \Phi(-\infty)], \tag{102}$$

proven in Appendix C for functions Φ whose derivative decreases faster than $1/|y|$ at infinity. Applying Eq. (102) to $\Phi(y) = M(\mathsf{u}_m, y)$, we can rewrite Eq. (98) as

$$\hat{R}[v] - \hat{R}[0] = -\frac{1}{2}\int_k g_k^{-2} G(k, \mathsf{u}_m)|v_k|^2 + 2T^2\int_{-\infty}^{\infty} dy\, y[M(\mathsf{u}_m, y) - \tanh(y)]. \tag{103}$$

This result can also be derived via an alternative route, providing a useful check of the above formalism: In Eq. (86), we can directly separate out the contribution from the most distant states by writing $\hat{G}_{ab}(k) = \bar{G}_{ab}(k) + \hat{G}(k, 0)(1 - n\delta_{ab})$, with $\bar{G}^c(k) = 0$ and $\bar{G}(k, 0) = 0$. One can easily check that the piece $\hat{G}(k, 0)(1 - n\delta_{ab})$ produces the first term in Eq. (103). The remaining part leads to the same expression as Eq. (86), with the replacement $\hat{G} \to \bar{G}$. The only difference in the subsequent evaluation is that there is no need for a convolution in the end, since $\bar{G}^c(k) = 0$. This establishes Eq. (103).

Note that the first term in Eq. (103) has the expected form for the contribution from the plateau $0 \leq \mathsf{u} \leq \mathsf{u}_m$ [cf. Eqs. (44) and (48)], with a coefficient of $|v_k|^2$

$$-\frac{1}{2}g_k^{-2} G(k, \mathsf{u}_m) = -\frac{1}{2}T\sigma(\mathsf{u}_m) = \tilde{B}'(0), \tag{104}$$

independent of k. Clearly, this term is the only contribution in the case of a replica-symmetric solution. We now show that it also gives the dominant contribution at large v^2 of order $O(N^0)$, but $v^2 \gg L^{-d}$.

1. Limit of $L^d v^2 \gg 1$

In this case, Eq. (99) can be rewritten as

$$-\frac{1}{2}(M'' + 2\mathsf{u}M'M) = \frac{dM}{dq} \to 0 \tag{105}$$

since q is large (from now on, we denote ∂_y by a prime). One can integrate this equation to $M' + \mathsf{u}(M^2 - 1) = 0$, where the integration constant (with respect to y) is fixed by the fact that $M(\mathsf{u}_c, y) \to 1$ for large y, which cannot be changed by the evolution (99). The solution of Eq. (105) is then $M(\mathsf{u}, y) = \tanh(\mathsf{u}y)$. One can check that the flow of M is attracted to this simple "fixed point" as $\mathsf{u} \to \mathsf{u}_m$, if $v \gg v_*$, with v_* defined below. In that case, the second term in Eq. (103) becomes

$$2T^2 \int_{-\infty}^{\infty} dy y[\tanh(\mathsf{u}_m y) - \tanh(y)]$$
$$= 4T^2 \left(\frac{1}{\mathsf{u}_m^2} - 1 \right) \int_0^{\infty} dy y[\tanh(y) - 1], \tag{106}$$

and the large-v behavior of the second cumulant in this $v^2 = O(1)$ regime is, thus,

$$\hat{R}[0] - \hat{R}[v] \overset{v\to\infty}{\approx} \frac{T\sigma(\mathsf{u}_m)}{2} \int_x v_x^2 + \frac{\pi^2}{6} T^2 \left(\frac{1}{\mathsf{u}_m^2} - 1 \right). \tag{107}$$

The leading behavior is quadratic in v and corresponds to the contribution of the most distant states to the full (inverse) correlation. Hence, it should match the result obtained in the FRG for the regime $v^2 \sim N$ [cf. Eqs. (47) and (48) or, equivalently, Eqs. (77) and (78)]. Indeed, it does.

For a uniform $v_x = v$ and in the limit $T \to 0$, one finds for both models (8) and (9), using Eqs. (20) and (22),

$$\hat{R}[0] - \hat{R}[v] \overset{v\to\infty}{\approx} \frac{m^{2-\theta} v^2 L^d}{A(2-\theta)} + \frac{\pi^2}{6A^2} m^{-2\theta}. \tag{108}$$

This suggests a crossover around $v \sim v_*$ defined as

$$m^2 L^d v_*^2 = m^{-\theta} \leftrightarrow v_* = (mL)^{-d/2} m^{-\zeta}. \tag{109}$$

The physical meaning of this crossover scale will be discussed in more detail in the context of the models with one-step RSB below (cf. Sec. III E).

2. Perturbation expansion for $L^d v^2 \ll 1$

Since for $q(\mathsf{u}) = 0$, one has $M(\mathsf{u}, y) = \tanh(y) := m_0(y)$, there is a uniquely defined expansion in powers of q, which, since $q \sim v^2$, is equivalent to the direct expansion in powers of v^2 of Sec. III A:

$$M(\mathsf{u}, y) = m_0(y) + m_1(\mathsf{u}, y) + m_2(\mathsf{u}, y) + \cdots . \tag{110}$$

Each $m_n(\mathsf{u}, y)$ contains only terms of degree q^n. They satisfy the recursion

$$\dot{m}_n = -\frac{1}{2}\dot{q}(\mathsf{u}) \left[m''_{n-1} + \mathsf{u} \left(\sum_{p=0}^{n-1} m_p m_{n-p-1} \right)' \right], \tag{111}$$

where here and below dots denote ∂_{u}. The initial conditions are $m_n(\mathsf{u}_c, y) = 0$. The final result for $\hat{R}[v]$ is

$$\hat{R}[v] - \hat{R}[0] = -2T^2 q(0) + 2T^2 \sum_{n\geq 1} \int_{-\infty}^{\infty} dy\, y m_n(\mathsf{u}_m, y)$$
$$=: \sum_{n\geq 1} R_n[v], \tag{112}$$

where we recall that $4T^2 q(\mathsf{u}) = \int_k g_k^{-2} |v_k|^2 G(k, \mathsf{u})$. Hence, R_n contains all terms of degree $q^n \sim v^{2n}$, and we are, thus, effectively computing the derivatives at the origin, $\hat{R}^{(2n)}[v=0]$.

This calculation is performed in Appendix D, and the results are, indeed, consistent with the direct expansion of Sec. III A although the method is quite different. The lowest order term reads

$$R_1[v] = -2T^2 \int_0^1 q(\mathsf{u}) d\mathsf{u} = -\frac{1}{2} \int_k g_k^{-2} [\tilde{G}(k) - G^c(k)] |v_k|^2, \tag{113}$$

using that $\int_0^1 G(\mathsf{u}) = \tilde{G} - G^c$, recovering the results (62) and (69) which yield, at small v, the full result of Mézard-Parisi for the correlation function.

The next-order term is

$$R_2[v] = \frac{2}{3} T^2 \left(\int_0^1 d\mathsf{u}\, q^2(\mathsf{u}) - \left[\int_0^1 d\mathsf{u} q(\mathsf{u}) \right]^2 \right). \tag{114}$$

As discussed in Refs. 8, 22, 38, 48, and 49, the fourth derivative at zero of the FRG function $R^{(4)}[0]$ is a direct measure of susceptibility fluctuations. Indeed, we find that our present result has the general form of susceptibility fluctuations within a Parisi ansatz, defined and derived in Ref. 46.

3. Thermal boundary layer: General formula

It is possible to resum the derivatives, order by order in temperature, and derive the thermal boundary layer (TBL) form:

$$\hat{R}[v] - \hat{R}[0] = -\frac{1}{2} \int_k g_k^{-2} \tilde{G}_{T=0}(k) |v_k|^2 + T^3 \hat{r}_1[\hat{v}] + T^4 \hat{r}_2[\hat{v}]$$
$$+ \cdots , \tag{115}$$

where the first term is the "zero-temperature limit" of the leading small-v quadratic term,[74] and the higher-order terms in the expansion in T are scaling functions of the boundary-layer variable:

$$\hat{v}_k = v_k / T, \tag{116}$$

$$q(\mathsf{u}) = \frac{1}{4}\int_k g_k^{-2}|\hat{v}_k|^2 G(k,\mathsf{u}). \quad (117)$$

This structure, which appears already in the one-loop FRG, can be computed exactly in the large-N limit here.

This structure appears already in the one-loop FRG, where one finds that, at $T>0$, the nonanalyticity of $R[v]$ is thermally rounded.[22,31,32] Since temperature is irrelevant in the RG sense when $\theta>0$, this rounding occurs only in a layer determined by $vm^{\zeta}\sim Tm^{\theta}$, which becomes smaller and smaller as $T\to 0$, hence the name thermal boundary layer. Here, we compute its exact expression in the large-N limit.

We now perform an expansion (slightly more formal) which allows us to obtain Eq. (115). The idea, looking at Eq. (99), is that the nonlinear term contains an extra factor of u and that for $\mathsf{u}_m\leq\mathsf{u}\leq\mathsf{u}_c$ one has $\mathsf{u}\sim T$. Hence, it is natural to expand in the nonlinearity to generate a low-temperature expansion. Of course, this must be checked *a posteriori*. Further, we find it more convenient to use $q(\mathsf{u})$ instead of u to parametrize the ultrametric distance. Thus, rewriting Eq. (99) as $\partial_q M=-\frac{1}{2}[M''+\mathsf{u}(M^2)']$, and expanding $M=M_0+M_1+\cdots$, formally in powers of u, we have to solve the hierarchy:

$$\partial_q M_0 = -\frac{1}{2}M_0'', \quad (118)$$

$$\partial_q M_1 = -\frac{1}{2}(M_1''+2\mathsf{u}M_0M_0'), \quad (119)$$

$$\partial_q M_n = -\frac{1}{2}\left(M_n''+2\mathsf{u}\sum_{p=0}^{n-1}M_pM_{n-1-p}'\right). \quad (120)$$

Note that this hierarchy is formally similar to Eq. (111), apart from a shift in the index of the linear term on the right hand side (RHS), which indicates that we actually perform a different resummation.

The initial condition is $M_0(\mathsf{u}_c,y)=\tanh(y)$, $M_{n\geq 1}(\mathsf{u}_c,y)=0$. Again, primes stand for ∂_y. We define

$$\hat{R}[v]-\hat{R}[0]=\mathcal{R}_0[v]+\mathcal{R}_1[v]+\cdots, \quad (121)$$

$$\mathcal{R}_0[v] = -2T^2q(0)+2T^2\int_{-\infty}^{\infty}dy\, y[M_0(q(\mathsf{u}_m),y)-\tanh(y)], \quad (122)$$

$$\mathcal{R}_{n\geq 1}[v]=2T^2\int_{-\infty}^{\infty}dy\, yM_n(q(\mathsf{u}_m),y), \quad (123)$$

where we use the notation $\mathcal{R}_n$ to distinguish from the expansion in powers of q discussed in the previous section, and different from the $\hat{r}_i[v]$ defined in Eq. (115).

The equation for M_0 is a simple diffusion equation with solution

$$M_0(q(\mathsf{u}),y)=\langle\tanh(y+\sqrt{q(\mathsf{u}_c,\mathsf{u})}z)\rangle_z, \quad (124)$$

$$q(\mathsf{u}_c,\mathsf{u}) := q(\mathsf{u}_c)-q(\mathsf{u}). \quad (125)$$

Thanks to the identity (102), when $M_0(q(\mathsf{u}_m),y)$ from Eq. (124) is substituted into Eq. (122), we obtain

$$\mathcal{R}_0[v]=-2T^2q(\mathsf{u}_c), \quad (126)$$

whereby the terms proportional to $q(0)=q(\mathsf{u}_m)$ cancel. In the limit $T\to 0$, Eq. (126) becomes the same as the first term in Eq. (115), since

$$\tilde{G}(k)=G^c(k)+(1-\mathsf{u}_c)G(k,\mathsf{u}_c)+\int_0^{\mathsf{u}_c}d\mathsf{u}\,G(k,\mathsf{u})\overset{T\to 0}{\approx}G(k,\mathsf{u}_c). \quad (127)$$

Here, we used G^c, $\mathsf{u}_c\sim T$, and the fact that $G(k,\mathsf{u})$ has a finite limit as $T\to 0$.

To obtain the next-order term, $\mathcal{R}_1[v]$, we solve Eq. (119):

$$M_1(q,y)=-\int_q^{q(\mathsf{u}_c)}dq'\,dy'\mathcal{D}(q,y;q',y')\mathsf{u}(q')\times[(M_0M_0')(q',y')], \quad (128)$$

where

$$\mathcal{D}(q,y;q',y')=-\frac{\theta(q'-q)}{\sqrt{2\pi(q'-q)}}\exp\left[-\frac{(y-y')^2}{2(q'-q)}\right] \quad (129)$$

is the (reverse) diffusion kernel satisfying $(\partial_q+\frac{1}{2}\partial_y^2)\mathcal{D}=\delta(q-q')\delta(y-y')$, and $\mathsf{u}(q)$ is the inverse function of $q(\mathsf{u})$ for $\mathsf{u}_m<\mathsf{u}<\mathsf{u}_c$. Equation (128) can be rewritten as

$$M_1(q,y)=\int_q^{q(\mathsf{u}_c)}dq'\,\mathsf{u}(q')\langle(M_0M_0')(q',y+z\sqrt{q'-q})\rangle_z, \quad (130)$$

which when inserted into Eq. (123) gives

$$\mathcal{R}_1[v]=2T^2\int_{q(0)}^{q(\mathsf{u}_c)}dq'\,\mathsf{u}(q')\times\int_{-\infty}^{\infty}dy\,y\langle(M_0M_0')(q',y+z\sqrt{q'-q(0)})\rangle_z. \quad (131)$$

We can now use the identity (102) for $\Phi=M_0M_0'$, which has rapidly decreasing derivatives and satisfies $\Phi(\pm\infty)=0$. This yields

$$\mathcal{R}_1[v]=2T^2\int_{q(0)}^{q(\mathsf{u}_c)}dq\,\mathsf{u}(q)\int_{-\infty}^{\infty}dy\,y(M_0M_0')(q,y).$$

Integrating by parts over y and using the solution (124) for M_0, one finally obtains

$$\mathcal{R}_1[v] = T^2 \int_{q(0)}^{q(\mathsf{u}_c)} dq\, \mathsf{u}(q) \int_{-\infty}^{\infty} dy [1 - \langle \tanh(y + z_1 \sqrt{q(\mathsf{u}_c) - q}) \tanh(y + z_2 \sqrt{q(\mathsf{u}_c) - q}) \rangle_{z_1,z_2}]. \quad (132)$$

Note that we have used $(M_0^2 - 1)$ as primitive of $2M_0 M_0'$, since we need it to vanish for large argument. Using

$$\psi(a-b) := \int_{-\infty}^{\infty} dy [1 - \tanh(y+b)\tanh(y+a)] = 2(a-b)\coth(a-b), \quad (133)$$

we obtain the exact scaling functional for the thermal boundary layer:[75]

$$\mathcal{R}_1[v] = T^3 r_1[\hat{v}], \quad (134)$$

$$r_1[\hat{v}] = 2\int_{q_m}^{q_c} dq\, \hat{\mathsf{u}}(q) \langle z\sqrt{2(q_c - q)} \coth(z\sqrt{2(q_c-q)}) \rangle_z, \quad (135)$$

where

$$\hat{\mathsf{u}}(q) := \frac{\mathsf{u}(q)}{T} \quad (136)$$

has a finite limit as $T \to 0$, where we introduced the definitions

$$q_c := q(\mathsf{u}_c) = q(1) = \frac{1}{4}\int_k g_k^{-2} |\hat{v}_k|^2 G(k, \mathsf{u}_c), \quad (137)$$

$$q_m := q(\mathsf{u}_m) = q(0) = \frac{T\sigma(0)}{4}\int_k |\hat{v}_k|^2, \quad (138)$$

$$\tilde{q} = \frac{1}{4}\int_k g_k^{-2} |\hat{v}_k|^2 \tilde{G}(k). \quad (139)$$

4. Thermal boundary layer: Uniform v and scaling function for m→0

Let us consider here a uniform $v_x = v$ for which one has

$$q(\mathsf{u}) = \frac{m^4 \hat{v}^2 L^d}{4} G(k=0, \mathsf{u}). \quad (140)$$

Here and below, we define

$$G(\hat{\mathsf{u}}) = G(k=0, \mathsf{u} = T\hat{\mathsf{u}}). \quad (141)$$

One can rewrite $r_1[\hat{v}] \equiv L^d r_1(\hat{v})$ with

$$r_1[\hat{v}] = \frac{m^4 \hat{v}^2 L^d}{2} \int_{G_m}^{G_c} dG\, \hat{\mathsf{u}}(G) \left\langle z \frac{m^2 |\hat{v}| L^{d/2}}{2} \sqrt{2(G_c - G)} \times \coth\left[z \frac{m^2 |\hat{v}| L^{d/2}}{2} \sqrt{2(G_c - G)} \right] \right\rangle_z, \quad (142)$$

where here we denote $G_m := G(\mathsf{u}_m)$ and $G_c := G(\mathsf{u}_c)$ (not to be confused with the connected correlator G^c). Let us now specify to models (23) and (24). One finds

$$G(\hat{\mathsf{u}}) = \frac{8}{A(4-\theta^2)} \frac{1}{m^{2+\theta}} - \frac{2}{2+\theta} \frac{A^{2/\theta}}{\hat{u}^{1+2/\theta}}, \quad (143)$$

where A was given in Eq. (23). Hence,

$$\hat{\mathsf{u}}(G) = \frac{A m^\theta (4 - 2\theta)^{\theta/(2+\theta)}}{[8 - (4-\theta^2) A m^{2+\theta} G]^{\theta/(2+\theta)}}, \quad (144)$$

with $\hat{\mathsf{u}}_c = A m_c^\theta$, $A m^{2+\theta} G_m = \frac{2}{2-\theta}$, and $A m^{2+\theta} G_c = \frac{8}{4-\theta^2} - \frac{2}{2+\theta}\left(\frac{m}{m_c}\right)^{2+\theta}$. Using Eq. (144), we obtain the TBL function as a double integral in Eq. (142). In the limit $m \ll m_c$, this simplifies to

$$r_1[\hat{v}] = m^2 \hat{v}^2 L^d H_\theta\left(\frac{1}{\sqrt{2A}} \frac{\hat{v}}{v_* m^\theta} \right),$$

$$H_\theta(x) = \frac{1}{2}\left(\frac{2}{2+\theta}\right)^{\theta/(2+\theta)} \int_0^{2/(2+\theta)} \frac{dt}{t^{\theta/(2+\theta)}} \langle zx\sqrt{t} \coth(zx\sqrt{t}) \rangle_z, \quad (145)$$

where $v_* = L^{-d/2} m^{-1-\left(\frac{\theta}{2}\right)}$ is the scale obtained in Eq. (109). Further, from Eq. (23), A depends only on d and γ. The scaling function H_θ depends only on θ, while the argument is scaled by the characteristic displacement v_* multiplied by the scaled temperature Tm^θ. This indicates that the scaling function of the thermal boundary layer exhibits universality for $\theta > 0$ since only scales of order $1/m$ contribute to the final scaling function, all features of $q(\mathsf{u})$ with $\mathsf{u} \gg \mathsf{u}_m$ being subdominant.

5. Nonanalytic cusp from the T→0 limit of the thermal boundary layer

The TBL functional (134) exhibits a non-trivial large-argument limit, $\hat{v} = v/T \to \infty$ (or, equivalently, $q_c \to \infty$):

$$r_1[\hat{v}] \approx \frac{4}{\sqrt{\pi}} \int_{q_m}^{q_c} dq\, \hat{\mathsf{u}}(q) \sqrt{q_c - q}, \quad (146)$$

using that $\langle |z| \rangle_z = \sqrt{2/\pi}$. This limit must match the $T=0$ limit of the functional $R[v]$, denoted $R_{T=0}[v]$. More precisely, as we will show in the next section, r_1 must match the cubic term $\sim v^3$ of $R_{T=0}[v]$, i.e., the cusp nonanalyticity.

We now perform an explicit calculation for a uniform $v_x = v$. From Eq. (142), one finds in the limit of large $\hat{v} L^{d/2}$:

$$L^d \mathcal{R}_1(v) = \mathcal{R}_1[v] \approx \rho (m^4 v^2 L^d / 4)^{3/2}, \quad (147)$$

$$\rho = \frac{4}{\sqrt{\pi}} \int_{G_m}^{G_c} dG\, \hat{\mathsf{u}}(G) \sqrt{G(\mathsf{u}_c) - G}, \tag{148}$$

which produces a cusp nonanalyticity at zero temperature. The coefficient ρ can be computed explicitly for models (23) and (24) using Eqs. (143) and (144), and one finds

$$\rho = \frac{16}{3}\sqrt{\frac{2}{\pi A}} m_c^{\theta} \left(\frac{m^{-2-\theta} - m_c^{-2-\theta}}{2+\theta} \right)^{3/2} {}_2F_1\left[\frac{3}{2}, \frac{\theta}{2+\theta}, \frac{5}{2}, 1 - \left(\frac{m_c}{m} \right)^{2+\theta} \right]. \tag{149}$$

One can check that in the limit $m \ll m_c$, one has $\rho \sim m^{-(3+\theta/2)}$ and that the prefactor agrees, using Eq. (147), with the one obtained from the large-$\hat{v}$ limit of Eq. (145). We have, thus, obtained the exact leading nonanalyticity at zero temperature: it consists in a linear cusp in the force correlator, $-N^{-1}\Sigma_i \partial_{v_i}^2 R[v] \sim |v|$. This nonanalyticity is of the same kind (i.e., proportional to $|v|$) as the one found in the standard FRG (e.g., to one loop for any N) and in the large-N FRG in the regime $v^2 \sim N$, which will be discussed in detail in the next section. However, there are differences in the dependence of the amplitude of the cusp on m, L, and N. Anticipating the results of Sec. IV, they can be summarized as follows. In the regime $m \ll m_c$, one finds

$$\begin{aligned}
\hat{R}_{T=0}[v] - \hat{R}_{T=0}[0] &= L^d[\hat{R}_{T=0}(v) - \hat{R}_{T=0}(v)] \\
&= \frac{C_1}{m^{2\theta}} \left(\frac{v}{v_*} \right)^2 \left[1 - b\frac{|v|}{v_*} + O\left(\frac{v^2}{v_*^2} \right) \right], \\
v^2 &= O\left(\frac{N^0}{L^{d/2}} \right), \\
&= \frac{C_N}{m^{2\theta}} \left(\frac{v}{v_*} \right)^2 \left[1 - a\frac{|v|}{v_c} + O\left(\frac{v^2}{v_c^2} \right) \right], \\
v^2 &= O(NL^0),
\end{aligned} \tag{150}$$

where a, b, as well as C_1, C_N are numerical prefactors (with $C_1/C_N = G_c/G_m > 1$). Note that the two scales $v_* = (mL)^{-d/2} m^{-\zeta}$ and $v_c = \sqrt{N} m^{-\zeta}$ are very different. The nonanalytic corrections in the regime $v^2 = O(L^{-d/2} N^0)$ are related to the occurrence of shocks in the system, as the quadratic well is moved. Their contribution starts dominating once $v > v_*$.

From Eq. (149), one finds that the amplitude of the cusp is zero at the Larkin mass m_c, and then grows linearly as a function of $m_c - m$. This is in contrast to the large-v regime, where the amplitude jumps to a finite value at m_c [cf. Eq. (265) below].

Let us finally point out that a cusp nonanalyticity proportional to $|v|$ in the regime $v^2 = O(L^{-d/2} N^0)$ was found in Ref. 47, but with an amplitude scaling differently with m. This resulted from a calculation of a rather different observable which is reviewed in Appendix E. A closely related cusp singularity was also found in the study of shocks in Burger's turbulence.[71] (For a recent discussion of their relation to FRG, see Ref. 48.)

It is important to note that the nonanalyticity found here at $T=0$ in the regime $v = O(1)$ is a robust feature that occurs irrespective of the type of the ultrametric RSB scheme (whether continuous or one-step, marginally or fully stable). As will be discussed below, it reflects the switches in the minimum energy, and shocklike jumps in position, which occur as the energies of two states cross upon moving the harmonic well. It is, not surprisingly, rounded by temperature. In that sense, it has some similarities with shocks discussed for interfaces $N=1$ and for Burger's turbulence. In contrast, in Sec. IV, the cusp in the regime $v^2 = O(N)$ will be seen to rely on the marginality of the RSB scheme with respect to clustering fluctuations on the largest scales. That type of marginality only occurs naturally for systems exhibiting continuous RSB. As we will see, in that case, a cusp occurs even at finite T, in contrast to the above discussed nonanalyticity which forms only in the limit $T=0$. As we will discuss later, it is related to a more global transformation of the set of states as v is varied.

6. $T \to 0$ limit of $R[v]$

The above described perturbation expansion is also perfectly suited to analyze the limit $T=0$, where it turns into a rigorous expansion in $|v|$. A similar expansion was pointed out in Ref. 47. To exhibit the dependence on T and v, we define $q = v^2 L^d \gamma / T^2$ by introducing the reduced coupling function:

$$\gamma(\hat{\mathsf{u}}) = \frac{1}{4} \int_k g_k^{-2} \left[\frac{|v_k|^2}{v^2 L^d} G(k, \mathsf{u} = T\hat{\mathsf{u}}) \right], \tag{151}$$

where in this section we denote by v^2 a suitable average of v_k, such as $v^2 L^d = \int_x v_x^2 = \int_k v_k^2$, such that $v_k / |v| L^{d/2}$ is just a form factor. As mentioned before, $\gamma(\hat{\mathsf{u}})$ and its inverse $\hat{\mathsf{u}}(\gamma)$ have finite $T=0$ limits, taking values between $\gamma(\hat{\mathsf{u}}_{c,m}) = \gamma_{c,m}$ and $\hat{\mathsf{u}}_{c,m}$, respectively. After rescaling $y \equiv |v| L^{d/2} \hat{y} / T$, the evolution equation (99) for $M(q,y) \equiv \hat{M}(\gamma, \hat{y})$ becomes

$$\partial_\gamma \hat{M} = -\frac{1}{2} [\partial_{\hat{y}}^2 \hat{M} + |v| L^{d/2} \hat{\mathsf{u}}(\gamma) \partial_{\hat{y}} (\hat{M}^2)], \tag{152}$$

$$\hat{M}(\hat{\mathsf{u}}_c, \hat{y}) = \tanh\left(\frac{L^{d/2}|v|\hat{y}}{T} \right) \overset{T\to 0}{\to} \mathrm{sign}(\hat{y}), \tag{153}$$

and the second cumulant takes the form

$$\hat{R}[v] - \hat{R}[0] \overset{T=0}{=} -\frac{1}{2} \int_k g_k^{-2} G_{T=0}(k, \hat{\mathsf{u}}_m) |v_k|^2 + 2v^2 L^d \int_{-\infty}^{\infty} d\hat{y}\, \hat{y} [\hat{M}(\hat{\mathsf{u}}_m, \hat{y}) - \mathrm{sign}(\hat{y})]. \tag{154}$$

From Eq. (152), it is easy to see that the above described procedure corresponds to a power series expansion in $|v|$, the term corresponding to $\mathcal{R}_n^{T=0}[v]$ being proportional to $|v|^{2+n}$. We will show below that in the case of a one-step RSB, the zero-temperature correlator can be obtained in closed form.

7. Comparison with the thermal boundary layer from droplet arguments

It is interesting to note certain analogies with formulas obtained from droplet arguments, where one assumes rare quasidegeneracies of the ground state. In $d=0$, it was found in Refs. 48 and 49 that

$$\hat{R}''_{ij}(v) \coloneqq \partial^2_{v^i v^j}\hat{R}(v) = \hat{R}''_{ij}(0) + m^4 T\left\langle y^i y^j F\left(m^2 y \cdot \frac{v}{T}\right)\right\rangle_y + O(T^2), \quad (155)$$

$$F(z) = \frac{z}{4}\coth\left(\frac{z}{2}\right) - \frac{1}{2} = \frac{1}{4}\left[\psi\left(\frac{z}{2}\right) - 2\right], \quad (156)$$

where $y \equiv u^{21} = u^2 - u^1$ is the difference between the center-of-mass displacement of the ground state (u^1) and of the excitation (u^2). They are characterized by a (unnormalized) distribution $D(y) = P(y, E=0)$, where $P(y,E)dydE$ is the (normalized) joint distribution of position and energy differences between the two states. Here, we denote $\langle \ldots \rangle_y \coloneqq \int dy \ldots D(y)$, which can be normalized using the STS identity $\langle y_i y_j \rangle_y = 2\delta_{ij}/m^2$. In some simple cases (e.g., the Sinai model, corresponding to $N=1$ with random-field disorder), $D(y)$ is known analytically. The above formula can be generalized[48,49] to any d:

$$\hat{R}[v] = \frac{1}{2}\int_{xy} \left.\frac{\delta \hat{R}[v]}{\delta v_x^i \delta v_y^j}\right|_{v=0} v_x^i v_y^j + T^3\left\langle \mathcal{F}\left(\int_{xx'} g^{-1}_{xx'} v_x \cdot u^{12}_{x'}/T\right)\right\rangle_{u^{12}}, \quad (157)$$

with $\mathcal{F}''(z) = F(z)$, and a formula for all cumulants was also obtained.

Given the similarities between the formulas (155) and (134), it is tempting to interpret the latter in terms of a droplet size density, summed over all ultrametric distances u. To this end, we rewrite Eq. (134) for uniform $\hat{v} = v/T$ as

$$L^d \mathcal{R}_1(v) = \hat{v}^2 T^3 \int_{\hat{q}_m}^{\hat{q}_c} d\hat{q}\, \hat{\mathsf{u}}(\hat{q}) \langle \psi(|\hat{v}|\sqrt{2(\hat{q}_c - \hat{q})}z)\rangle_z, \quad (158)$$

where we note that $\hat{q}(\hat{\mathsf{u}}) \coloneqq q(\hat{\mathsf{u}})/\hat{v}^2$ and its inverse function are independent of $\hat{v}$.

As shown in Appendix F, the force correlator splits into a longitudinal and a transverse part, describing forces parallel and orthogonal to the displacement vector $\vec{v}$. Note that due to the $O(N)$ symmetry, the correlator is only a function of $|v|$. The TBL contribution to the force correlators is $L^d \Delta_L^{(1)}(v) = -L^d \mathcal{R}_1''(|v|)$ and $L^d \Delta_T^{(1)}(v) = -L^d \mathcal{R}_1'(|v|)/|v|$, respectively. They can be cast in the form (for details, see Appendix F)

$$-L^d \Delta^{(1)}_{L,T}(v) = T\int_0^\infty db\, \rho^{\mathrm{RSB}}_{L,T}(b)\psi(b|\hat{v}|), \quad (159)$$

with the densities

$$\rho^{\mathrm{RSB}}_L(b) = \int_{\hat{q}_m}^{\hat{q}_c} d\hat{q}\, \hat{\mathsf{u}}(\hat{q}) \langle (z^4 - z^2)\delta(b - z\sqrt{2(\hat{q}_c - \hat{q})})\rangle_z, \quad (160)$$

$$\rho^{\mathrm{RSB}}_T(b) = \int_{\hat{q}_m}^{\hat{q}_c} d\hat{q}\, \hat{\mathsf{u}}(\hat{q}) \langle (1 + z^2)\delta(b - z\sqrt{2(\hat{q}_c - \hat{q})})\rangle_z. \quad (161)$$

This has precisely the same form as the droplet expressions for the force correlators, which from Eq. (155) are found as

$$-\Delta^{\mathrm{drop}}_{L,T}(v) = \hat{R}''(0) - m^2 T + T\int_0^\infty db\, \rho^{\mathrm{drop}}_{L,T}(b)\psi(b|\hat{v}|) + O(T^2), \quad (162)$$

where $R''(0) \equiv \partial^2_{v_i} R(v=0)$ (for any fixed i), and the densities $\rho^{\mathrm{drop}}_{L,T}(b)$ are given in Eq. (F5). Note also that formulas (132) and (133), and the appearance of the function ψ, bear similarities to expressions obtained in the case $N=1$ for averages over a uniform density of shocks rounded by temperature.[48,49]

In order to go further in the comparison and extract observables such as shock and droplet density and their size distribution, a more detailed description of higher moments is needed for the present model. Work in this direction is in progress.

D. Case of one-step replica symmetry breaking ($d \leq 2$, $\gamma \geq \gamma_c$)

As mentioned before, the GVM saddle point for a one-step situation is characterized by the "breakpoint" u_c [$\equiv \mathsf{u}_1$ in the notation of Eq. (89)] and the two self-energy parameters $\sigma_{0,1}$ (26). Similarly, the correlation function $G(k,\mathsf{u})$ and the coupling $q(\mathsf{u})$ assume only two off-diagonal values $G_{0,1}$ and $q_{0,1}$. The former has the following interpretation: The measure on configuration space describing fluctuations both due to disorder and thermal noise can be constructed independently for each mode k, following Ref. 46.

For the displacement in each environment, one picks a set of "state centers" u_k^α as[76]

$$u_k^\alpha = u_k^0 + \sqrt{G_1(k) - G_0(k)}\,\xi_k^\alpha, \quad (163)$$

$$u_k^0 = \sqrt{G_0(k)}\,\xi_k^0, \quad (164)$$

where the ξ_k^0 and ξ_k^α are chosen from independent univariate Gaussian distributions. Note that in a given environment, the (infinite) set of u_k^α is globally displaced by the same (random) u_k^0. Each state corresponds to a partial Gibbs measure which is assigned a weight W_α (with $\sum_\alpha W_\alpha = 1$), such that the total Gibbs measure in this environment is the weighted superposition of the partial Gibbs measures, i.e., in one thermal realization, one picks a state α with probability W_α and the mode u_k takes the value

$$u_k = u_k^\alpha + \sqrt{\tilde{G}(k) - G_1(k)}\,\eta_k^\alpha, \quad (165)$$

where η_k^α are chosen from independent univariate Gaussian distributions and account for thermal noise inside a given state. In each environment, the weights W_α are independent random variables chosen from the distribution $P(W) \sim_{W\to\infty} W^{-(1+\mathsf{u}_c)}$, the glass transition corresponding to the divergence of its first moment at large W, which implies that only a few states dominate the total Gibbs measure.[77] An analogous construction applies in the case of continuous RSB, where the obvious generalization of the above to K-step RSB has to be taken to the limit $K\to\infty$.

With a general one-step ansatz of the form (14), we obtain the correlation functions:

$$G_0(k) = T\sigma_0 g_k^2, \tag{166}$$

$$G_1(k) = T\sigma_0 g_k^2 + \frac{T}{\mathsf{u}_c}\left(g_k - \frac{1}{g_k^{-1}+\Sigma_1}\right), \tag{167}$$

where $\Sigma_1 := [\sigma](\mathsf{u}_c) = \mathsf{u}_c(\sigma_1-\sigma_0)$. As always, on the saddle point, STS implies $G^c(k)=Tg_k$, and we note

$$\tilde{G}(k) = G^c(k) + \mathsf{u}_c G_0(k) + (1-\mathsf{u}_c)G_1(k). \tag{168}$$

With such a one-step ansatz, the GVM free-energy density takes the form[46]

$$\phi(\mathsf{u}_c) \equiv \frac{\mathcal{F}(\mathsf{u}_c)}{NL^d} = f_0 - \frac{1}{2T}\sum_b B\left(2\int_k \tilde{G}(k) - G_{ab}(k)\right) + \frac{1}{2}\int_k\left[g_k^{-1}\tilde{G}(k) - \frac{T}{n}\,\mathrm{Tr}\log G(k)\right] \tag{169a}$$

$$= \tilde{f}_0 + \frac{1}{2T}[\mathsf{u}_c B(\chi_0) + (1-\mathsf{u}_c)B(\chi_1)] + \frac{T}{2}\frac{1-\mathsf{u}_c}{\mathsf{u}_c}\int_k\left[\frac{\Sigma_1}{k^2+m^2+\Sigma_1} - \ln\left(\frac{k^2+m^2+\Sigma_1}{k^2+m^2}\right)\right], \tag{169b}$$

where we denote the square of transverse intra- or interstate fluctuations as

$$\chi_{0,1} = 2\int_k [\tilde{G}(k) - G_{0,1}(k)], \tag{170}$$

and we have absorbed quantities that depend only on T and m, but not on u_c and Σ_1, into the constants f_0 and $\tilde{f}_0$. The free-energy density (169a) is minimized with respect to G by the saddle point satisfying $\delta\mathcal{F}/\delta G_{ab}=0$ [Eq. (15)], taking the one-step form

$$\sigma_{0,1} = -\frac{2}{T}B'(\chi_{0,1}). \tag{171}$$

In order to describe equilibrium thermodynamics, the breakpoint u_c has to be chosen so as to extremize (*maximize*) $\mathcal{F}$, as usual in replica treatments. However, other choices of u_c are of physical interest as well, as discussed in detail below.

1. Instability of the replica-symmetric solution

Let us derive the phase diagram in the one-step case. For simplicity, we restrict to $d<2$ and $\Lambda/m_c=\infty$. We recall that we use the natural units introduced in Sec. II. Performing the integrals, the free-energy density reads (dropping the constant $\tilde{f}$)

$$\phi(\mathsf{u}_c) \equiv \frac{\mathcal{F}(\mathsf{u}_c)}{NL^d} = \frac{1}{2T}[\mathsf{u}_c B(\chi_0) + (1-\mathsf{u}_c)B(\chi_1)] + \frac{A_d T}{\epsilon(2-d)}\frac{1-\mathsf{u}_c}{\mathsf{u}_c}\left\{\frac{\Sigma_1}{(m^2+\Sigma_1)^{(2-d)/2}} - \frac{2}{d}[(m^2+\Sigma_1)^{d/2} - m^d]\right\}, \tag{172}$$

where we have used

$$\int_q \frac{1}{1+q^2} = \frac{\Gamma(1-d/2)}{(4\pi)^{d/2}} = \frac{2A_d}{\epsilon(2-d)}. \tag{173}$$

In $d=0$ (a particle), the last line of Eq. (172) becomes $-2\ln(1+\Sigma_1/m^2)$. In $\phi(\mathsf{u}_c)$ above, Σ_1 and u_c can be considered as two independent variational parameters. The variation with respect to Σ_1 (at fixed u_c) yields back the saddle-point equation:

$$\Sigma_1 = -\frac{2\mathsf{u}_c}{T}[B'(\chi_1) - B'(\chi_0)], \tag{174}$$

where from Eq. (170) one has

$$\chi_0 = \frac{4A_d}{\epsilon(2-d)}\frac{T}{\mathsf{u}_c}\left[\frac{1}{m^{2-d}} - \frac{1-\mathsf{u}_c}{(m^2+\Sigma_1)^{1-d/2}}\right],$$

$$\chi_1 = \frac{4A_d}{\epsilon(2-d)}\frac{T}{(m^2+\Sigma_1)^{1-d/2}}. \tag{175}$$

The replica-symmetric solution ($\mathsf{u}_c=1$, $\chi_1=\chi_0=\chi^{\mathrm{RS}}$, and $\Sigma_1=0$) is valid at high temperature and/or large mass, but becomes unstable when the condition

$$\frac{4A_d}{\epsilon m^\epsilon}B''(\chi^{\mathrm{RS}}[m,T_c]) = 1 \tag{176}$$

is met, with $\chi^{\mathrm{RS}} = \frac{4A_d}{\epsilon(2-d)}Tm^{d-2}$. This defines a unique function $T_c(m)$ for masses $m \le m_c$ smaller than the zero-temperature critical mass:[78]

$$m_c = m_c(T=0) = \left[\frac{4A_d}{\epsilon}B''(0)\right]^{1/\epsilon}. \tag{177}$$

The function $T_c(m)$ describes the location of a continuous glass transition toward a one-step RSB phase for $m_c \ge m \ge m_*$. Here, m_* denotes the mass where $T_c(m)$ attains its maximum. For $m<m_*$, the line $T_c(m)$ has little physical significance, since in that regime the glass transition occurs in a discontinuous manner at $T>T_c(m)$, as will be discussed below.

It is interesting to note[46] from Eqs. (163)–(165), using Eqs. (166)–(168), that as $m\to 0$ the thermal fluctuations of the displacement field u within a state, $\tilde{G}-G_1=T/(k^2+m^2+\Sigma_1)$, remain bounded and massive, and occur only at the Larkin scale.

By contrast, the rms difference in displacement between two states in a given sample, $u^{\alpha}-u^{\alpha'}$, scales as $G_1-G_0=\frac{T}{\mathsf{u}_c}\Big[\frac{1}{k^2+m^2}-\frac{1}{k^2+m^2+\Sigma_1}\Big]$. Hence, the thermal fluctuations between states, which are active at any $T>0$ in a given sample, occur at all scales up to $1/m$. Note that these rms differences in displacement have a finite $T=0^+$ limit if T/u_c goes to a constant in that limit (which is generally the case as shown below). These fluctuations are responsible for the roughness of the manifold $\zeta=(2-d)/2$ with a nonzero amplitude even as $T\to 0$.

Finally, sample-to-sample fluctuations include, in addition, the term $G_0\sim T\sigma_0/(k^2+m^2)^2$, whose mass dependence is controlled by σ_0. These fluctuations also occur at all scales smaller than $1/m$.

2. Metastable states and configurational entropy

The breakpoint $0<\mathsf{u}_c<1$ is *a priori* a free parameter of the one-step ansatz. In order to describe the thermodynamic equilibrium, one should choose $\mathsf{u}_c=\mathsf{u}_c^{\mathrm{eq}}$, which extremizes the free energy:

$$\frac{d\phi}{d\mathsf{u}_c}(\mathsf{u}_c^{\mathrm{eq}})=0 \quad \text{(equilibrium)} \tag{178}$$

(at fixed Σ_1) as was done in Ref. 46. As in most glassy problems with a one-step structure, at low temperatures $T\ll T_c$ the equilibrium breakpoint is proportional to the temperature[79] $\mathsf{u}_c^{\mathrm{eq}}\approx T\omega^{\mathrm{eq}}$. This is shown in Appendix G, where ω^{eq} is computed as well.

However, the function $\phi(\mathsf{u}_c)$ encodes much more information than just the equilibrium physics. It can be interpreted[80] as the quenched "replicated free energy," i.e., the free-energy density per replica of a set of u_c clones (replica) which are bound to remain in the same metastable state of the energy landscape. With this interpretation, one can alternatively write the total free energy as a sum over states. Their number $\mathcal{N}(f)$ at fixed free-energy density f increases exponentially with the volume and N. One, thus, introduces the configurational entropy, or complexity, $\Sigma(f)=\log[\mathcal{N}(f)]/NL^d$. The total Boltzmann weight of u_c clones can then be written as

$$\exp[-NL^d\beta\mathsf{u}_c\phi(\mathsf{u}_c)]\approx\int df\,\exp\{-NL^d[\beta\mathsf{u}_c f-\Sigma(f)]\}, \tag{179}$$

where $\beta=1/T$. In the large-N limit, the configurational entropy becomes the Legendre transform of the replicated free energy:

$$\beta\mathsf{u}_c\phi(\mathsf{u}_c)=\beta\mathsf{u}_c f-\Sigma(f),\quad \Sigma'(f)=\beta\mathsf{u}_c. \tag{180}$$

Knowing $\phi(\mathsf{u}_c)$, one easily obtains an implicit parametrization of the configurational entropy as a function of the free-energy density:

$$f=\frac{d[\mathsf{u}_c\phi(\mathsf{u}_c)]}{d\mathsf{u}_c}=\phi(\mathsf{u}_c)+\mathsf{u}_c\phi'(\mathsf{u}_c), \tag{181}$$

$$\Sigma=\beta\mathsf{u}_c^2\phi'(\mathsf{u}_c). \tag{182}$$

We see, in particular, that the equilibrium prescription (178) corresponds to choosing the states with vanishing configurational entropy. Since the configurational entropy is an increasing function of f, the so selected states have the lowest free-energy density in typical samples and, thus, describe indeed the quenched equilibrium free energy.

However, the equilibrium may not be possible to reach dynamically, which suggests a different choice for u_c. The choice is constrained by the requirement that the one-step solution be stable (as was the case for $\mathsf{u}_c=\mathsf{u}_c^{\mathrm{eq}}$).

Metastable states of the free-energy density above the equilibrium value f^{eq} are described by breakpoints in the range $\mathsf{u}_c^{\mathrm{th}}<\mathsf{u}_c<\mathsf{u}_c^{\mathrm{eq}}$, where the lower boundary is determined by the so-called replicon instability of the one-step scheme, i.e., the condition[81]

$$\frac{4A_d}{\epsilon(m^2+\Sigma_1)^{\epsilon/2}}B''(\chi_1)=1 \quad \text{(threshold)}. \tag{183}$$

A comparison with Eq. (178) shows that at fixed temperature $T<T_c(m_*)$, this implies $m^2+\Sigma_1=m_c^2(T)$, where $m_c(T)>m_*$ is uniquely defined as the solution of $T_c(m_c(T))=T$. One can prove that solutions of the one-step saddle-point equations with condition (183) exist for all $T<T_c(m_*)$ and $m<m_c(T)$ (but nowhere outside this parameter regime).[82] The states described by $\mathsf{u}_c^{\mathrm{th}}$ are merely marginally stable and are often referred to as "threshold states." Since they are usually the most abundant metastable states of the system, they are most likely to trap the dynamics after a fast temperature quench for $m<m_*$.

Another choice for u_c of interest is the value $\mathsf{u}_c=\mathsf{u}_c^{\mathrm{cp}}>\mathsf{u}_c^{\mathrm{eq}}$, where the one-step scheme becomes unstable with respect to a clustering fluctuation among the existing states.[81] The latter is equivalent to the condition

$$\frac{4A_d}{\epsilon m^{\epsilon}}B''(\chi_0)=1 \quad \text{(cusp for FRG at large } v). \tag{184}$$

This condition ensures that the second cumulant in the regime $v^2\sim N$ is nonanalytic at $v=0$, as we will discuss in Sec. IV B 4.

We emphasize that the kind of marginal stability imposed by Eq. (184) is clearly distinct from the marginality (183) due to the replicon mode, which is usually imposed to select dynamical threshold states in one-step systems.[83] The latter is also the marginality property of continuous RSB systems that ensures the presence of collective soft modes in classical[84] and quantum mean-field spin, elastic, or electron glasses,[85–88] and leads to a universal, saturated pseudogap in the local field distribution of spin and electron glasses.[89–91]

While the replicon instability (183) indicates the fragility toward fragmentation of existing states into substates, the condition (184) signals the instability toward the formation of clusters among previously equivalent states. When m

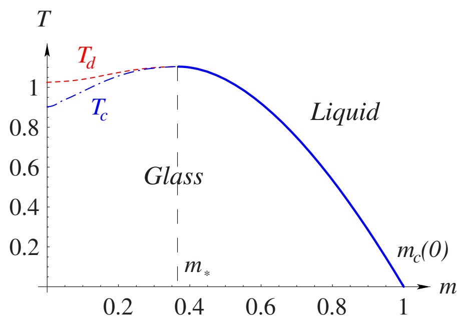

FIG. 4. (Color online) The breakpoint u_c as a function of m at constant temperature $T=0.8$ in the glass phase $[m<m_c(T)=0.673]$ for model (23) in $d=1$. The labels cp, eq, and th indicate threshold, equilibrium, and cusp states. Notice that u^{cp} exceeds 1 at small enough m. The same would be true for u^{eq} and u^{th} for $T^{\max}>T>T_c(0)$ and $T^{\max}>T>T_d(0)$, respectively.

$\leqslant m_c$, these two instabilities involve rather different length scales. This can be seen as follows: The replicon instability corresponds to each state u_k^α in Eq. (163), giving birth to a new cluster of substates labeled by β, $u_k^\alpha \to u_k^{\alpha,\beta}=u_k^\alpha+\delta u_k^\beta$, where each δu_k^β occurs with a probability W'_β (with $\Sigma_\beta W'_\beta=1$). This rearrangment implied by the additional substructure involves scales of order $1/m_c$ since $dG(\mathsf{u}) = T\, d\sigma(\mathsf{u})/(g_k^{-1}+[\sigma](\mathsf{u}))^2$ with $[\sigma](\mathsf{u}\geqslant \mathsf{u}_c)=\Sigma_1 \sim m_c^2$. On the contrary, Eq. (184) signals the instability toward u_k^0 splitting into several clusters $u_k^0 \to u_k^0+\delta u_k^\beta$, generating substates $u_k^{\beta,\alpha}$. This rearranges the original u_k^α into clusters labeled by β, and obviously involves scales up to $1/m$.

The above two kinds of instabilities have been analyzed in detail in the context of the spherical p-spin model in Ref. 92. More recently, they have been discussed in the context of lattice-glass models[93] and optimization problems,[94–96] where they are sometimes referred to as instabilities of the first (clustering) and second (fragmentation) kind.[97] They also appear as the instabilities driving the transitions between the two types of one-step phases adjacent to an intermediate two-step RSB phase in certain mixed spherical spin models.[98]

For model (23) in $d=1$, i.e., the directed polymer problem, we have checked explicitly that $\mathsf{u}_c^{\text{th}}<\mathsf{u}_c^{\text{eq}}<\mathsf{u}_c^{\text{cp}}$, and we expect this to be generally true for one-step solutions. This is illustrated in Fig. 5. For the associated configurational entropies, this implies $\Sigma^{\text{th}}>\Sigma^{\text{eq}}=0>\Sigma^{\text{cp}}$, and thus, the states selected by the clustering instability (184) have negative configurational entropy. Anticipating the analysis of Sec. IV B 4, we conclude that samples exhibiting nonanalytic shocklike behavior in the regime $v^2\sim N$ where a FRG equation was previously derived, correspond to exponentially rare realizations of the disorder occurring with probability $P\sim\exp[-NL^d|\Sigma(\mathsf{u}_c^{\text{cp}})|]$, as derived explicitly in Appendix G.

Note that upon approaching the limit of a marginal one-step solution, i.e., for $d\leqslant 2$ and $\gamma\downarrow\gamma_c$, the three values $\mathsf{u}_c^{\text{th}}<\mathsf{u}_c^{\text{eq}}<\mathsf{u}_c^{\text{cp}}$ merge and the one-step saddle point becomes simultaneously marginal with respect to both instabilities discussed above.

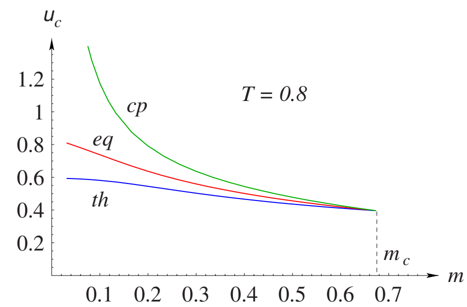

FIG. 5. (Color online) Phase diagram for model (23) in $d=1$. The solid line for $m>m_*$ indicates a continuous glass transition, where the renormalized force correlator $\tilde{B}'(x)$ displays a cusp at the origin. For smaller mass, $m<m_*$, the glass transition toward the one-step RSB phase (as a function of T) is discontinuous and takes place dynamically as a freezing transition at T_d, or, if equilibrium can be attained, as a genuine thermodynamic transition at the lower temperature T_c. A similar phase diagram applies in $d<2$ for model (23) and model (24) with $\gamma>\gamma_c$.

3. Phase diagram

In this section, we establish the phase diagram and discuss some of the subtleties associated with the choice of u_c. The situation is closely analogous to a particle in a random environment ($d=0$) analyzed in Ref. 99. The phase diagram of a typical case, model (23) in $d=1$, is shown in Fig. 4, and explicit values given in the analysis below refer to this specific case.

The glass phase exhibits everywhere one-step RSB. Right on the instability line $T_c(m)$ where Eq. (176) is obeyed, there is only one admissible value for u_c:

$$\mathsf{u}_c^{\text{crit}}(m) = -\frac{T_c(m)I_2^2(m)}{I_3(m)}\frac{B'''(\chi^{\text{RS}})}{B''(\chi^{\text{RS}})} = -\frac{4A_d}{\epsilon^2}\frac{T_c(m)}{m^{2-d}}\frac{B'''(\chi^{\text{RS}})}{B''(\chi^{\text{RS}})}, \tag{185}$$

which yields the fluctuation-dissipation ratio relating response and correlations at the glass transition.[99] It increases monotonously with decreasing m, and reaches $\mathsf{u}_c^{\text{crit}}=1$ at $m=m_*$ $[=1/e=0.3678$, with $T_c^{\max}=T_c(m_*)=3/e=1.1036$ in $d=1$ for model (23) where $A_1=3/4]$. For states to be dynamically or thermodynamically of significance, u must always be smaller than 1, and thus, the line $T_c(m)$ loses its significance below m_*.

For $m>m_*$, the glass transition is continuous in the sense that G_1-G_0 smoothly goes to 0 as $T\uparrow T_c(m)$. For $m<m_*$, the temperature-driven transition is discontinuous with a sudden jump between intervalley and intravalley correlations occurring at some $T\in[T_c(m),T_c^{\max}]$. The location of the transition depends on the point of view. From a thermodynamic (*static*) standpoint, the glass transition takes place at the line given by $\mathsf{u}_c^{\text{eq}}(m,T)=1$, indicating that the replica symmetry must be broken spontaneously to extremize the free energy, which gives rise to a nonanalyticity in the free energy. For model (23), one finds the explicit result

$$T_c(m=0) = \left(\frac{2A_d}{d\epsilon}(2e)^{d/2}\right)^{-2/\epsilon} \overset{d=1}{=} 0.9028. \quad (186)$$

However, metastable states exist already at higher temperature. In the mean-field limit $N\to\infty$, they induce a *dynamical* freezing transition at the line $T_d(m)$ defined by $\mathsf{u}_c^{\mathrm{th}}(m,T_d)=1$. For model (23), one finds

$$T_d(m=0) = \left(\frac{e2^{d/2}A_d}{\epsilon}\right)^{-2/\epsilon} \overset{d=1}{=} 1.0268. \quad (187)$$

The resulting phase diagram is naturally very similar to the one for a particle in a random environment (the limit $d=0$ of a random manifold),[99] and it also strongly resembles that of the spherical p-spin model, whereby the mass m takes the role of the external field h.[92] In the latter the glass, phase is known to be everywhere of one-step nature, the transition (at fixed h) being continuous for $|h|>h_*$ and discontinuous for $|h|<h_*$.

4. Second cumulant

To evaluate the second cumulant of the renormalized disorder potential $\hat{V}$, we introduce as before the coupling $q_{0,1}$, connected to $G_{0,1}$ via

$$q_{0,1} = \frac{1}{4T^2}\int_k g_k^{-2}G_{0,1}(k)|v_k|^2. \quad (188)$$

We need to apply the recursion relations (93) only once (since here $K=1$) to calculate

$$g_1(y) \equiv \exp[\mathsf{u}_c\psi_1(y)] = e^{(\tilde{q}-q(1))/2\mathsf{u}_c}\langle[2\cosh(y + z\sqrt{q_1-q_0})]^{\mathsf{u}_c}\rangle_z, \quad (189)$$

and using similar steps as in the derivation of Eqs. (86) and (103), we obtain

$$\hat{R}[v]-\hat{R}[0] = -2T^2q_0 - 2T^2\int_{-\infty}^{\infty}dy\{\psi_1(y)-\ln[2\cosh(y)]\}. \quad (190)$$

Recalling that $q^c=\tilde{q}-[\mathsf{u}_cq_0+(1-\mathsf{u}_c)q_1]=0$, one can see that $\psi_1(y)-\ln[2\cosh(y)]\sim q^c/2=0$ at large $|y|$, and thus, the integral in Eq. (190) indeed converges. In the following, we examine various limits of this formula.

5. Large L^dv^2

Let us introduce the notation $Q=q_1-q_0$. At large v (large Q), one can use that

$$\langle(2\cosh(y+z\sqrt{Q}))^{\mathsf{u}_c}\rangle_z \overset{Q\to\infty}{\sim} 2\cosh(\mathsf{u}_cy)e^{\mathsf{u}_c^2Q/2},$$

as can be shown using a saddle-point method. This yields the large-v limit:

$$\hat{R}[v]-\hat{R}[0] \overset{v\to\infty}{\sim} -2T^2q_0 - 2T^2\frac{1}{\mathsf{u}_c}\int_{-\infty}^{\infty}dy\{\ln[2\cosh(y\mathsf{u}_c)] - \mathsf{u}_c\ln[2\cosh(y)]\}. \quad (191)$$

Evaluating the integral, we find the final result:

$$\hat{R}[0]-\hat{R}[v] \overset{v\to\infty}{\sim} \frac{T}{2}\sigma(0)\int_x v_x^2 + \frac{\pi^2T^2}{6}\left(\frac{1}{\mathsf{u}_c^2}-1\right), \quad (192)$$

which matches the full RSB result (107) if we formally replace u_m by u_c. These two expressions are, indeed, identical in the case of a marginal one-step solution, as it occurs in $d=2$. In that case, $\theta=0$, and the analysis of the crossover to large v in Sec. III C 1 remains unchanged.

6. Small L^dv^2

For small L^dv^2, one can expand in Q as follows:

$$\begin{aligned}\psi_1(y)-\ln[2\cosh(y)] &= \frac{1}{\mathsf{u}_c}\ln\langle e^{\mathsf{u}_c[\ln\cosh(y+z\sqrt{Q})-\ln\cosh(y)]}\rangle_z + \frac{\tilde{q}-q(1)}{2}\\ &= \frac{1}{2}(1-\mathsf{u}_c)[1-\tanh^2(y)]Q + \cdots,\end{aligned} \quad (193)$$

where $q^c=0$ was used. Performing the y integrals, one eventually finds

$$\hat{R}[v]-\hat{R}[0] = -2T^2q_0 - 2T^2(1-\mathsf{u}_c)\left[Q - \frac{\mathsf{u}_c}{3}Q^2 + \frac{4\mathsf{u}_c}{45}Q^3 + \frac{4\mathsf{u}_c}{315}(3u_c-5)Q^4 + O(Q^5)\right]. \quad (194)$$

As it must be, the leading term is

$$\hat{R}[v]-\hat{R}[0] = -2T^2\int_0^1 q(\mathsf{u})d\mathsf{u}, \quad (195)$$

which yields the GVM result for two-point correlations. Indeed, Eq. (195) matches expression (113), which should not depend on the RSB scheme. Similarly, inserting the one-step form for $q(\mathsf{u})$ in Eq. (114), one checks that it reproduces the second-order term from Eq. (194). In fact, one can check that Eqs. (194) and (114) agree with

$$\begin{aligned}\hat{R}[v]-\hat{R}[0] = -2T^2\Bigg[&\mathrm{tr}(q) + \frac{1}{3}\mathrm{tr}(q^2) + \frac{4}{45}\left(\sum_b q_{ab}^3 + 2\,\mathrm{tr}(q^3) - 3\,\mathrm{tr}(q^2)\mathrm{tr}(q)\right) + \frac{4}{315}\Big(-3\,\mathrm{tr}(q^4) - 12[\mathrm{tr}(q^2)]^2\\ &+ 30\,\mathrm{tr}(q^2)[\mathrm{tr}(q)]^2 + 5\sum_b q_{ab}^4 - 20\,\mathrm{tr}(q)\sum_b q_{ab}^3 + O(q^5)\Big)\Bigg],\end{aligned} \quad (196)$$

where we have used $q^c=0$ and defined $\mathrm{tr}(A)=\lim_{n\to 0}\frac{1}{n}\mathrm{Tr}(A)$. Note that $\Sigma_b q_{ab}^3=\mathrm{tr}((q\cdot q)q)$, where the dot is the Hadamard product.

7. Low-T expansion

Let us now consider the low-T expansion, i.e., the thermal boundary layer, using similar notations as in Sec. III C 3. In the $T\to 0$ limit, $\mathsf{u}_c\to 0$, but $\hat{\mathsf{u}}_c\equiv \mathsf{u}_c/T\to \omega^{\text{eq}}$ has a nonzero limit, and so do q_0 and q_1 when expressed in terms of fixed $\hat{v}=v/T$, as in Eq. (116). Hence, it is convenient to define, for the present one-step case, an expansion in u_c (Ref. 100) analogous to Eq. (121):

$$\hat{R}[v]-\hat{R}[0]=\sum_{p=0}^{\infty}\mathcal{R}_p[v], \qquad (197)$$

obtained by expanding Eq. (193) in powers of u_c at fixed Q. This yields

$$\mathcal{R}_0[v]=-2T^2q_1, \qquad (198)$$

$$\mathcal{R}_1[v]=-T^2\mathsf{u}_c\int_{-\infty}^{\infty}dy\{\langle[\ln\cosh(y+z\sqrt{Q})]^2\rangle_z - \langle\ln\cosh(y+z\sqrt{Q})\rangle_z^2-Q\}, \qquad (199)$$

$$\mathcal{R}_{p\geq 2}[v]=-2T^2\frac{\mathsf{u}_c^p}{(p+1)!}\int_{-\infty}^{\infty}dy\langle[\ln\cosh(y+z\sqrt{Q}) - \ln\cosh(y)]^{p+1}\rangle_z^c. \qquad (200)$$

The expression for $\mathcal{R}_0$ has been simplified using an integration by parts and the identity (102), and is found to match the result (126) for the continuous case. The term $\tilde{q}-q_1=-\mathsf{u}_cQ$ has been included in $\mathcal{R}_1$. The term multiplied by u_c^p in Eq. (200) is the $(p+1)$th connected average (cumulant), as indicated by the superscript c. After a calculation summarized in Appendix H, we finally obtain the thermal boundary layer:

$$\mathcal{R}_1[v]=2T^2\mathsf{u}_c\int_0^Q dq\langle z\sqrt{2q}\coth(z\sqrt{2q})\rangle_z, \qquad (201)$$

which agrees with the result for continuous RSB (134) as expected, since both formulas should apply for the borderline case of a marginal one-step solution.

8. Cusp and full correlator at T=0

The case of one-step RSB is sufficiently simple to allow for a complete calculation of the nonanalytic $T=0$ limit of the full functional $\hat{R}[v]$ in the regime $v^2\sim 1$. Let us define the variable:

$$w:=\mathsf{u}_c\sqrt{Q}=\frac{\hat{\mathsf{u}}_c}{2}\left[\int_k g_k^{-2}[G_1(k)-G_0(k)]|v_k|^2\right]^{1/2}, \qquad (202)$$

which will be shown to be of order $O(1)$ when the crossover to the shock-dominated regime occurs [see Eq. (211) below]. It tends to a finite limit as $T\to 0$. For a uniform $v_x=v$, this becomes

$$w=\frac{1}{2}[L^d\hat{\mathsf{u}}_c^2v^2m^4(G_1-G_0)]^{1/2}=\frac{v}{2v_*}\left[\frac{\hat{\mathsf{u}}_c}{m^\theta}\left(\frac{\Sigma_1}{m^2+\Sigma_1}\right)\right]^{1/2}, \qquad (203)$$

with $G_{0,1}\equiv G_{0,1}(k=0)$ as given by Eqs. (166) and (167). Note that the characteristic scale for v (determined by $w\approx 1$) is not exactly the scale $v_*=L^{-d/2}m^{-1-(\theta/2)}$ for shocks found for continuous RSB in Eq. (109), but rather (for $m\ll\Sigma_1$) $\sim v_*^{\text{1step}}=v_*m^{\theta/2}\sim L^{-d/2}m^{-1}$. However, the two scales become the same in the case of marginal one-step RSB since there $\theta=0$.

Let us first obtain the $T=0$ cusp for a uniform $v_x=v$ by taking the limit of large v/T of the thermal boundary layer. In that limit, expression (201) tends to[101]

$$L^d\mathcal{R}_1^{T=0}(v)=2\hat{\mathsf{u}}_c\int_0^{(w/\hat{\mathsf{u}}_c)^2}dq'\langle|z|\sqrt{2q'}\rangle_z = \frac{1}{\hat{\mathsf{u}}_c^2}\frac{8w^3}{3\sqrt{\pi}} = \frac{(mL^{d/2}|v|)^3}{3(\pi\hat{\mathsf{u}}_c)^{1/2}}\left(\frac{\Sigma_1}{m^2+\Sigma_1}\right)^{3/2}, \qquad (204)$$

using $\langle|z|\rangle_z=\sqrt{2/\pi}$. This finite nonzero limit as $T\to 0$ (cf. Appendix G) is, thus the exact expression for the leading nonanalyticity of $\hat{R}[v]-\hat{R}[0]$ at $T=0$, which is again cubic $\sim|v|^3$ (corresponding to a "linear cusp" of the force correlator $-\hat{R}''[v]$). Note that in this regime, $v^2\sim L^{-d}$, the cusp exists irrespective of the choice of u_c, including the equilibrium solution. This is to be contrasted to the regime $v^2\sim N$, where, in the case of a nonmarginal one-step solution, a cusp exists only for the choice $\mathsf{u}_c=\mathsf{u}^{\text{cp}}$ (see the discussion in Sec. IV B 4).

We now obtain the full functional $\hat{R}_{T=0}[v]$ for arbitrary v_x, using the variable w defined in Eq. (202). By using Eq. (189) in Eq. (190) and taking the limit of small u_c, we find at $T=0$:

$$\hat{R}[v]-\hat{R}[0]|_{T=0}=-\frac{1}{2}\int_k g_k^{-2}G_0^{T=0}(k)|v_k|^2+\mathcal{R}_{T=0}(w), \qquad (205)$$

where

$$\mathcal{R}_{T=0}(w)=-\frac{2}{\hat{\mathsf{u}}_c^2}\int_{-\infty}^{\infty}d\hat{y}\left[-\frac{w^2}{2}+\ln\langle e^{|\hat{y}+zw|}\rangle_z-|\hat{y}|\right] = -\frac{w^2}{\hat{\mathsf{u}}_c^2}\int_0^{\infty}\frac{8\hat{y}\,d\hat{y}}{1+\dfrac{\exp(2w\hat{y})\{1+\text{erf}[(w+\hat{y})/\sqrt{2}]\}}{1+\text{erf}[(w-\hat{y})/\sqrt{2}]}} = \begin{cases}-\dfrac{w^2}{\hat{\mathsf{u}}_c^2}\left[2-\dfrac{8|w|}{3\sqrt{\pi}}+O(w^2)\right], & w\ll 1\\ -\dfrac{\pi^2}{6\hat{\mathsf{u}}_c^2}, & w\gg 1.\end{cases} \qquad (206)$$

From the expansion for $w\ll 1$, we again recover Eq. (204) with, in the uniform-v case, $\mathcal{R}_{T=0}(w)\to L^d\mathcal{R}_1^{T=0}(v)$. The asymptotics for $w\gg 1$ is in agreement with the result (192) for continuous RSB (with $\hat{\mathsf{u}}_m\to\hat{\mathsf{u}}_c$).

From this expression, one can compute the force correlator, which, from $O(N)$ symmetry, splits in transverse and longitudinal parts as defined in Appendix F.

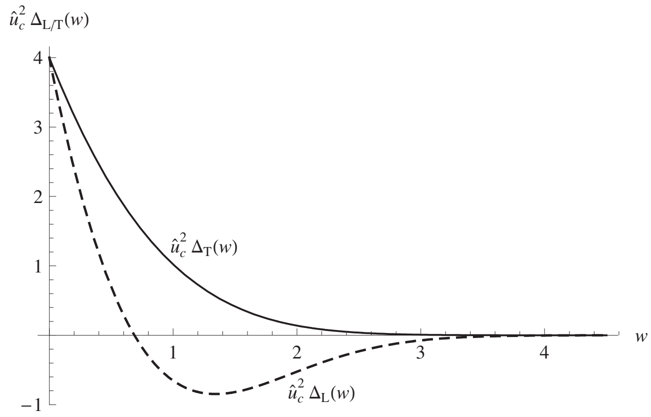

FIG. 6. Nonanalytic contribution to the force correlator in longitudinal $\Delta_L(w)$ and transversal $\Delta_T(w)$ directions, at $T=0$ in the case of one-step RSB. The rescaled displacement w is defined in Eq. (203).

The nonanalytic parts of the longitudinal and transverse force correlators in the regime $v^2 \sim L^{-d/2}$ are proportional to $-\mathcal{R}''_{T=0}(w)$ and $-\frac{\mathcal{R}'_{T=0}(w)}{w}$, respectively. They are plotted in Fig. 6, both exhibiting a linear cusp at the origin. Note that the full correlator of the force, in addition, contains a constant which derives from the v^2 term in Eq. (205). Further decay from this constant to zero at infinity occurs (for any $\gamma>0$) in the regime $v^2 \sim N$.

E. Interpretation of v_* and the thermal boundary layer

What happens to the manifold as the center of the harmonic well is moved? Let us first focus on the case of a one-step RSB for which the construction of the statistical measure is significantly simpler and was recalled in Eqs. (163) and (164). From this construction, we know that at low temperatures a certain state center ξ_k^α dominates, but there is at least one excited state which differs in energy by a typical amount T/u_c. Changing the position of the harmonic well by an amount v shifts the relative energies of these two low lying configurations (states), noted $u^{1,2}$, by an amount

$$\Delta E = \int_k g_k^{-1} v_k \cdot [u^1(k) - u^2(k)]. \tag{207}$$

One can expect a switch from one state to the other, and thus a macroscopic jump, as the energies of two states cross. This occurs typically when $|\Delta E| \sim T/\mathsf{u}_c = \hat{\mathsf{u}}_c^{-1}$. Recalling that $\overline{[u^1(k)-u^2(k)]^2}$ is of the order of $G_1(k)-G_0(k)$, one finds

$$\overline{\Delta E^2} = 2\int_k g_k^{-2}|v_k|^2[G_1(k) - G_0(k)]. \tag{208}$$

Hence, comparing with Eq. (202), the jump occurs typically when

$$w \sim O(1). \tag{209}$$

We, thus, understand the scale of variation of the functional $\hat{R}[u]$ given by Eqs. (205) and (206). The argument is even simpler for a uniform center v ($v_k = L^{d/2} v\,\delta_{k,0}$) which couples only to the $k=0$ mode of the excitation, the energy shift being $m^2 L^{d/2} v[u^1(0)-u^2(0)]$. Since $\overline{[u^1(0)-u^2(0)]^2} = 2(G_1 - G_0)$, we see that the energy shift (207) competes with the typical excitation energy $\hat{\mathsf{u}}_c^{-1}$ when v is of the order of $v_*^{1\text{step}}$ as defined below Eq. (203). Since the energy difference is finite, the jump is thermally smoothed at finite temperature, but turns into a sharp shock for $T\to 0$, which is at the root of the nonanalyticity in Eq. (206).

We can obtain better insight into the physics for shifts of order $v \sim v_*^{1\text{step}}$ by examining the force correlator. We consider uniform v for simplicity. To be specific, we define $-\hat{R}''(v) \coloneqq -\partial_{|v|}^2 R(v)$, which corresponds to the longitudinal force correlator. From Eq. (205), we see that for $v \gg v_*^{1\text{step}}$, the correlator is simply constant and equal to

$$-\hat{R}''(v \gg v_*^{1\text{step}}) = m^4 G_0(k=0). \tag{210}$$

This has a simple interpretation in terms of the hierarchical construction (163) and (164): One can imagine the states (characterized by ξ^α) as parabolic potential valleys within a big parabolic potential valley as determined by the global center u_k^0, and accordingly write schematically $V(u) = V_0(u^0) + V_\alpha(\xi^\alpha)$ for the total potential. For $v \gg v_*^{1\text{step}}$, the manifold has jumped to a different state center, and, therefore, the part of the force arising from $V'_\alpha(\xi^\alpha)$ does not contribute to the correlator. However, u^0 is very robust under shifts of $v \ll N^{1/2}$, and jumps only once $v^2 \sim N$, as we will see in the next section. The force corresponding to the big valley, $V'_0(u^0)$, thus remains constant. Since the disorder potential competes against the quadratic well $L^d m^2 (u^0)^2/2$, that part of the force is of order $V'_0(u) \sim L^{d/2} m^2 u^0_{k=0}$, which leads to Eq. (210).

For $v \ll v_*^{1\text{step}}$, we see from Eq. (204) that the force correlator behaves as

$$-\hat{R}''(v \ll v_*^{1\text{ step}}) = m^2\left[m^2 G_1(k=0) - \frac{|v|}{v_*^{1\text{ step}}}\frac{2}{(\pi\hat{\mathsf{u}}_c)^{1/2}}\left(\frac{\Sigma_1}{m^2+\Sigma_1}\right)^{3/2}\right]. \tag{211}$$

The first term can be understood as m^4 times the *intrastate* correlator $\langle u^2\rangle^{(\alpha)}$. The force correlations rapidly decrease with growing v. Indeed, we can understand the nonanalytic piece $\sim |v|$ as being due to shocks which occur with a finite density along the v axis. Note the large prefactor $\sim L^{d/2}$ of $|v|$: It indicates that the product of the density and size of shocks scales as $\sim L^{d/2}$, that is, in such a way that the system size rather than $1/m$ acts as a cutoff. Further work is in progress to clarify the properties and the distribution of these shocks.

Let us close the discussion of shocks by sketching the analysis in the case of continuous RSB. The typical scale in that case, $v_* = v_*^{1\text{step}} m^{-\theta/2}$, can be retrieved by the same argument as above for the one-step RSB. However, now the energy difference between two states at ultrametric distance u is typically of order T/u. This competes with the energy shift induced by the displacement of the well:

$$\overline{\Delta E^2} = 2\int_k g_k^{-2}|v_k|^2[G(\mathsf{u}_c,k) - G(\mathsf{u},k)] \sim \frac{L^d v^2 m^4}{\hat{\mathsf{u}}^{1+2/\theta}}. \tag{212}$$

The largest response is due to transitions between states differing at the largest scales, i.e., $\mathsf{u}\approx\mathsf{u}_m\sim m^\theta$. The above energy comparison at this scale immediately yields v_*. However, there is no sharp selection of shocks that involves the highest hierarchy scale. Smaller shocks contribute as well, even though their weight decreases with increasing u characterizing the shock. Note that from the construction of the measure of pure states, it is clear that when a shock occurs at scale $\mathsf{u}=\mathsf{u}_r$ (in a finite K-step RSB scheme), the whole subhierarchy of state centers u_k^s with $K\geqslant s\geqslant r$ changes. Note that, in general, shocks characterized by a larger u correspond to smaller spatial rearrangements.

IV. REGIME $v^2\sim N$

We now compute the functional $\hat{W}[v]=W[j=(g^{-1}v)/T]$ defined in Sec. II C and, more explicitly, its second cumulant part $\hat{R}[v]$, in the regime $v^2\sim N$. This is the standard regime for the large-N analysis, and in Refs. 11 and 13, the associated saddle-point equation was obtained. There the focus was on the calculation of the effective action $\Gamma[u]$, and, in particular, its two-replica component $R[u]$, part of which will be of use here, too, to obtain $\hat{W}[v]$ and $\hat{R}[v]$. We find, as announced in Sec. II C, that the functionals $\hat{R}$ and R are identical. The calculations carried out here are, however, rather different in spirit from the one in Refs. 11 and 13. We obtain $\hat{R}[v]$ from imposing external fields $v^a=\pm v$ to two groups of replicas, whereas in Refs. 11 and 13, the case of $u^{ab}\neq 0$ for all $a\neq b$ was considered. It is reassuring that the two approaches yield consistent results. The advantage of the present approach is that it includes RSB effects, and hence, it provides a complete derivation of the FRG equation on all length scales (below *and* above the Larkin scale).

A. General saddle point

To analyze the saddle point in the regime $v^2\sim N$, it is convenient to introduce the rescaled variables:

$$\tilde{u} = \frac{u}{\sqrt{N}}, \quad \tilde{v} = \frac{v}{\sqrt{N}}. \tag{213}$$

We can now rewrite the definition (59) and decouple the partition sum with the help of two auxiliary fields as

$$e^{\hat{W}[v]} = \overline{\prod_a Z_V\left[j^a = \frac{g^{-1}v^a}{T}\right]} = \int \mathcal{D}[\tilde{u}]\mathcal{D}[\chi]\mathcal{D}[\sigma]e^{-N\mathcal{S}},$$

$$\mathcal{S} = \frac{1}{T}\sum_a \int_k g_k^{-1}\left(\frac{1}{2}\tilde{u}_{-k}^a\cdot\tilde{u}_k^a - \tilde{v}_{-k}^a\cdot\tilde{u}_k^a\right) + \int_x\left[U(\chi_x) + \frac{1}{2}\sum_{ab}\sigma_x^{ab}(\chi_x^{ab} - \tilde{u}_x^a\cdot\tilde{u}_x^b)\right], \tag{214}$$

where the replica matrix field χ_x^{ab} has been introduced through a purely imaginary Lagrange multiplier matrix σ_x^{ab}. A standard choice, as in previous sections, is $g_k^{-1}=k^2+m^2$, but our analysis is more general. We have also included the source term shifting the center of mass. U is a function of an $n\times n$ replica matrix[102] $\tilde{u}\tilde{u}\equiv\tilde{u}^a\cdot\tilde{u}^b$:

$$U(\tilde{u}\tilde{u}) = -\frac{1}{2T^2}\sum_{ab}B((\tilde{u}^a-\tilde{u}^b)^2) - \frac{1}{3!T^3}\sum_{abc}S^{(3)}(\ldots) + \cdots, \tag{215}$$

containing the information about the bare disorder via its cumulants, e.g., its second cumulant being [as in Eq. (7)]

$$R_0(u) = NB(\tilde{u}^2). \tag{216}$$

Note that the rescaling (213) was performed in order to make explicit the appearance of a factor of N in front of the action $\mathcal{S}$, which allows for a saddle-point analysis. One now explicitly performs the functional integration over the field u_x to obtain

$$e^{\hat{W}[v]} = \int \mathcal{D}[\chi]\mathcal{D}[\sigma]e^{-NS[\chi,\sigma,\tilde{v}]}, \tag{217}$$

$$S[\chi,\sigma,\tilde{v}] = \frac{1}{2}\mathrm{Tr}\ln\left[\frac{1}{T}(g^{-1}-\sigma)\right] + \int_x\left[U(\chi_x) + \sum_{ab}\frac{1}{2T}\sigma_x^{ab}\chi_x^{ab}\right] - \frac{1}{2T}\sum_{ab}\int_{x,x'}\tilde{v}_x^a[(g-g\sigma g)^{-1}]_{xx'}^{ab}\tilde{v}_{x'}^b, \tag{218}$$

where the inversions and the trace are performed in both replica and spatial-coordinate space. We use the shorthand $g^{-1}\equiv(g^{-1})_{xy}^{ab}=g_{xx'}^{-1}\delta^{ab}$, which is diagonal in replica space.

Equation (217) has now the standard form for a saddle-point evaluation of the functional $\hat{W}[v]=:N\tilde{W}[\tilde{v}]$ except that the saddle point is not, in general, uniform in space. At dominant order in $1/N$, we obtain

$$\tilde{W}[\tilde{v}] = \frac{1}{N}\ln\sum_{\mathrm{sp}}(e^{-NS[\chi_{\tilde{v}},\sigma_{\tilde{v}},\tilde{v}]}). \tag{219}$$

We have allowed for different saddle points ("sp") to contribute. To alleviate notations, we did not add an index indicating the different saddle points to $\chi_{\tilde{v}}$ and $\sigma_{\tilde{v}}$. They depend on $\tilde{v}_x$ and are the solutions of the saddle-point equations obtained, respectively, by setting to zero the functional derivatives (at fixed $\tilde{v}_x$):

$$\left.\frac{\delta S[\chi_{\tilde{v}},\sigma_{\tilde{v}},\tilde{v}]}{\delta\sigma_x^{ab}}\right|_{\chi=\chi_{\tilde{v}},\ \sigma=\sigma_{\tilde{v}}} = 0, \tag{220}$$

$$\left.\frac{\delta S[\chi,\sigma,\tilde{v}]}{\delta \chi_x^{ab}}\right|_{\chi=\chi_{\tilde{v}},\ \sigma=\sigma_{\tilde{v}}} = 0. \tag{221}$$

Solving these equations, one can obtain $\hat{R}[v]$ from its definition (54).

The explicit form of the saddle-point equations is

$$(\chi_{\tilde{v}})_x^{ab} = (G_{\tilde{v}})_{xx}^{ab} + \frac{1}{T^2}(G_{\tilde{v}}{:}g^{-1}{:}\tilde{v})_x^a \cdot (G_{\tilde{v}}{:}g^{-1}{:}\tilde{v})_x^b$$
$$\equiv (G_{\tilde{v}})_{xx}^{ab} + \tilde{u}_x^a \tilde{u}_x^b, \tag{222}$$

$$(\sigma_{\tilde{v}})_x^{ab} = -2T\frac{\partial}{\partial \chi^{ab}} U((\chi_{\tilde{v}})_x), \tag{223}$$

$$TG_{\tilde{v}}^{-1} = g^{-1} - \sigma_{\tilde{v}}, \tag{224}$$

where $G_{\tilde{v}}$ is a matrix with both replica indices and spatial coordinates; thus, inversion is carried out for both. The notation for the N-component vector $(G{:}\tilde{j})_x^b := \Sigma_c \int_y G_{xy}^{bc} \tilde{j}_y^c$ is a shorthand for a matrix product, but consistent with our above conventions, we do not write the vector indices of j explicitly. We have defined the average displacement induced by the source:

$$\tilde{u}_x^a \equiv \tilde{u}_x^a(v) := \frac{1}{T}(G_{\tilde{v}}{:}g^{-1}{:}\tilde{v})_x^a. \tag{225}$$

It is a function of v and of the chosen sp, and to simplify notations, we drop, in what follows, the dependence on v except when an ambiguity arises. As detailed in Refs. 11 and 13, $\tilde{u}(v)$ arises in performing the Legendre transform to obtain $\Gamma[u]$ from $W[v]$, as one may see from Eq. (29) and (52), i.e.,

$$\Gamma[u] + W[v] = \frac{1}{T} u{:}g^{-1}{:}v, \tag{226}$$

$$u = Tg{:}\frac{\delta W[v]}{\delta v}, \tag{227}$$

and using that for a given saddle point:

$$\tilde{W}_{\text{sp}}[\tilde{v}] = -S[\chi_{\tilde{v}}, \sigma_{\tilde{v}}, \tilde{v}]. \tag{228}$$

Taking the total derivative with respect to $\tilde{v}$, which is equivalent to differentiating only the explicit $\tilde{v}$ dependence in Eq. (220), one recovers Eq. (225). While in Refs. 11 and 13 we had chosen sources $\tilde{v}^a - \tilde{v}^b \neq 0$ such that $\tilde{u}^a - \tilde{u}^b \neq 0$ and, therefore, assumed a unique saddle point, here we allow for spontaneous RSB and, hence, for many saddle points. In general, the set of saddle points will include the set of all permutations π which leave $\tilde{v}$ invariant,[103] i.e., $\tilde{v}^{\pi(a)} = \tilde{v}^a$ for all $a = 1, \ldots, n$. Hence, the $\tilde{u}_x^a(v)$ in Eq. (225) is identical to a partial average $\langle u_x^a \rangle_\pi$ (corresponding to a single saddle point labeled by π), while the thermodynamic average corresponds to the full average over all equivalent saddle points, $\langle u_x^a \rangle = \Sigma_\pi \langle u_x^a \rangle_\pi$. In the limit $\tilde{v} \to 0$, the saddle-point equations (222) become identical to the saddle-point equations of the GVM, with $G_v \to G$ and $\sigma_v \to \sigma$ taking the values of the solution given by Mézard-Parisi (see also below). Performing the sum over equivalent saddle points sp in Eq. (219), one recovers the results of Sec. III.

B. Analysis for a uniform v

According to the general strategy to compute $\hat{R}[v]$, as described in Sec. III C, we now solve the saddle-point equations (220) and (221), specifying the source $\tilde{v}_x^a = \tilde{v}_x(1, 1, \ldots, -1, \ldots, -1)$ with $n/2$ entries $+1$, and $n/2$ entries -1. For simplicity, we restrict here to a uniform $v_x = v$, for which $\hat{R}[\{v_x = v\}] = L^d \hat{R}(v)$. From the definition (54) and the replica-sum expansion (79), one has

$$L^{-d}\tilde{W}[v] = \frac{m^2}{2T} n \tilde{v}^2 + \frac{1}{2T^2}\frac{n^2}{2}\hat{B}(4\tilde{v}^2) + O(n^3),$$

$$\hat{R}(v) = N\hat{B}(\tilde{v}^2), \tag{229}$$

up to a (v-independent) constant. The matrices $\chi_{\tilde{v}}$ and σ are now independent of x, and $G_{\tilde{v}}$ is translationally invariant. We parametrize the $n \times n$ replica matrix $\chi_{\tilde{v}}$ by

$$\chi_{\tilde{v}} = \begin{pmatrix} \chi_1 & \chi_{2\tilde{v}} \\ \chi_{2\tilde{v}} & \chi_1 \end{pmatrix}, \tag{230}$$

where we anticipate that the diagonal blocks will turn out to be independent of $\tilde{v}$. We use similar notations for σ and G:

$$\sigma_{\tilde{v}} = \begin{pmatrix} \sigma_1 & \sigma_{2\tilde{v}} \\ \sigma_{2\tilde{v}} & \sigma_1 \end{pmatrix}, \quad G_{\tilde{v}}(k) = \begin{pmatrix} G_1(k) & G_{2\tilde{v}}(k) \\ G_{2\tilde{v}}(k) & G_1(k) \end{pmatrix}. \tag{231}$$

Note that σ_1 and G_1 should not be confused with the variables used for the one-step solution. The saddle-point equations (222)–(224) now become

$$\chi_1 = \tilde{u}^2 \mathbb{J} + \int_k G_1(k), \tag{232}$$

$$\chi_{2\tilde{v}} = -\tilde{u}^2 \mathbb{J} + \int_k G_{2\tilde{v}}(k), \tag{233}$$

$$TG_{\tilde{v}}^{-1}(k) = \begin{pmatrix} g_k^{-1}\mathbb{1} - \sigma_1 & -\sigma_{2\tilde{v}} \\ -\sigma_{2\tilde{v}} & g_k^{-1}\mathbb{1} - \sigma_1 \end{pmatrix}, \tag{234}$$

$$\sigma_{\tilde{v}}^{ab} = -2T\frac{\partial}{\partial \chi^{ab}} U(\chi_{\tilde{v}}), \tag{235}$$

and must be solved for a given value of $\tilde{v}$. We have introduced the notation $\mathbb{J} \equiv 1_{n/2}$ and $\mathbb{1}$ for the $\frac{n}{2} \times \frac{n}{2}$ matrices:

$$\mathbb{J}^{ab} = 1, \quad \mathbb{1}^{ab} = \delta^{ab}. \tag{236}$$

In general, we expect that χ_1^{ab} is an ultrametric matrix while $\chi_{2\tilde{v}}^{ab} = \chi_{2\tilde{v}} \mathbb{J}^{ab}$, and similarly, for σ_1^{ab} and $\sigma_{2\tilde{v}}^{ab}$. This ansatz for the solution is motivated by the expectation that states in different groups will be very distant in phase space (at least, as distant as the farthest equilibrium states, as described by $\mathsf{u}=0$), and thus, their mutual overlap will not depend on the specific replica in either of the groups. Further, we have $\tilde{u}_x^a = \tilde{u}(1,1,\ldots,-1,\ldots,-1)$, and one can show that our ansatz implies

$$\tilde{u}_x^a = \tilde{v}_x^a, \tag{237}$$

which means that the average displacement is tied to the center of the harmonic well. This holds because Eq. (225) implies $Tg_k\tilde{u}_k=[G_1^c(k)-G_{2\tilde{v}}^c(k)]\tilde{v}_k$, where $G_1^c(k)=\Sigma_b G_{1,ab}(k)$ (the sum being restricted to the $n/2$ replica in the same group as a) and $G_{2\tilde{v}}^c(k)=\Sigma_b G_{2\tilde{v},ab}(k)$ (the sum being restricted to the $n/2$ replica in the group not containing a). Within our ansatz, as $n\to 0$, $G_1^c(k)=Tg_k$ and $G_{2\tilde{v}}^c(k)$ vanish [see Eq. (242) below], which establishes Eq. (237).

To evaluate Eq. (235), let us split the set of indices a into two groups: a_+ for the first $n/2$ replicas, i.e., those for which $\tilde{v}^a=\tilde{v}$, and a_- for the remaining $n/2$ replicas, and consider for simplicity a bare model with Gaussian disorder:[104]

$$\begin{aligned} U(\chi_{\tilde{v}}) = &-\frac{1}{2T^2}\sum_{a_+,b_+} B(\chi_1^{aa}+\chi_1^{bb}-\chi_1^{ab}-\chi_1^{ba}) \\ &-\frac{1}{2T^2}\sum_{a_-,b_-} B(\chi_1^{aa}+\chi_1^{bb}-\chi_1^{ab}-\chi_1^{ba}) \\ &-\frac{1}{T^2}\sum_{a_-,b_+} B(\chi_1^{aa}+\chi_1^{bb}-\chi_{2\tilde{v}}^{ab}-\chi_{2\tilde{v}}^{ba}). \end{aligned} \tag{238}$$

One can easily see that Eqs. (235) and (238) imply the STS property $\sigma^c=\Sigma_a\sigma_{\tilde{v}}^{ab}=0$. Applying the inversion formulas (34)–(36) to Eq. (234), we find the exact relation (to all orders of n) $G^c=G_1^c+G_{2\tilde{v}}^c=Tg_k$ from the connected part (234). Further, to lowest order in n, one finds [cf. Eq. (40) and (41)]

$$[G_1](k,\mathsf{u}) = Tg_k - \frac{T}{g_k^{-1}+[\sigma_1](\mathsf{u})}, \tag{239}$$

$$G_1(k,0) = g_k^2 T\sigma_1(0), \tag{240}$$

$$G_{2\tilde{v}} = g_k^2 T\sigma_{2\tilde{v}}, \tag{241}$$

and to precision $O(n)$:

$$G_1^c(k) = Tg_k - (n/2)g_k^2T\sigma_{2\tilde{v}},$$

$$G_{2\tilde{v}}^c(k) = (n/2)g_k^2T\sigma_{2\tilde{v}}. \tag{242}$$

Up to negligible corrections of order $O(n)$, the saddle-point equations for the diagonal blocks are the same as those in the regime $v=O(1)$ [cf. Eq. (14) and (15)], independent of the external field $\tilde{v}$:

$$\begin{aligned} \sigma_1^{ab} = -\frac{2}{T}\Bigg[& B'(\chi_1^{aa}+\chi_1^{bb}-2\chi_1^{ab}) \\ &- \delta_{ab}\sum_{c_+} B'(\chi_1^{aa}+\chi_1^{cc}-2\chi_1^{ac})\Bigg], \end{aligned}$$

for a and b in the + group. An analogous equation holds for the − diagonal block. This is not surprising since the external field v does not separate the replica within a group. Since these saddle-point equations have a unique physical solution, we will identify $\sigma_1\equiv\sigma$ henceforth, and also drop the subscripts 1 on G_1 and χ_1. In Parisi's parametrization of ultrametric matrices, the saddle-point equation is conveniently rewritten as

$$\sigma(\mathsf{u}) = -\frac{2}{T}B'\left(2\int_k [\tilde{G}(k)-G(k,\mathsf{u})]\right), \tag{243}$$

$$\tilde{\sigma} = \int_0^1 \sigma(\mathsf{u})d\mathsf{u}. \tag{244}$$

The saddle-point equation for the off-diagonal part is

$$\sigma_{2\tilde{v}}^{ab} = -\frac{2}{T}B'(\chi^{aa}+\chi^{bb}-2\chi_{2\tilde{v}}^{ab}), \tag{245}$$

which within our ansatz $\sigma_{2\tilde{v}}^{ab}=\sigma_{2\tilde{v}}\mathbb{J}^{ab}$ reduces to a single equation

$$\sigma_{2\tilde{v}} = -\frac{2}{T}B'\left(4\tilde{v}^2+2\int_k[\tilde{G}(k)-G_{2\tilde{v}}(k)]\right). \tag{246}$$

Before analyzing these equations, let us indicate how to extract $\hat{R}(v)$ from its solution. Let us first rewrite the part of the action at the saddle point which depends explicitly on v (in fact, on $v\cdot v$):

$$\begin{aligned} \frac{S[\chi_{\tilde{v}},\sigma_{\tilde{v}},\tilde{v}]|_{\text{expl}}}{L^d} &= -\frac{m^4}{2T^2}\tilde{v}^aG_{\tilde{v}}^{ab}(k=0)\tilde{v}^b \\ &= -\frac{m^4}{2T^2}n\tilde{v}^2[G^c(k=0)-G_{2\tilde{v}}^c(k=0)] \\ &= \tilde{v}^2\left(-\frac{m^2}{2T}n+\frac{\sigma_{2\tilde{v}}}{2T}n^2\right). \end{aligned} \tag{247}$$

Since the derivative of $\tilde{W}_{\text{sp}}[\tilde{v}]=-S[\chi_{\tilde{v}},\sigma_{\tilde{v}},\tilde{v}]$, with respect to $\tilde{v}$ (in fact, with respect to $\tilde{v}\cdot\tilde{v}$) only involves the explicit part, we find, and comparing with Eq. (229),

$$-\frac{2}{T}\hat{B}'(4\tilde{v}^2) = \sigma_{2\tilde{v}}. \tag{248}$$

We now discuss various cases according to whether or not the replica symmetry is broken in the diagonal block (the saddle point of the GVM), indicating whether or not the system is in a glass phase.

1. Replica-symmetric region

Assuming replica symmetry, $\sigma(\mathsf{u})=\sigma^{\mathrm{RS}}$, we have

$$G(k) = Tg_k\mathbb{1} + T\sigma^{\mathrm{RS}}g_k^2\mathbb{J}, \tag{249}$$

$$G_{2\tilde{v}}(k) = T\sigma^{\mathrm{RS}}_{2\tilde{v}}g_k^2\mathbb{J}. \tag{250}$$

This reduces the saddle-point equation (243) to

$$\sigma^{\mathrm{RS}} = -\frac{2}{T}B'(2TI_1), \tag{251}$$

independent of $\tilde{v}$, and Eq. (246) becomes

$$\sigma^{\mathrm{RS}}_{2\tilde{v}} = -\frac{2}{T}B'(4\tilde{v}^2 + 2T\{I_1 + [\sigma^{\mathrm{RS}} - \sigma^{\mathrm{RS}}_{2\tilde{v}}]I_2\}), \tag{252}$$

where $I_n=\int_k g_k^n$. Comparing with Eq. (251), we see that $\sigma^{\mathrm{RS}}_{2,\tilde{v}=0}=\sigma_{\mathrm{RS}}$, as is expected in the absence of external fields.

2. Identification with functional renormalization group below the Larkin scale

It is convenient to introduce the function $\tilde{B}'$ via the change of variables:

$$-\frac{2}{T}\tilde{B}'(4\tilde{v}^2) \equiv \sigma^{\mathrm{RS}}_{2\tilde{v}}. \tag{253}$$

Plugging it into Eq. (246), we see that it satisfies exactly the self-consistency equation (33):

$$\tilde{B}'(x) = B'(x + 2TI_1 + 4[\tilde{B}'(x) - \tilde{B}'(0)]I_2) \tag{254}$$

as derived in Ref. 13 for the second cumulant function of $\tilde{B}(x)$, which occurs in the effective action [defined there via $R(u)=N\tilde{B}(\tilde{u}^2)$]. Since Eq. (254) uniquely specifies $\tilde{B}$ up to a constant, a comparison of Eqs. (253) and (248) shows that

$$\tilde{B}'(x) = \hat{B}'(x), \tag{255}$$

i.e., we have recovered, in the glassy regime, the general identity $\hat{R}=R$ announced in Eqs. (57) and (78).

From the self-consistency equation (254), a FRG equation for $\hat{B}(x)$ can be derived [following, cf. Eqs. (6.1)–(6.8) in Ref. 13]

$$-m\partial_m\hat{B}'(x) = \hat{B}''(x)\left[4(m\partial_m I_2)[\hat{B}'(0) - \hat{B}'(x)] - \frac{2m\partial_m TI_1}{1 + 4I_2\hat{B}''(0)}\right], \tag{256}$$

with initial condition $\hat{B}(x)=B(x)$ for $m=+\infty$.

At this stage, we only know that the FRG equation (256) is valid in the replica-symmetric region, i.e., for $m>m_c(T)$ (see discussion in Sec. II B). At the Larkin mass, $\hat{B}''(0)$ diverges, signaling a cusp in the force correlator, as can be seen from the conditions (17) and (254). Hence, at $m=m_c^+$, Eq. (256) is still valid, but the second term (involving the temperature explicitly) is negligibly small there and can be dropped. It is now crucial to establish how to continue this equation *below* the Larkin mass. To this end, we compute $\hat{B}(x)$ explicitly beyond the Larkin mass, i.e., in the glassy region, where RSB occurs within the replica groups, and derive the correct FRG equation for $m<m_c$.

3. Self-consistency equation for the second cumulant below the Larkin mass

The saddle-point equation (246) together with Eq. (248) yields the correct continuation of the self-consistency equation (254) below the Larkin mass:

$$\hat{B}'(x) = B'\left(x + 2\int_k \tilde{G}(k) + 4\hat{B}'(x)I_2\right). \tag{257}$$

We expect that

$$\hat{B}'(0) = -\frac{T}{2}\sigma(\mathsf{u}=0) \tag{258}$$

remains valid when replica symmetry is broken [with, of course, a different and nontrivial value for $\sigma(0)$] since it expresses the equality $\sigma(\mathsf{u}=0)=\sigma_{2,\tilde{v}=0}$ between the self-energy associated with distant equilibrium states and that associated with the coupling among the two replica groups in the limit of zero forcing, $\tilde{v}\to 0$. Indeed, one can check using Eq. (240) that Eq. (258) is a solution of Eq. (257), given that Eq. (243) holds. Note that Eq. (258) ensures that the function $\hat{B}(\tilde{v}^2)$ perfectly matches the large v^2 limit of the $v^2=O(1)$ results (107) and (192), irrespective of the scheme of RSB, as it should.

Equation (257) can be rewritten in a form similar to Eq. (254):

$$\begin{aligned}\hat{B}'(x) &= B'\left(x + 2TI_1 + 4I_2[\hat{B}'(x) - \hat{B}'(0)] + 2\int_k A_k\right)\\ &= B'(\chi_0 + x + 4I_2[\hat{B}'(x) - \hat{B}'(0)]),\end{aligned} \tag{259}$$

where

$$\chi_0 := 2\int_k [\tilde{G}(k) - G(k,0)] \tag{260}$$

and

$$A_k = \tilde{G}(k) - Tg_k - T\sigma(0)g_k^2 = \int_0^1 d\mathsf{u}[G(k,\mathsf{u}) - G(k,0)] \tag{261}$$

is an *anomaly* which is nonzero if and only if the replica symmetry is broken. [To get the second line in Eq. (261), we used the generally valid inversion formula $G(k,0)=T\sigma(0)g_k^2$.]

4. Correlator and functional renormalization group equation below the Larkin mass

From Eq. (259), we easily obtain the behavior of the force correlator, $-\hat{B}'(x)$, at small argument. If the RSB solution is marginally stable with respect to a clustering instability at the largest scales, i.e., if the condition

$$1 = 4I_2 B''(\chi_0), \tag{262}$$

holds, with χ_0 defined in Eq. (260), one finds a nonanalytic cusp in the correlator:

$$-\hat{B}'(x) = \frac{T\sigma(0)}{2} - \left[\frac{-2x}{(4I_2)^3 B'''(\chi_0)}\right]^{1/2} + O(x). \tag{263}$$

This type of marginality is automatically ensured in the case of continuous RSB, which is marginal with respect to fluctuations on all scales (see Appendix I) including those corresponding to u_m, which entails Eq. (262). For a one-step solution, however, it occurs naturally only on the transition line $T_c(m)$ for $m > m_*$, while in the glass phase, it requires the specific choice $\mathsf{u}_c = \mathsf{u}^{\text{cp}}$ [cf. Eq. (184)]. In the case of a nonmarginal one-step solution, the latter choice differs from the value of u_c corresponding to thermodynamic equilibrium, and was shown to describe rare disorder configurations in Sec. III D 2. On the other hand, for a fully stable saddle point with $1 > 4I_2 B''(\chi_0)$, one finds the regular correlator:

$$-\hat{B}'(x) = \frac{T\sigma(0)}{2} - \frac{xB''(\chi_0)}{1 - 4I_2 B''(\chi_0)} + O(x^2). \tag{264}$$

We emphasize the difference between these results and the generic nonanalyticity (147) and (204) found in the regime $v = O(1)$ at $T = 0$, occurring irrespective of the RSB scheme. The cusp in the regime $v = O(\sqrt{N})$ analyzed here is present even at finite temperature, provided the RSB scheme is marginally stable in the sense of condition (262). The nonanalyticity, thus, reflects the criticality of the system being at the brink of an instability toward an additional clustering of the topmost level of an ultrametric structure. In the one-step case, the instability is toward a two-step RSB with an additional step in the lower plateau.[92,98]

Taking a derivative of Eq. (257) with respect to x and using it to simplify Eq. (256), one finds[13] repeating the steps of Eqs. (6.4)–(6.6) in Ref. 13:

$$-m\partial_m \hat{B}'(x) = \hat{B}''(x)\{4m\partial_m I_2[\hat{B}'(0) - \hat{B}'(x)] + A(m)\}, \tag{265}$$

where

$$A(m) = -2m\partial_m\left[TI_1 + \int_k A_k\right] + 4I_2 m\partial_m \hat{B}'(0)$$
$$= -2m\partial_m \int_k \tilde{G}(k) + 2T\sigma(0)m\partial_m I_2. \tag{266}$$

This equation is the general FRG equation valid in all regimes. In the nonglassy RS regime, $A_k = 0$ and the amplitude $A(m)$ is identical to the last term in Eq. (256). In the glassy region, Eq. (265) is certainly valid for all $x > 0$, and it is also valid at $x = 0$ if $\hat{B}''(0) < \infty$, i.e., if the RSB solution is not marginal in the sense of Eq. (262). However, even if the solution is marginal, and hence $\hat{B}''(0)$ is infinite [i.e., $\hat{B}'(x)$ exhibits a cusp], both sides of the equation have a nontrivial limit at $x = 0^+$, which yields another valid equation as can be checked using Eq. (263). Another useful expression for $A(m)$ is obtained by rewriting the second equation in formula (266) as

$$A(m) = -m\partial_m \chi_0 - 2TI_2 m\partial_m \sigma(0), \tag{267}$$

where we used definitions (260) and (261). The second term in Eq. (267) can be rewritten using the saddle-point equation (243) at $u = 0$, and taking a derivative with respect to m, one obtains

$$A(m) = -[1 - 4I_2 B''(\chi_0)]m\partial_m \chi_0, \tag{268}$$

a formula valid in all cases and regimes. We already point out and will discuss further below that the amplitude $A(m)$ vanishes if the marginality condition (262) is met.

Let us now analyze in more detail the case of continuous RSB which includes as a limiting case the marginal one-step case occurring in $d \leq 2$ with $\gamma = \gamma_c(d)$. In Ref. 13, it was found that the consistent FRG equation[105] for $m < m_c(T)$ was Eq. (265) without the last term, i.e., $A(m) = 0$. As we discussed above, this matches the established equation (33) at $m = m_c^+$. The validity of Eq. (265) for $m < m_c$ was inferred from the study of the FRG equation in inverted variables $x = x(\hat{B}')$, noting that for models (23) and (24) the FRG flow *completely stops* at $m = m_c^+$ (the beta function is identically zero; hence, its natural continuation is to remain zero below m_c). In Sec. VIII D of Ref. 13, the analysis of the FRG flow was extended to an arbitrary bare model [i.e., an arbitrary $B(x)$]. It was found that the natural continuation is such that the function $\tilde{B}'$ retains a cusp for all $m \leq m_c$. This was found to coincide with the marginality condition at u_m, and hence, lead to Eqs. (262) and (263).

From the above general expression (268), we see that the vanishing of the amplitude $A(m) = 0$ is a direct consequence of the marginality of the continuous RSB at $\mathsf{u} = \mathsf{u}_m$, i.e., condition (262), and, thus, confirms the correctness of the assumption made in Ref. 13. In addition, we discover here that the cusp can be avoided if there is a nonzero amplitude $A(m)$. This possibility was naturally not considered in Ref. 13, where the analysis was based on the self-consistency equation without anomaly and the ensuing FRG equation. While the amplitude $A(m)$ always vanishes in the case of continuous RSB, a zero amplitude requires a specific choice of the breakpoint $\mathsf{u}_c = \mathsf{u}^{\text{cp}}$ in the case of one-step RSB, as discussed in the next section.

C. Discussion of the functional renormalization group flow

1. General considerations

Let us analyze the generalized self-consistency Eq. (259) for the renormalized correlator function $\hat{B}'(x)$. It depends only on the (given) bare disorder function $B'(x)$ and a number $\chi_0 = \chi_0(m, T)$, defined in Eq. (260). This is the only input from the saddle-point solution in the regime $v \sim O(1)$, which introduces an anomaly in the glass phase. We emphasize again that in the case of one-step RSB, χ_0 does not only depend on T and m, but also on the choice of the breakpoint u_c.

Since the force correlator (the derivative of the potential correlator) scales like $\hat{B}' \sim m^{-2\theta+d+2\zeta}$, with typical values of the argument scaling as $m^{-2\zeta}$, it is natural to define the rescaled force correlator (as in Refs. 11 and 13)

$$\tilde{b}'(\hat{x}) \coloneqq \frac{4A_d}{m^{-2\theta+d+2\zeta}} \hat{B}'(m^{-2\zeta}\hat{x}). \tag{269}$$

At this stage, if we ignore all other information from the $v \sim O(1)$ regime, the two exponents ζ and θ are undetermined. Let us assume for now that they can be fixed by requiring that $\tilde{b}'(\hat{x})$ reaches a nontrivial fixed point. From Eq. (259), one deduces that $\tilde{b}'$ satisfies the equation

$$\tilde{b}'(\hat{x}) = \frac{4A_d}{m^{2-\theta}} B'\left(\chi_0 + m^{-2\zeta}\left(\hat{x} + \frac{\tilde{b}'(\hat{x}) - \tilde{b}'(0)}{\epsilon}\right)\right), \tag{270}$$

where we have used $I_2 = A_d/(\epsilon m^\epsilon)$ in the limit of infinite cutoff, and consequently set $\theta = d-2+2\zeta$, as expected, so that the last two terms in the argument of B' (the bare disorder) scale the same way. The only information needed from the $v \sim O(1)$ regime is the value of χ_0, given by the saddle-point solution. It fixes the value of $\tilde{b}'$ at the origin:

$$\tilde{b}'_0(m,T) \coloneqq \tilde{b}'(0) = \frac{4A_d}{m^{2-\theta}} B'(\chi_0) = -\frac{4A_d}{m^{2-\theta}} \frac{T\sigma(0)}{2}. \tag{271}$$

The above two equations then completely determine the FRG flow of $\tilde{b}'$, describing the evolution of the force correlator as the mass m is decreased. The corresponding flow equation was given in Eq. (265). Here, we directly solve Eq. (270) focusing on models (23) and (24), which admit simple solutions. We distinguish the case of continuous RSB (full or marginal one step), which we only briefly recall since it was discussed in detail in Ref. 13, and nonmarginal one-step RSB which requires a different and thorough analysis. The difference between the two cases can be grasped immediately. For continuous RSB, comparing Eqs. (271) and (25), valid in that case for models (23) and (24), we immediately see that $\tilde{b}'(0)$ reaches a fixed-point value with the same choice of exponents as in the $v \sim O(1)$ regime. By contrast, Eqs. (170) and (174) suggest a rapid decrease of $\tilde{b}'(0)$ as $m \to 0$ as discussed below.

Some features are independent of the RSB scheme and worth mentioning. Consider model (23), $B(x) = e^{-x}$. If one makes the choice $\zeta = 0$, then $\tilde{b}'(\hat{x})$ is the solution of

$$\tilde{b}'(\hat{x}) = \tilde{b}'_0 \exp\left[-\hat{x} - \frac{\tilde{b}'(\hat{x}) - \tilde{b}'_0}{\epsilon}\right], \tag{272}$$

which has clearly a fixed-point form provided $\tilde{b}'_0$, given by

$$\tilde{b}'_0 = -\frac{4A_d}{m^\epsilon} \exp[-\chi_0(m,T)], \tag{273}$$

reaches a fixed point as $m \to 0$. Similarly for model (24), $B'(x) = [1 + \frac{x}{\gamma}]^{-\gamma}$, and Eq. (271) together with the choice $\zeta = \zeta(\gamma) = \epsilon/[2(1+\gamma)]$ leads to the equation

$$\tilde{b}'_0 = -\frac{4A_d}{m^{\epsilon[\gamma/(1+\gamma)]}} \left[1 + \frac{\chi_0(m,T)}{\gamma}\right]^{-\gamma}. \tag{274}$$

Upon inversion, this allows us to simplify Eq. (270) for the rescaled force correlator as

$$\tilde{b}'(\hat{x}) = \tilde{b}'_0 \left[1 + \left(\frac{|\tilde{b}'_0|}{4A_d}\right)^{1/\gamma} \frac{1}{\gamma}\left(\hat{x} + \frac{\tilde{b}'(\hat{x}) - \tilde{b}'_0}{\epsilon}\right)\right]^{-\gamma}, \tag{275}$$

which reaches a fixed point if $\tilde{b}'_0$ does. Note that these expressions, as well as Eq. (270), are valid for all m, both above and below the Larkin mass.

2. Functional renormalization group flow for continuous replica symmetry breaking

As discussed in Ref. 13 for models (23) and (24), the flow is particularly simple. The structure of Eqs. (272) and (275) implies that $\tilde{b}'(\hat{x}) = \Phi(\hat{x} + \hat{x}_0)$ is always given by the same master function Φ, shifted by an amount $\hat{x}_0$ which depends on m only through $\tilde{b}'_0$. For model (23), the master function is the solution of $\Phi(x) = -\epsilon \exp[-x - 1 - \Phi(x)/\epsilon]$. The shift $\hat{x}_0$ must be positive, and $\hat{x}_0 = 0$ leads to a cusp (infinite slope) at the origin. In the case of continuous RSB, $\hat{x}_0$ freezes to zero as m decreases below $m_c(T)$. One checks that $\tilde{b}'_0$ reaches its fixed point value at $m = m_c(T)$:

$$-\tilde{b}'_0 = \epsilon, \tag{276a}$$

$$-\tilde{b}'_0 = \epsilon\left[\frac{4A_d}{\epsilon}\right]^{1/(1+\gamma)}, \tag{276b}$$

and remains constant everywhere in the glass phase. This implies, in particular, that $\tilde{b}'$ reaches its fixed point already at the phase transition $m_c(T)$ and sticks to it for all smaller m, a result inferred in Refs. 11 and 13 from the vanishing of the beta function at $m_c(T)$. The FRG flow for models with continuous RSB is illustrated in Fig. 7.

As shown in Ref. 13 for models different from Eqs. (276a) and (276b), and such that there is continuous RSB for all $m < m_c(T)$, such as linear combinations of Eqs. (276a) and (276b) with various powers, the flow is slightly more involved. For $m > m_c(T)$, the flow is not a simple translation in x, but the shape also changes as irrelevant parts of $\hat{B}'(x)$ decay. At $m = m_c(T)$, a cusp appears and remains for all $m < m_c(T)$ as $\tilde{b}'_0$ (and the shape of the function) converges slowly toward one of the above fixed-point values (276).

In the continuous RSB case, the existence of this family of nonanalytic fixed points is related to the vanishing of the amplitude $A(m)$ in the FRG equation. In Ref. 13, they were

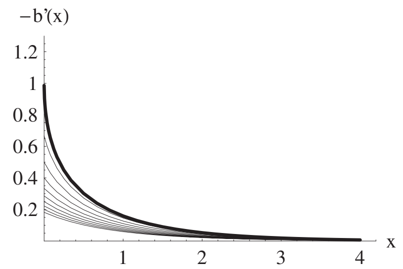

FIG. 7. FRG flow of the renormalized and rescaled correlator $\tilde{b}'(\hat{x})$ for model (276a) in $d=3$. The reduced temperature was chosen to be $\hat{T}=0.5$ and the curves correspond to $1 \leq m/m_c(\hat{T}) \leq 5.5$ in steps of 0.5, from top to bottom. For $m<m_c(\hat{T})$, the force correlator sticks to its fixed point $\tilde{b}'_*$ (thick line) as given by Eq. (272) with $\tilde{b}'_*(0)=\epsilon=1$. Due to the specific form of $B(x)$ in models (276a) and (276b), the flow reduces to an m-dependent horizontal shift of an otherwise constant master function $\Phi(x)$.

derived directly from Eq. (265) assuming $A(m)=0$. For $d>2$ and $d<2$, $\gamma \geq \gamma_c$, they lead to the same exponents $\zeta=\zeta(\gamma)$ and $\theta=\theta(\gamma)$ as the study of the $v^2=O(1)$ GVM regime (cf. Ref. 46). Hence, all parts of the effective action scale consistently. Note that in the limit case $d<2$ and $\gamma=\gamma_c=2/(2-d)$, the glass phase is described by a marginal one-step RSB solution. As discussed in details in Ref. 13 (Sec. VI D and Appendix F), the high-temperature phase $T>T_c$ is described by a line of analytic fixed points which solve Eq. (270) with $\zeta=(2-d)/2=\zeta(\gamma_c)$ and $\theta=\theta(\gamma_c)=0$. In that phase, $\tilde{b}'(x)$ converges to one of these fixed points. This line of fixed points terminates on a cuspy fixed point, toward which $\tilde{b}'(x)$ converge for $T<T_c$, and which has the forms (275) and (276) with $\gamma=\gamma_c$.

By contrast, in the non-marginal one-step case, both for models (276a) and (276b), the shift $\hat{x}_0$ generically vanishes only at $m_c(T)$ and becomes positive again in the glass phase, unless the choice $\mathsf{u}=\mathsf{u}^{\mathrm{cp}}$ is made for the breakpoint, as we now discuss (see also Fig. 8).

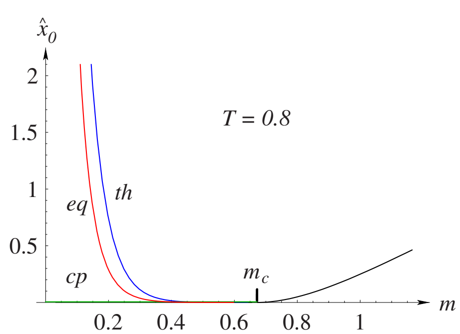

FIG. 8. (Color online) The shifts $\hat{x}_0$ as a function of m at constant temperature $T=0.8$ for model (276a) in $d=1$. The minimal shift $\hat{x}_0=0$ is attained at the glass transition $m=m_c(T)=0.673$ and signals a cuspy correlator. In the glass phase, only the cusp condition $\mathsf{u}=\mathsf{u}^{\mathrm{cp}}$ maintains $\hat{x}_0=0$ and, hence, a cusp. Equilibrium and threshold states have regular correlators ($\hat{x}_0>0$) in the glass phase.

D. Functional renormalization group flow: Physics for one-step replica symmetry breaking

1. Main analysis of functional renormalization group flow for one-step replica symmetry breaking

The situation is radically different in the case where the saddle point is solved by a nonmarginal one-step RSB scheme. This happens for $d<2$ and $\gamma>\gamma_c(d)=2/(2-d)$. As discussed in Sec. III D 2, one may consider several possible choices for the breakpoint u_c. To interpret what is actually computed in each case, one should go back to the definition (50) of the observable $\hat{V}[v]$, whose second cumulant is computed here in the regime $v^2 \sim N$.

Let us first discuss the choice $\mathsf{u}_c=\mathsf{u}_c^{\mathrm{eq}}$, where one computes the cumulant of the observable $\hat{V}[v]=\hat{V}^{\mathrm{eq}}[v]$ defined as the *equilibrium free energy* of a manifold (i.e., a directed polymer, $d=1$, or a particle, $d=0$), in an external quadratic well at position v and nonzero temperature T, in the limit of infinite N. More precisely, for every m, this prescription selects the metastable states of the lowest free-energy density in typical disorder. This condition is by definition equivalent to requiring the configurational entropy to remain fixed to $\Sigma=0$ as m varies, and thus, closely resembles the "isocomplexity" condition often used to describe the rapid quench in systems undergoing one-step RSB.[106,107]

The first observation is that for $m<m_c(T)$, $A(m)>0$ and this "anomalous" term acts as an "effective temperature" in the FRG equation (265) which avoids the occurrence of a cusp, similarly as a finite temperature does in the case of finite N. Let us evaluate this amplitude at low temperature (i.e., away from the glass phase boundary, $T<T_c$) and $m \to 0$. One has

$$\chi_0 \approx \frac{4A_d}{\epsilon(2-d)} \frac{T}{\mathsf{u}_c} m^{d-2}, \tag{277}$$

and as shown in Appendix G, $T/\mathsf{u}_c^{th}=1/\hat{\mathsf{u}}_c^{\mathrm{eq}}$ has a finite limit as $T \to 0$. Hence, χ_0 diverges as $m \to 0$ and, for model (276a), $B''(\chi_0)=-B'(\chi_0)=e^{-\chi_0}$ decays exponentially fast to zero. For model (276b), $4I_2B''(\chi_0) \sim m^{-2+(2-d)\gamma}$; hence, in all cases where $\gamma>\gamma_c$, one finds

$$A(m) \approx -m\partial_m \chi_0 \approx \frac{4A_d}{\epsilon} \frac{T}{\mathsf{u}_c} m^{d-2}. \tag{278}$$

This term in the FRG equation (265) has precisely the same form and scaling as a standard (one loop) temperature term[108] with $T \to T/\mathsf{u}_c$, avoiding the occurrence of a cusp. Remarkably, this temperature takes, in the limit $m \to 0$, the same value as the effective temperature T_{eff} which arises in the modified fluctuation-dissipation relation in such systems.[2,99]

Let us now discuss in more detail the solution of the self-consistent equation (270). We start with model (276b). If in Eq. (269) we choose the exponent values from the region $v^2 \sim O(1)$, i.e., $\zeta=(2-d)/2$ and $\theta=d-2+2\zeta=0$, we find that

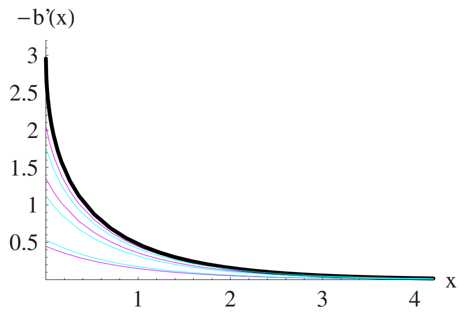

FIG. 9. (Color online) FRG flow of the equilibrium correlator $\tilde{b}'(\hat{x})$ for model (276a) in $d=1$, at the reduced temperature $T=T_{\max}/2$. The dashed lines (light blue) correspond to $m/m_c(T)=\{2,1.5,1.25\}$, from bottom to top, and the dotted lines (purple) to $m/m_c(T)=\{0.4,0.3,0.2\}$ from top to bottom. Note that the correlator only exhibits a cusp exactly at the continuous transition, $m=m_c(T)$, with $\tilde{b}_0'(m_c(T))=\epsilon=3$ (thick line). Due to the specific properties of model (276a), the correlator always equals the same master function, displaced by an m-dependent horizontal shift $\hat{x}_0$.

$$\tilde{b}_0' \sim m^{-2\tilde{\theta}}, \quad \tilde{\theta}=1-\frac{2-d}{2}\gamma, \tag{279}$$

where $\tilde{\theta}<0$ for $\gamma>\gamma_c$. Hence, with this scaling, the second cumulant in the region $v^2\sim O(N)$ tends to zero. To study this flow for $m\to 0$, one can instead use the choice $\theta\to\tilde{\theta}$ in Eq. (269) and find a fixed point for the scaled function defined in that way. Indeed, one can check easily that with the same $\zeta=(2-d)/2$, as $m\to 0$,

$$\hat{B}'(x)=m^{2-2\tilde{\theta}}\tilde{b}^{*\prime}(xm^{2\zeta}), \tag{280}$$

$$b^{*\prime}(\hat{x})=\gamma^{\gamma}\left[\frac{4A_d}{\epsilon(2-d)}\frac{T}{\mathsf{u}_c}+\hat{x}\right]^{-\gamma}, \tag{281}$$

which indicates that the force fluctuations are reduced by a factor $m^{-2\tilde{\theta}}$ in the region $v^2\sim O(N)$ as compared to the region $v^2\sim O(1)$. For model (276a), also obtained by taking $\gamma\to\infty$, the effect is even stronger, the decay of correlations being exponential of the form

$$\hat{B}'(x)\sim \exp\left(-\frac{1}{m^{2\zeta}}\frac{4A_d}{\epsilon(2-d)}\frac{T}{\mathsf{u}_c}\right)e^{-x}, \tag{282}$$

which cannot be put in the form of a scaling function as in Eq. (269). The equilibrium flow for that case in $d=1$ is shown in Fig. 9. It simply amounts to the horizontal shifting of the master function $\Phi(x)$ by $\hat{x}_0^{\rm eq}$, which is plotted in Fig. 8. While the correlator first grows with decreasing mass in the high-temperature phase (like in $d>2$), it decreases again within the glassy phase. The reason is that as m decreases below m_c, the stability of the one-step energy landscape increases and suppresses sample-to-sample fluctuations of the global shift u_k^0 of the states, which, in turn, sets the scale for force fluctuations.

2. Forces correlator, shocks, and the cusp

In the limit $\gamma\to\gamma_c$, one has $\tilde{\theta}\to 0$, as one recovers the marginal one-step solution,[109] and $\hat{B}'(0)$ then scales in the same way in the two regimes $v^2\sim 1$ and $v^2\sim N$. As noted previously, the value of $\hat{B}'(0)$ from the $v^2\sim N$ regime described by FRG is proportional to the contribution of the lower plateau to the two-point correlation at $k=0$. It also gives the sample-to-sample fluctuations of the global shift of states, u_k^0, in a given sample (163). While in the case of continuous RSB they scale as the relative fluctuations of the states, this is not the case for the nonmarginal one step, since there $G_0(k)$ (and σ_0) is much smaller than $G_1(k)-G_0(k)$. In the nonmarginal one-step case, it is the upper plateau which dominates the two-point correlation (for any $k\ll 1/m_c$). Upon moving the potential well by $v\sim N^{1/2}$, the global shift of states becomes a function of v, $u_k^0=u_k^0(v)$, the connected correlator of $u_k^0(0)$ and $u_k^0(v)$ being described by $G_{2v}(k)$. In this regime, the free energies are of order N, and one may expect that configurations centered around $u_k^0(0)$ or $u_k^0(v)$ differ typically by quantities of order $E(N)$, which diverge as $N\to\infty$ (at least, as $N^{1/2}$). In that case, when two levels cross as a function of v, the switching of the equilibrium position takes place as a function of the scaling variable $E(N)/T$. Hence, it turns into sharp jumps as $N\to\infty$ even at finite T.

If these jumps are of order $N^{1/2}$ in the displacement v, they show up as a nonanalyticity in the force correlator. This is what is observed in the case of marginal one-step and continuous RSB. On the other hand, stable (i.e., nonmarginal) one-step systems seem to have a much smoother landscape, leading to an analytic response of the system to a displacement of the well. This indicates that if there are shocks, their size does not scale with $N^{1/2}$, i.e., the system proceeds in small and effectively rounded jumps in contrast to the marginal cases.

The nonanalytic response of systems with continuous RSB is tightly bound to their marginal stability with respect to clustering. This criticality of the system implies an anomalous response to a field (v) pulling apart two replica groups, whereby the above argument suggests that this proceeds via the occurrence of shocks of size $N^{1/2}$. Notice that the presence of the nonanalyticity only relies on the marginality at u_m, whereas it is insensitive to the marginality of the RSB scheme at larger u (deeper down in the ultrametric hierarchy). This indicates that the shocks are really associated with jumps on the largest scales involving $u_k^0(v)$. That is, the whole hierarchy of states is affected, and not only part of it, as it can happen in the regime $v^2\sim 1$.

3. Some subtleties of the functional renormalization group flow for one-step replica symmetry breaking

Although we have focused on the flow at small m, interesting features also happen around the Larkin mass. At m_c, a cusp appears and $A(m)$ first vanishes at $m=m_c$, but then becomes positive again. This behavior indicates that a bifurcation in the lowest free-energy state occurs at m_c, where metastable states appear and the system is critical. However, the further evolution of the system for $m<m_c$ is smooth in the

sense that the system becomes uncritical again, with no further bifurcations occurring. This is seen to translate into a response which is regular when the harmonic well is displaced by v with $v^2 \sim N$.

To complete the discussion of the equilibrium FRG flow, we mention a subtlety (corresponding to the choice $\mathsf{u}_c = \mathsf{u}_c^{\text{eq}}$) which arises for temperatures in the range $T \in [T_c(0), T_c^{\max}]$. An inspection of the phase diagram in Fig. 4 shows that as $m \to 0$, the thermodynamic equilibrium is given by a replica-symmetric saddle point in the GVM, which is reached from the glassy phase by a *discontinuous* transition upon decreasing T. In that temperature regime, one natural continuation of the FRG flow from large to small mass is to maintain the condition $d\phi/d\mathsf{u}_c = 0$, defining $\mathsf{u}_c^{\text{“eq”}}$ even though it corresponds to $\mathsf{u}_c^{\text{“eq”}} > 1$ in the region where the genuine equilibrium is described by a RS solution. This reflects the fact that the selected states are thermodynamically irrelevant, in the sense that their Gibbs weight is negligible. Nevertheless, there are small corners of phase space where metastable states exist even when the mass is small, and among those states, the ones selected by $\mathsf{u}_c^{\text{“eq”}}$ still correspond to those with the lowest available free-energy density in typical disorder. We have verified that this branch of one-step solutions, indeed, exists down to $m=0$ for all temperatures $T < T^{\max}$.

We now turn to the discussion of other possible choices for the breakpoint. If one chooses $\mathsf{u}_c = \mathsf{u}_c^{\text{th}}$, one presumably computes the cumulant of an observable, $\hat{V}[v] = \hat{V}[v]^{\text{th}}$, defined as the free energy of the threshold states for the manifold in an external quadratic well at position v. These threshold states being known to be relevant for the dynamics, we may conjecture that the quantity computed using this criterion will find an interpretation as a part of the dynamical effective action. Note that under this prescription, the configurational entropy of the selected states, $\Sigma^{\text{th}}(m)$, grows with decreasing mass, reflecting either the bifurcation or birth of threshold states.

Another choice of breakpoint, and the only one which leads to a cusp, is $\mathsf{u}_c = \mathsf{u}^{\text{cp}}$. Then the amplitude $A(m) = 0$. Hence, it leads to similar fixed points as for the continuous RSB case. In particular, it yields a fixed point of $\tilde{b}_0'$ and freezes the renormalized correlator to the cuspy shape it attains at $m_c(T)$. The exponents are then the same, i.e., $\zeta = \zeta(\gamma)$. Note then that $\theta = \theta(\gamma) < 0$, which means that the temperature is relevant. That such a choice can be made was conjectured in Refs. 11 and 13 for $T=0$. Here, we show it to be possible at any temperature. It is not difficult to prove that one-step solutions satisfying the cusp condition (184) exist for all $T \leq T_{\max}$ and $m < m_c(T)$. Note, however, that one finds $\mathsf{u}^{\text{cp}} > 1$ for $m < m_*$ and $T > \tilde{T}_c(m)$, where $\tilde{T}_c(m)$ is the (unphysical) branch of the instability line defined by Eq. (176) (see Fig. 4).

A natural question is then as follows: What observable would be selected by this process? As discussed in Sec. III D 2, the choice u^{cp} appears to select metastable states that only exist in rare disorder configurations (the smaller m, the rarer). It remains to be understood whether such an observable could be constructed by imposing some constraint on the metastable states.

E. Nonuniform v

The above analysis is easily generalized to a nonuniform v_x, and allows us to compute the functional $\hat{R}[v]$ for a nonuniform v_x in the regime $v^2 \sim N$, where it takes the form $\hat{R}[v] = N\hat{B}[v^2]$ where $\hat{B}[v^2] := \hat{B}[\{\tilde{v}_x^2\}_x]$, i.e., it is a functional of the field $\tilde{v}_x^2$. We just give the final saddle-point equations and the resulting self-consistent equation for $\hat{B}$, which generalize the one obtained in Ref. 13 (for $R[v]$) in the replica-symmetric region [see Eq. (3.31) there with the correspondence in notations $\frac{\delta \tilde{U}_0[v \cdot v]}{\delta(v^a(x) \cdot v^b(x))} \to \sigma_{\tilde{v}}(x)$]. One easily sees that the diagonal blocks (in the space of two replica groups) are again independent of $\tilde{v}_x$ and, therefore, independent of x, and thus, simply correspond to the MP solution. Generalizing Eq. (246), the saddle-point equation in the off-diagonal sector yields a single equation, which now involves space indices:

$$\sigma_{2,\tilde{v}}(x) = -\frac{2}{T}B'\left(4\tilde{v}_x^2 + 2\left[\int_k \tilde{G}(k)\right] - 2G_{2,\tilde{v}}^{xx}\right), \quad (283)$$

where

$$G_{2,\tilde{v}}^{xx} = T\int_y g^2(x-y)\sigma_{2,\tilde{v}}(y), \quad (284)$$

which generalizes Eq. (241). As in the uniform case, $\sigma_{2,\tilde{v}=0}(x) = \sigma(0)$. Solving for the function $\sigma_{2,\tilde{v}}(x)$ yields the desired functional since

which is the analog of Eq. (248). These equations generalize Eq. (259) to a nonuniform field $\tilde{v}_x$. It would be interesting to see whether FRG equations can be derived also for the nonlocal parts of the functional $\hat{B}$, but this is left for future investigation.

V. DISCUSSION AND CONCLUSION

We have computed the renormalized disorder correlator $R(v)$ in the large-N limit for an elastic manifold in a $O(N)$ symmetric random potential in the presence of an external quadratic well. It was obtained as a physical observable describing the correlation in free energy when the center of the quadratic well is varied by v. It contains direct information about shocks, i.e., abrupt switches between two competing equilibrium positions that occur as v is varied. We have demonstrated the existence of two large-N scaling regimes $v^2 \sim 1$ and $v^2 \sim N$, and obtain closed expressions in each regime, and their zero- and low-temperature limits. Our results provide a direct connection between the GVM approach ($v=0$) using replica symmetry breaking saddle points and previous large-N FRG approaches.

We found that as v is increased, shocks start to occur at a uniform displacement of the well of order $v \sim v_* \sim L^{-d/2}$, which decreases with system size or, equivalently, for a nonuniform displacement v_x of order 1, but confined to a bounded region of volume 1 in space.[110] These shocks are rounded by temperature, but turn into a nonanalytic cusp of the force correlator at $T=0$. Our results bear some similarities to shocks found in Burger's turbulence in large dimension. The shocks can be interpreted within the RSB picture of an ultrametric phase space, which predicts that in a given disorder environment there exist several *states*, all centered within a single *big valley* whose position itself fluctuates from sample to sample. The shock regime $v \lesssim v_*$ then describes the energy crossing between states as the harmonic well is shifted, and, accordingly, it is sensitive to the replica symmetry breaking structure of the GVM approach. In particular, one finds that all GVM saddle points related by replica permutations contribute to the computation of observables. Beyond this regime, the force correlator remains constant in a large interval $N^{1/2} \gg v > v_*$, which reflects the sample-to sample fluctuations of the force density associated with the big valley, itself related to the sample-to-sample fluctuations of the global displacement u^0 of the valley.

This value of the force correlator matches perfectly with the value obtained from FRG calculations in the regime $v^2 \sim N$. In that regime, it was found that FRG recovers only the fluctuations among most distant states, which is governed by the (nontrivial) lower plateau of the self-energy function, σ_0. It is now clear that the FRG in this regime captures the shock structure of the big valley position $u^0(v)$. Indeed, imposing a position of the well on the scale $v^2 \sim N$ affects the global shift u^0 itself, which may lead to shocks. We have computed the decaying correlations between $u^0(0)$ and $u^0(v)$, as well as the force correlator. In the case of systems with continuous or marginal one-step RSB, such as manifolds in $2 \leqslant d \leqslant 4$ or directed polymers in long-range correlated disorder, we have found that their marginality toward a clustering instability implies a cusp also in this second scaling regime $v^2 \sim N$. This reflects the fact that the shift of the center of the well provokes shocks which are abrupt even at finite T because they involve the crossing of energies which scale with N. By establishing the persistence of the nonanalytic force correlator throughout the regime of small m and T, we have proved that the previously obtained FRG flow had been correctly extended into the glassy regime.

A major step forward has been achieved in the case where the regime $v^2 \sim 1$ displays a nonmarginal one-step RSB, a problem which was left open in the previous FRG study. In particular, we have found that in the regime $v^2 \sim N$, the force correlator is nonanalytic only at the glass transition, but not within the glassy regime. We interpret the latter in terms of a smooth energy landscape, where the manifold evolves smoothly (on the scale $N^{1/2}$) as the center of the harmonic well is varied. In the glassy regime, the disorder correlator becomes strongly suppressed with decreasing mass, which is a consequence of the increasing stability of the one-step landscape and the associated smallness of sample-to-sample fluctuations of u^0. Further, we have shown how the exact FRG equations in the regime $v^2 \sim N$ can be extended into the glassy regime, and how replica symmetry breaking translates into an anomaly in the FRG flow equation. Moreover, the possibility of studying nonequilibrium branches of metastable states in a one-step system by tuning the breakpoint parameter u_c was found to be equivalent to tuning the anomaly in the FRG equation.

The present study raises many questions. First, at finite N, the two scaling regimes in v are not clearly distinct. The main task is then to determine which aspect of either regime will persist at finite N. Until now, the FRG flow equation in the loop expansion seemed to connect more directly to the regime $v^2 \sim N$. In particular, one then expects that the shocks of the regime $v^2 \sim N$ should become rounded by temperature at finite N, as was found in FRG calculations in the loop expansion and for $N=1$. However, the present study raises the possibility of a different regime in the FRG accessible only at smaller v. The interpretation of the cusp at $T=0$ in terms of shocks remains valid, and offers an interesting venue for future studies going beyond the mean-field picture of switching between states. These concepts also generalize to other disordered systems, e.g., to spin glasses, where the statistics and properties of shocks can be studied by similar methods. Work is in progress in this direction. This should yield valuable new insight into the structure of the phase space and elementary excitations, such as droplets.

Note added in proof. Recently, we became aware of the work of Yoshino and Rizzo[115] which studies related spin models and obtains results on shocks and cusps similar to those discussed in the present work for the regime $v^2 \sim 1$.

ACKNOWLEDGMENTS

We wish to thank Leon Balents for useful discussions at an early stage of this work (in relation to Ref. 47) on the possibility of several scaling regimes at large N and on issues concerning the thermal boundary layer. We also thank J. P. Bouchaud, M. Mézard, and A. Middleton for interesting discussions. M.M. was supported by Grant No. PA002-113151 from the Swiss National Fund for Scientific Research. P.L.D. and K.W. acknowledge support from ANR program blan05-0099-01. We acknowledge the hospitality of the KITP where part of this work was accomplished.

APPENDIX A: RESTORING DIMENSIONS

In the main body of the text, we used the natural units r_f for transverse lengths, μ_c for the mass (and $1/\mu_c$ for longitudinal lengths in $d>0$), and E_c for energies. In order to recover the full dependence on the parameters B_0, r_f, and c, one simply has to restore the dimensionful units so as to render all quantities dimensionless:

masses and longitudinal length scales:

$$m,k,\Lambda \to \frac{1}{\mu_c}[m,k,\Lambda],$$

$$L \to L\mu_c,$$

temperature and energy densities:

$$T \to T/E_c,$$

$$\phi,f \to \frac{1}{E_c\mu_c^d}[\phi,f],$$

transverse fluctuations:

$$u,v \to \frac{1}{r_f}[u,v],$$

$$G(k=0) \to \frac{\mu_c^d}{r_f^2} G(k=0),$$

$$\int_k G(k),\chi \to \frac{1}{r_f^2}\left[\int_k G(k),\chi\right],$$

self-energy and other auxiliary functions:

$$\sigma,\Sigma_1,g^{-1}(k) \to \frac{r_f^2}{\mu_c^d E_c}\left[\sigma,\Sigma_1,g^{-1}\left(\frac{k}{\mu_c}\right)\right],$$

$$I_n \to \frac{E_c}{r_f^2}\left(\frac{E_c \mu_c^d}{r_f^2}\right)^{n-1} I_n,$$

$$\hat{B}^{(n)}(z) \to \frac{r_f^{2n}}{\mu_c^d E_c^2}\hat{B}^{(n)}\left(\frac{z}{r_f^2}\right),$$

$$\hat{R}(v) \to \frac{1}{\mu_c^d E_c^2}\hat{R}\left(\frac{v}{r_f}\right),$$

$$\hat{R}[v],R_n,\mathcal{R}_n \to \frac{1}{E_c^2}\left[\hat{R}\left[\frac{v}{r_f}\right],R_n,\mathcal{R}_n\right],$$

$$\hat{W},q,Q,\mathsf{u},\tilde{b} \to \hat{W},q,Q,\mathsf{u},\tilde{b}. \tag{A1}$$

With these substitutions, all equations turn into dimensionless identities, whereby in some cases additional factors of $c=\mu_c^{d-2}E_c r_f^2$ need to be restored. Note that amplitudes such as A being dimensionless are unchanged.

APPENDIX B: DIRECT EXPANSION OF $\hat{W}$ TO ORDER v^4

The perturbative expansion of Eq. (61) to second order requires

$$P_{abcd}^{(2)} := \sum_\pi{}' G_{ab}^{(\pi)} G_{cd}^{(\pi)}. \tag{B1}$$

In the case of two sets of replica with $v^a=v^{12}/2$ for $a=1,\ldots,n/2$ and $v^a=-v^{12}/2$ for $a=n/2+1,\ldots,n$, one has $G_{ab}=q_{ab}/2$ with q_{ab} defined in Eq. (87). As for the sum $P_{ab}^{(1)}:=\Sigma_\pi' G_{ab}^{(\pi)}=\alpha\delta_{ab}+\beta$ [cf. Eq. (68)], replica symmetry restricts this tensor to take the form

$$\begin{aligned}P_{abcd}^{(2)} &= A\delta_{abcd} + B(\delta_{abc}+\delta_{abd}+\delta_{acd}+\delta_{bcd}) + C_1\delta_{ab}\delta_{cd}\\ &\quad + C_2(\delta_{ac}\delta_{bd}+\delta_{ad}\delta_{bc}) + D_1(\delta_{ab}+\delta_{cd})\\ &\quad + D_2(\delta_{ac}+\delta_{ad}+\delta_{bc}+\delta_{bd}) + E,\end{aligned} \tag{B2}$$

the coefficients of which can be obtained by solving the system of linear constraints arising from the identities

$$\sum_a P_{abcd}^{(2)} = G^c P_{cd}^{(1)},$$

$$\delta_{ab}P_{abcd}^{(2)} = \tilde{G} P_{cd}^{(1)},$$

$$\sum_a \delta_{ac}\delta_{bd}P_{abcd}^{(2)} = \sum_a G_{ab}^2.$$

The quantity of interest for the second-order expansion of Eq. (61) is the second cumulant:

$$\hat{W}[v]^{(2)} = \frac{1}{2}\left[\sum_{abcd} v^a v^b v^c v^d P_{abcd}^{(2)} - \left(\sum_{abcd} v^a v^b P_{ab}^{(1)}\right)^2\right]. \tag{B3}$$

For the case of two-replica groups, one obtains the final result:

$$\begin{aligned}\hat{W}[v]^{(2)} &= \frac{1}{2}v^4[nA + n^2(C_1+2C_2) - n^2\alpha^2]\\ &= \frac{v^4 n^2(2-n)}{(3-n)(1-n)^2}\left[\left(\sum_{a\neq 1} G_{1a}\right)^2 - (1-n)\sum_{a\neq 1} G_{1a}^2\right]\\ &= \frac{2v^4}{3}\left[\int_0^1 G^2(\mathsf{u})d\mathsf{u} - \left(\int_0^1 G(\mathsf{u})d\mathsf{u}\right)^2\right]n^2 + O(n^3).\end{aligned} \tag{B4}$$

From this, one derives Eq. (114) in the text by recalling that

$$R_2[v] = \lim_{n\to 0}\frac{4T^2}{n^2}\hat{W}[v]^{(2)} \tag{B5}$$

and $G(\mathsf{u})=q(\mathsf{u})/2$.

APPENDIX C: A USEFUL IDENTITY

For any function $\Phi(y)$ with derivatives decreasing strictly faster[111] than $1/|y|$ for large $|y|$, one has

$$\int_{-\infty}^{\infty} dy\, y[\Phi(y+z)+\Phi(y-z)-2\Phi(y)] = -z^2[\Phi(\infty) - \Phi(-\infty)]. \tag{C1}$$

Indeed,

$$\begin{aligned}&\int_{-\infty}^{\infty} dy\, y[\Phi(y+z)+\Phi(y-z)-2\Phi(y)]\\ &= \int_{-\infty}^{\infty} dy\, y \int_0^z dz'[\Phi'(y+z')-\Phi'(y-z')]\\ &= -\int_{-\infty}^{\infty} dy \int_0^z dz'[\Phi(y+z')-\Phi(y-z')]\\ &= -\int_{-\infty}^{\infty} dy \int_0^z dz' \int_{-z'}^{z'} dz''\, \Phi'(y+z'')\\ &= -[\Phi(\infty)-\Phi(-\infty)]\int_0^z dz' \int_{-z'}^{z'} dz''\\ &= -z^2[\Phi(\infty)-\Phi(-\infty)].\end{aligned}$$

Applied to integrals over Gaussian averages, normalized such that $\langle z^2\rangle_z=1$, Eq. (C1) implies

$$\int_{-\infty}^{\infty} dy\, y[\langle \Phi(y+\sqrt{Q}z)\rangle_z - \Phi(y)] = -\frac{Q}{2}[\Phi(\infty) - \Phi(-\infty)]. \tag{C2}$$

APPENDIX D: PERTURBATION EXPANSION FOR $L^d v^2 \ll 1$

Here, we compute the two lowest orders in the expansion defined in Sec. III C 2. The functions $m_{1,2}$ satisfy, from Eq. (111),

$$\dot{m}_1 = -\frac{1}{2}\dot{q}(\mathsf{u})[m_0'' + \mathsf{u}(m_0^2)'], \tag{D1}$$

$$\dot{m}_2 = -\frac{1}{2}\dot{q}(\mathsf{u})[m_1'' + \mathsf{u}(2m_0 m_1)'], \tag{D2}$$

To lowest order, using that

$$m_0'' + (m_0^2)' = 0, \tag{D3}$$

one has to solve

$$\dot{m}_1 = -\frac{1}{2}(1-\mathsf{u})\dot{q}(\mathsf{u})m_0''. \tag{D4}$$

The solution is

$$m_1 = p(\mathsf{u})m_0'', \quad p(\mathsf{u}) = \frac{1}{2}\int_{\mathsf{u}}^{\mathsf{u}_c} d\tilde{\mathsf{u}}(1-\tilde{\mathsf{u}})\dot{q}(\tilde{\mathsf{u}}). \tag{D5}$$

Integration by parts gives $2p(\mathsf{u}_m)=\int_0^1 d\mathsf{u}(1-\mathsf{u})\dot{q}(\mathsf{u})=-q(0)+\int_0^1 q(\mathsf{u})d\mathsf{u}$. The integration range can be extended to the interval $[0,1]$ since $\dot{q}=0$ outside $[\mathsf{u}_m,\mathsf{u}_c]$. By plugging this into Eq. (112) and using $\int_0^\infty y m_0''=-\int_0^\infty m_0'=-1$, the term proportional to $q(0)$ cancels and one obtains Eq. (113) in the text.

The next-order correction satisfies, from Eqs. (D5) and (D2),

$$\dot{m}_2 = -\frac{1}{2}\dot{q}(\mathsf{u})p(\mathsf{u})[m_0'''' + \mathsf{u}(2m_0 m_0'')']. \tag{D6}$$

This gives

$$m_2 = \frac{1}{2}m_0''''\int_{\mathsf{u}}^{\mathsf{u}_c} d\tilde{\mathsf{u}}\,\dot{q}p + (m_0 m_0'')'\int_{\mathsf{u}}^{\mathsf{u}_c} d\tilde{\mathsf{u}}\,\tilde{\mathsf{u}}\dot{q}p. \tag{D7}$$

In order to calculate Eq. (112), we need

$$\int_{-\infty}^{\infty} dy\, y m_0'''' = -[m_0'']_{-\infty}^{\infty} = 0, \tag{D8}$$

$$\int_{-\infty}^{\infty} dy\, y(m_0 m_0'')' = \int_{-\infty}^{\infty} dy\, m_0(m_0^2)' = \frac{4}{3}, \tag{D9}$$

where on the second line we used Eq. (D3). Inserting into Eq. (112) gives

$$R_2[v] = \frac{8}{3}T^2\int_0^1 d\mathsf{u}\,\mathsf{u}\dot{q}(\mathsf{u})p(\mathsf{u}), \tag{D10}$$

where $p(\mathsf{u})$ is defined in Eq. (D5). Substituting the definitions (D4) and (D5), $\mathsf{u}\dot{q}=2\dot{p}+\dot{q}$, integrating by parts, and using $p(1)=0$, one finds

$$\int_0^1 d\mathsf{u}\,\mathsf{u}\dot{q}(\mathsf{u})p(\mathsf{u}) = [p^2+qp]_0^1 - \frac{1}{2}\int_0^1 d\mathsf{u}(\mathsf{u}-1)q\dot{q}$$
$$= \frac{1}{4}\int_0^1 d\mathsf{u}\,q^2 - \frac{1}{4}q(0)^2 - p(0)[p(0)+q(0)], \tag{D11}$$

which with $p(0)=(1/2)[\int_0^1 d\mathsf{u}q - q(0)]$ yields the final result (114) in the text.

APPENDIX E: THERMAL BOUNDARY LAYER OF THE EFFECTIVE POTENTIAL CORRELATOR

Here, we revisit and complete the calculation of the effective potential defined in Ref. 47 in an attempt to connect with the FRG function $R(u)$. The effective potential studied there is constructed (see Ref. 47 for details) from the probability distribution for a given Fourier mode $u=u_k$ (denoted there $\vec{\phi}_0$) in a given environment. This sample dependent probability is denoted here $Z_V[u]$ (unnormalized) and there $\mathcal{P}_\Omega(\vec{\phi}_0)$. The authors then introduce the potential correlator:

$$\mathcal{V}(u-u') = -\lim_{n\to 0}\frac{\overline{Z(u)^{n/2}Z(u')^{n/2}} - \overline{Z(u)}^{n/2}\overline{Z(u')}^{n/2}}{(n/2)^2\beta^2}, \tag{E1}$$

describing the second moment of the effective potential $\tilde{V}(u)=\beta^{-1}\ln[Z(u)]$. This is the central object studied there. Although it is a very physical object, it is very different from the effective potential studied here $\hat{V}(v)$—which is also a physical observable—but involves a source (implemented via a quadratic well). As a result, $\tilde{V}(u)$ cannot be connected to the standard FRG.[112] Some discussion of the differences between the two approaches was given in Sec. VIII G of Ref. 13. Here, we discuss more of the differences in details, based on explicit calculation.

Since this version of an effective disorder is also interesting, it is worthy to push here further the calculation of Ref. 47. To avoid confusion between u (displacement field) and u (replica overlap), we replace everywhere $u\to v$, keeping in mind, however, that its physical meaning is different from the one (position of well center) given in the text. The above partition function can be evaluated via a saddle point as in the GVM:

$$\overline{\prod_{a=1}^{n} Z(v^a)} = \sum_{\pi} \exp\left[-\frac{\beta}{2} v^{\pi(a)} G_{ab}^{-1}(k) v^{\pi(b)}\right]$$
$$= \exp\left[-\frac{n\beta}{4}(k^2+m^2)(v^2+v'^2)\right]$$
$$\times \sum_{\pi} \exp\left[\frac{\beta}{2}(v^{\pi(a)}\sigma_{ab} v^{\pi(b)})\right]. \quad \text{(E2)}$$

In the same way as we derived $R[v]$, we can compute the correlator of $\tilde{\mathcal{V}}$ as

$$\mathcal{V}(v-v') = -2T^2 \int_{-\infty}^{\infty} dy\, y[\tilde{M}(0,y) - \tanh(y)],$$

where $\tilde{M}$ satisfies the same flow equation as M, but with the "inverse coupling":

$$\tilde{q}(\mathsf{u}) = \frac{\beta}{4}(v-v')^2 \sigma(\mathsf{u}). \quad \text{(E3)}$$

We can now apply our general expressions (126) and (134) to the above case and find for the thermal boundary layer:

$$-\mathcal{V}(v-v') = \mathcal{V}_0(v-v') + \mathcal{V}_1(v-v') + \cdots, \quad \text{(E4)}$$

where

$$\mathcal{V}_0(v-v') = -2T^2 \tilde{q}(\mathsf{u}_c) = -\frac{T\sigma(\mathsf{u}_c)}{2}(v-v')^2,$$

$$\mathcal{V}_1(v-v') = T^2 \int_{\mathsf{u}_m}^{\mathsf{u}_c} d\mathsf{u} \left(\mathsf{u}\frac{d\tilde{q}}{d\mathsf{u}}\right) \langle \psi(z\sqrt{2(\tilde{q}_c - \tilde{q})})\rangle_z$$
$$= (v-v')^2 \mathsf{u}_c \sigma_c (1+\gamma) \int_{m^\theta/m_c^\theta}^{1} dv\, v^{(2/\theta)-1}$$
$$\times \left\langle \psi\left(z\left|\frac{v-v'}{T}\right| \sqrt{\frac{T\sigma_c}{2}(1-v^{(2/)\theta-1})}\right)\right\rangle_z, \quad \text{(E5)}$$

where $\sigma_c = \sigma(\mathsf{u}_c)$. These formulas have well-defined limits as $T \to 0$ (recalling that $\mathsf{u}_c/T = A m_c^\theta$ and $T\sigma_c = 2m_c^{2-\theta}/[(2-\theta)A]$). For $m \to 0$, the last term reduces to

$$\mathcal{V}_1(v-v') \to \frac{(v-v')^3 \mathsf{u}_c \sigma_c (T\sigma_c)^{1/2}}{4} \frac{\Gamma[1+\theta/(2-\theta)]}{\Gamma[(5/2)+\theta/(2-\theta)]}.$$

With the notation introduced in Ref. 47 (for $d \geqslant 2$),

$$1+\gamma := \frac{2}{\theta} - 1 = \frac{4-d}{d-2}, \quad \text{(E6)}$$

$$g := \frac{1+\gamma}{8} \beta\sigma(\mathsf{u}_c) u_c^2 (v-v')^2, \quad \text{(E7)}$$

the above results can be recast into the form

$$\mathcal{V}(v-v') = -\mathcal{V}_0 - \mathcal{V}_1 = \frac{4}{(\beta \mathsf{u}_c)^2}\left[\frac{g}{1+\gamma} - \mathsf{u}_c^3 \Upsilon_2\left(\frac{g}{\mathsf{u}_c^2}\right)\right],$$

where

$$\Upsilon_2(x) = \frac{x}{2}\left\langle \int_0^1 dv\, v^{1+\gamma} \psi\left(z\sqrt{\frac{4x(1-v^{1+\gamma})}{1+\gamma}}\right)\right\rangle_z, \quad \text{(E8)}$$

and $\psi(x) = 2x\coth(x)$, as before. Using $\psi(x) \to 2|x|$ for large arguments, one further finds

$$\Upsilon_2(x) \overset{x\to\infty}{\to} \sqrt{2} x^{3/2}\left[\frac{1}{(1+\gamma)^{5/2}} \frac{\Gamma(1/(1+\gamma))}{\Gamma[(5/2)+1/(1+\gamma)]}\right].$$

The term in brackets is easily seen to tend to 1 as $1+\gamma = \epsilon/(d-2) \to 0$. Thus, $\Upsilon_2^{\epsilon\to 0}(x\to\infty) \to \sqrt{2}x^{3/2}$.[113]

For large arguments v, the flow of $\tilde{M}$ is attracted to an intermediate fixed point $\tilde{M}(\mathsf{u},y) \approx \tanh(\mathsf{u}y)$. This happens for a large coupling parameter $g \gg 1$ [or, more explicitly, for displacements such that $(v-v')^2 m_c^{2+\theta} \gg 1$]. If, in addition, the mass is sufficiently small, $(v-v')^2 \ll m^{-(2+\theta)}$, the correlator $\mathcal{V}$ is controlled by this intermediate fixed point and can be shown to scale as

$$\mathcal{V}(v-v') \sim g^{2\theta/(2+\theta)} \sim (v-v')^{4\theta/(2+\theta)}. \quad \text{(E9)}$$

An important difference to the FRG correlator $R(v)$ concerns the scale on which the nonanalyticity lives in $\mathcal{V}(v)$. Comparing $\mathcal{V}_0$ and $\mathcal{V}_1$, we find that higher-order terms become dominant for $v \geqslant v_{**} \sim m_c^{(2+\theta)/2}$, reflecting the fact that the effective potential correlator $\mathcal{V}$ is sensitive to physics on the Larkin scale, rather than to shocks occurring on the scale m, as is the case for the FRG correlator.

APPENDIX F: COMPARISON WITH THE THERMAL BOUNDARY LAYER FOR DROPLETS

Due to the $O(N)$ symmetry, the disorder correlator is only a function of $v = |\vec{v}|$ (for spatially uniform v). Accordingly, the force correlator splits into transverse and longitudinal parts:

$$-\partial_{v_i}\partial_{v_j}\hat{R}(v) = \Delta_L(v)\frac{v_i v_j}{v^2} + \Delta_T(v)\left(\delta_{ij} - \frac{v_i v_j}{v^2}\right), \quad \text{(F1)}$$

with $\Delta_L(v) = -\hat{R}''(v)$ and $\Delta_T(v) = -\frac{\hat{R}'(v)}{v}$, derivatives being with respect to $v = |\vec{v}|$. Both correlators are equal at $v=0$, so that $\partial_{v_i}\partial_{v_j}\hat{R}(v)$ is well defined and proportional to δ_{ij} at $v = 0$. Note that at large N, one has $\frac{1}{N}\Sigma_i \partial_{v_i}^2 \mathcal{R} = \Delta_T(v) + O(1/N)$, and hence, the transverse components dominate the average force correlator.

The TBL contribution to the droplet force correlator (155) can be expressed in terms of longitudinal and transverse correlators:

$$-\Delta_L^{\text{drop}}(v) = T\frac{m^4}{4}\left\langle y_1^2 \psi\left(\frac{m^2 y_1}{2}\hat{v}\right)\right\rangle_y, \quad \text{(F2)}$$

$$-\Delta_T^{\text{drop}}(v) = T\frac{m^4}{4}\left\langle y_2^2 \psi\left(\frac{m^2 y_1}{2}\hat{v}\right)\right\rangle_y, \quad \text{(F3)}$$

where $y_1 = y_\parallel$ denotes the component of y parallel to v, while y_2 is an arbitrary orthogonal component.

To make contact with expressions obtained for the manifolds, we recast these expressions into the form

$$-\Delta_{L,T}^{\rm drop}(v) = T\int db\, \rho_{L,T}^{\rm drop}(b)\psi(b|\hat{v}|), \tag{F4}$$

with the distributions

$$\rho_L^{\rm drop}(b) = \frac{2}{m^2}\int d^{N-1}y_\perp b^2 D\left(y_\parallel = \frac{2b}{m^2}, y_\perp\right),$$

$$\rho_T^{\rm drop}(b) = \frac{2}{m^2}\int d^{N-1}y_\perp \left(\frac{m^2 y_2}{2}\right)^2 D\left(y_\parallel = \frac{2b}{m^2}, y_\perp\right). \tag{F5}$$

In computing the force correlators (159), we have used that

$$\partial_{\hat{v}}\langle \hat{v}^2\psi(\hat{v}xz)\rangle_z = \left\langle 2\hat{v}\psi(\hat{v}xz) + \hat{v}z\frac{d}{dz}\psi(\hat{v}xz)\right\rangle_z = \langle \hat{v}(1+z^2)\psi(\hat{v}xz)\rangle_z, \tag{F6}$$

$$\partial_{\hat{v}}^2\langle \hat{v}^2\psi(\hat{v}xz)\rangle_z = \left\langle (1+z^2)\psi(\hat{v}xz) + z(1+z^2)\frac{d}{dz}\psi(\hat{v}xz)\right\rangle_z = \langle (z^4-z^2)\psi(\hat{v}xz)\rangle_z. \tag{F7}$$

APPENDIX G: ONE-STEP SADDLE POINTS IN THE GAUSSIAN VARIATIONAL METHOD AND THEIR LOW TEMPERATURE LIMITS

Here, we first give for completeness the general one-step saddle-point equations for the equilibrium statics, valid for any d and Λ. Equations (166)–(168), (170), (171), and (174) form a closed set of equations, which together with Eqs. (169) and (170) determines $\mathsf{u}_c = \mathsf{u}_c^{\rm eq}$:

$$0 = \frac{d\phi(\mathsf{u}_c)}{d\mathsf{u}_c} = \frac{1}{2T}[B(\chi_0) - B(\chi_1) - (\chi_0-\chi_1)B'(\chi_0)] - \frac{T}{2\mathsf{u}_c^2}\int_k \left[\frac{\Sigma_1}{g_k^{-1}+\Sigma_1} - \ln(1+\Sigma_1 g_k)\right]. \tag{G1}$$

The easiest way to show this is to consider Σ_1 and u_c as independent variational parameters of the saddle-point equations, such that $d\Sigma_1/d\mathsf{u}_c = 0$, and then use Eq. (175).

Let us now analyze the limit $T\to 0^+$ of the various one-step saddle points for $d<2$ and $\Lambda=\infty$. It is easy to see that the corresponding saddle-point equations (174) and (175) together with the three possible conditions (178) and (183), or (184) admit solutions of the form $\mathsf{u}_c = T\hat{\mathsf{u}}_c$ with finite $\hat{\mathsf{u}}_c$ as $T\to 0$:

$$\chi_0 = \frac{4A_d}{\epsilon(2-d)}\frac{1}{\hat{\mathsf{u}}_c}\left[\frac{1}{m^{2-d}} - \frac{1}{(m^2+\Sigma_1)^{1-d/2}}\right],$$

$$\chi_1 \sim T \to 0,$$

$$\Sigma_1 = -2\hat{\mathsf{u}}_c[B'(\chi_1) - B'(\chi_0)] \to -2\hat{\mathsf{u}}_c[B'(0) - B'(\chi_0)]. \tag{G2}$$

The three possible values for the breakpoint are

(i) existence of a cusp in the FRG in the large-v regime ($\hat{\mathsf{u}}_c = \hat{\mathsf{u}}_c^{\rm cp}$), i.e., condition (184):

$$\frac{4A_d}{\epsilon m^\epsilon}B''(\chi_0) = 1, \tag{G3}$$

(ii) the equilibrium static condition ($\hat{\mathsf{u}}_c = \hat{\mathsf{u}}_c^{\rm eq}$), which from Eq. (G1), using Eq. (173), reads

$$\frac{d\phi}{d\hat{\mathsf{u}}_c} = 0 = \frac{1}{2}[B(\chi_0) - B(0) - \chi_0 B'(\chi_0)] - \frac{A_d}{\epsilon(2-d)\hat{\mathsf{u}}_c^2}\left(\frac{\Sigma_1}{(m^2+\Sigma_1)^{1-(d/2)}} - \frac{2}{d}[(m^2+\Sigma_1)^{d/2} - m^d]\right), \tag{G4}$$

(iii) the condition (183) for threshold states ($\hat{\mathsf{u}}_c = \hat{\mathsf{u}}_c^{\rm th}$), which is equivalent to

$$\Sigma_1 = m_c^2(T) - m^2 \to m_c^2(0) - m^2. \tag{G5}$$

For concreteness, we give explicit results for model (276a) in the limit $m\to 0$; an illustration for general m and $d=1$ at a fixed temperature can be found in Fig. 4.

For small m, $B(\chi_0)\sim B'(\chi_0)\sim e^{-\chi_0}\to 0$ and $\sigma_0\to 0$. One finds, from Eq. (G1), *for any* $0<T<T_c$:

$$\mathsf{u}_c^{\rm eq} e^{d(1-\mathsf{u}_c^{\rm eq})/\epsilon} = \frac{T}{T_c}, \quad \Sigma_1^{\rm eq} = 2\frac{\mathsf{u}_c^{\rm eq}}{T}e^{-d\mathsf{u}_c^{\rm eq}/(2-d)}, \tag{G6}$$

where T_c is given in Eq. (186). Using condition (iii), one finds, for any $0<T<T_d$,

$$\mathsf{u}_c^{\rm th} e^{2(1-\mathsf{u}_c^{\rm th})/\epsilon} = \frac{T}{T_d}, \tag{G7}$$

$$\Sigma_1^{\rm th} = m_c^2(T) = 2\frac{\mathsf{u}_c^{\rm th}}{T}e^{-2\mathsf{u}_c^{\rm th}/(2-d)}, \tag{G8}$$

where T_d is the dynamical transition temperature given in Eq. (187). In the $T\to 0$ limit, one obtains[114]

$$\hat{\mathsf{u}}_c^{\rm eq} = \left[\frac{2^{1+(d/2)}A_d}{d\epsilon}\right]^{2/\epsilon} = \frac{1}{T_c\exp(d/\epsilon)} \overset{d=1}{=} 0.7937,$$

$$\hat{\mathsf{u}}_c^{\rm th} = \frac{m_c(0)^2}{2} = \frac{1}{2}\left(\frac{4A_d}{\epsilon}\right)^{2/\epsilon} \overset{d=1}{=} \frac{1}{2}. \tag{G9}$$

The cusp condition (G3) imposes that $\chi_0\sim\log m$, and from the saddle-point equations, it follows that

$$\hat{\mathsf{u}}_c^{\rm cp} \sim m^{d-2}/\log(1/m) \to \infty. \tag{G10}$$

We finally determine the $T\to 0$ limit of the configurational entropy associated to this branch of cuspy solutions, $\Sigma(\hat{\mathsf{u}}_c^{\rm cp}) = \hat{\mathsf{u}}_c^2\frac{d\phi}{d\hat{\mathsf{u}}_c}$. For $m \ll m_c$, one finds $\Sigma_1 \approx 2\hat{\mathsf{u}}_c^{\rm cp} \gg m$. Hence, the leading term in the configurational entropy is

$$\Sigma(\hat{u}_c^{\rm cp}) \approx (\hat{u}_c^{\rm cp})^2 \frac{d\phi}{d\hat{u}_c} \xrightarrow{T\to 0, m\to 0} -\frac{(\hat{u}_c^{\rm cp})^2}{2} \approx -8\left[\frac{A_d m^{d-2}}{(2-d)\epsilon \log(4A_d/\epsilon m^{\epsilon})}\right]^2, \tag{G11}$$

which is negative. Hence, the condition (G3) selects exponentially rare configurations.

APPENDIX H: THERMAL BOUNDARY LAYER IN THE CASE OF ONE-STEP REPLICA SYMMETRY BREAKING

Here, we prove that the thermal boundary layer in the one-step case can be written as

$$\mathcal{R}_1[v] = 2T^2 u_c V(\sqrt{Q}), \tag{H1}$$

where

$$V(\sqrt{Q}) = \int_0^Q dQ' \langle z\sqrt{2Q'} \coth(z\sqrt{2Q'})\rangle_z. \tag{H2}$$

Since both expressions at small Q are easily seen to be of order $O(Q)$, it is sufficient to show the equivalence for the second derivative with respect to $\sqrt{Q}$. Taking the second derivative of $\mathcal{R}_1[v]$ in Eq. (199), we find

$$\frac{1}{2T^2 u_c}\frac{\partial^2}{\partial(\sqrt{Q})^2}\mathcal{R}_1 = -\int_{-\infty}^{\infty} dy \langle z^2\Phi_z''(\Phi_z - \Phi) + z^2(\Phi_z')^2 - z^2\Phi_z''(\Phi_{z'} - \Phi) - zz'\Phi_z'\Phi_{z'}' - 1\rangle_{z,z'}, \tag{H3}$$

where $\Phi = \Phi(y) = \ln\cosh(y)$, $\Phi_z = \Phi(y + z\sqrt{Q})$, and primes denote derivatives with respect to y. After a partial integration (in y) of the terms containing Φ'', the expression simplifies to

$$\int_{-\infty}^{\infty} dy \langle z(z-z')(1-\Phi_z'\Phi_{z'}')\rangle_{z,z'} = \left\langle \frac{(z-z')^2}{2}\psi[(z-z')\sqrt{Q}]\right\rangle_{z,z'} = \langle z^2\psi(z\sqrt{2Q})\rangle_z, \tag{H4}$$

where $\psi(a) = 2a\coth(a)$ as in Eq. (133), and we have used the fact that $z+z'$ and $z-z'$ are independent Gaussian variables with variance 2.

On the other hand, one finds

$$V'(\sqrt{Q}) = 2\sqrt{Q}\langle z\sqrt{2Q}\coth(z\sqrt{2Q})\rangle_z,$$

$$V''(\sqrt{Q}) = \langle 4z\sqrt{2Q}\coth(z\sqrt{2Q})\rangle_z + \langle 2\sqrt{2Q}z^2\partial_z\coth(z\sqrt{2Q})\rangle_z = \langle 2\sqrt{2Q}z^3\coth(z\sqrt{2Q})\rangle_z = \langle z^2\psi(z\sqrt{2Q})\rangle_z, \tag{H5}$$

where we performed a partial integration in the second but last line (with the remaining term coming from the derivative of the measure $e^{-z^2/2}$), completing the proof.

APPENDIX I: GENERAL SOLUTION FOR CONTINUOUS REPLICA SYMMETRY BREAKING

The general continuous RSB solution has been derived in detail for the model $g_k^{-1} = k^2 + m^2$ in Ref. 13. Here, we sketch its generalization to arbitrary g_k^{-1}. A continuous RSB ansatz is always just marginally stable on all scales, as expressed in the present case by the identity

$$1 = 4B''\left(2\int_k \tilde{G}(k) - G(k,u)\right)\int_k \frac{1}{[g_k^{-1} + [\sigma](u)]^2}, \tag{I1}$$

for all $u_m < u < u_c$. Using Eq. (15), which in continuous form reads $\sigma(u) = -\frac{2}{T}B'(2\int_k \tilde{G}(k) - G(k,u))$, this leads to the relation

$$\sigma(u) = -\frac{2}{T}B'\left((B'')^{-1}\left(\frac{1}{4\int_k [g_k^{-1} + [\sigma](u)]^{-2}}\right)\right). \tag{I2}$$

Further, the relation $1/u = d\sigma/d[\sigma]$ allows one to solve for $\sigma(u)$.

In particular, using $[\sigma](u_m) = 0$, we find immediately the general expression for $\sigma(u_m) = \sigma(0)$:

$$\sigma(0) = \sigma(u_m) = -\frac{2}{T}B'\left((B'')^{-1}\left(\frac{1}{4I_2}\right)\right). \tag{I3}$$

[1] M. Mézard, G. Parisi, and M. A. Virasoro, *Spin Glass Theory and Beyond* (World Scientific, Singapore, 1987).

[2] L. F. Cugliandolo and J. Kurchan, Phys. Rev. Lett. **71**, 173 (1993).

[3] J.-P. Bouchaud, L. Cugliandolo, J. Kurchan, and M. Mézard, *Spin Glasses and Random Fields*, edited by A. P. Young (World Scientific, Singapore, 1997).

[4] D. S. Fisher, Phys. Rev. B **31**, 7233 (1985).

[5] D. S. Fisher, Phys. Rev. Lett. **56**, 1964 (1986).

[6] L. Balents and D. S. Fisher, Phys. Rev. B **48**, 5949 (1993).

[7] P. Chauve, P. Le Doussal, and K. J. Wiese, Phys. Rev. Lett. **86**, 1785 (2001).

[8] P. Chauve and P. Le Doussal, Phys. Rev. E **64**, 051102 (2001).

[9] S. Scheidl and Y. Dincer, arXiv:cond-mat/0006048 (unpublished).

[10] Yusuf Dincer, M.S. thesis, Universität Köln, 1999.

[11] P. Le Doussal and K. J. Wiese, Phys. Rev. Lett. **89**, 125702 (2002).

[12] P. Le Doussal, K. J. Wiese, and P. Chauve, Phys. Rev. E **69**, 026112 (2004).

[13] P. Le Doussal and K. J. Wiese, Phys. Rev. B **68**, 174202 (2003).

[14] P. Le Doussal and K. J. Wiese, Nucl. Phys. B **701**, 409 (2004).
[15] P. Le Doussal and K. J. Wiese, Phys. Rev. E **72**, 035101(R) (2005).
[16] D. E. Feldman, Phys. Rev. B **61**, 382 (2000).
[17] D. E. Feldman, Int. J. Mod. Phys. B **15**, 2945 (2001).
[18] D. E. Feldman, Phys. Rev. Lett. **88**, 177202 (2002).
[19] G. Tarjus and M. Tissier, Phys. Rev. Lett. **93**, 267008 (2004).
[20] L. Balents and P. Le Doussal, Europhys. Lett. **65**, 685 (2004).
[21] L. Balents and P. Le Doussal, Phys. Rev. E **69**, 061107 (2004).
[22] L. Balents and P. Le Doussal, Ann. Phys. (N.Y.) **315**, 213 (2005).
[23] P. Le Doussal and K. J. Wiese, Phys. Rev. Lett. **96**, 197202 (2006).
[24] P. Le Doussal and K. J. Wiese, Phys. Rev. Lett. **98**, 269704 (2007).
[25] G. Tarjus and M. Tissier, Phys. Rev. Lett. **96**, 087202 (2006).
[26] G. Tarjus and M. Tissier, Phys. Rev. B **74**, 214419 (2006).
[27] A. Fedorenko, P. Le Doussal and K. J. Wiese, Phys. Rev. E **74**, 041110 (2006).
[28] A. A. Fedorenko, P. Le Doussal, and K. J. Wiese, Phys. Rev. E **74**, 061109 (2006).
[29] T. Nattermann, S. Stepanow, L. H. Tang, and H. Leschhorn, J. Phys. II **2**, 1483 (1992).
[30] O. Narayan and D. S. Fisher, Phys. Rev. B **48**, 7030 (1993).
[31] P. Chauve, T. Giamarchi, and P. Le Doussal, Europhys. Lett. **44**, 110 (1998).
[32] P. Chauve, T. Giamarchi, and P. Le Doussal, Phys. Rev. B **62**, 6241 (2000).
[33] P. Le Doussal, K. J. Wiese, and P. Chauve, Phys. Rev. B **66**, 174201 (2002).
[34] P. Le Doussal and K. J. Wiese, Phys. Rev. E **67**, 016121 (2003).
[35] P. Le Doussal and K. J. Wiese, Phys. Rev. E **68**, 046118 (2003).
[36] P. Le Doussal, K. J. Wiese, E. Raphael, and R. Golestanian, Phys. Rev. Lett. **96**, 015702 (2006).
[37] G. Blatter, M. V. Feigel'man, V. B. Geshkenbein, A. I. Larkin, and V. M. Vinokur, Rev. Mod. Phys. **66**, 1125 (1994).
[38] T. Nattermann and S. Scheidl, Adv. Phys. **49**, 607 (2000).
[39] T. Giamarchi and P. Le Doussal, Phys. Rev. Lett. **72**, 1530 (1994).
[40] T. Giamarchi and P. Le Doussal, Phys. Rev. B **52**, 1242 (1995).
[41] T. Giamarchi and P. Le Doussal, *Spin Glasses and Random Fields*, edited by A. P. Young (World Scientific, Singapore, 1997).
[42] T. Nattermann, *Spin Glasses and Random Fields*, edited by A. P. Young (World Scientific, Singapore, 1997).
[43] A. Aharony, Y. Imry, and S. K. Ma, Phys. Rev. Lett. **37**, 1364 (1976).
[44] G. Grinstein, Phys. Rev. Lett. **37**, 944 (1976).
[45] K. B. Efetov and A. I. Larkin, Sov. Phys. JETP **45**, 1236 (1977).
[46] M. Mézard and G. Parisi, J. Phys. I **1**, 809 (1991).
[47] L. Balents, J. P. Bouchaud, and M. Mézard, J. Phys. I **6**, 1007 (1996).
[48] P. Le Doussal, Europhys. Lett. **76**, 457 (2006).
[49] P. Le Doussal (unpublished).
[50] M. Kardar, G. Parisi, and Y.-C. Zhang, Phys. Rev. Lett. **56**, 889 (1986).
[51] E. Frey and U. C. Täuber, Phys. Rev. E **50**, 1024 (1994).
[52] M. Lässig, Nucl. Phys. B **448**, 559 (1995).
[53] K. J. Wiese, Phys. Rev. E **56**, 5013 (1997).
[54] K. J. Wiese, J. Stat. Phys. **93**, 143 (1998).
[55] A. A. Middleton, P. Le Doussal and K. J. Wiese, Phys. Rev. Lett. **98**, 155701 (2007).
[56] P. Le Doussal and K. J. Wiese, Europhys. Lett. **77**, 66001 (2007).
[57] A. Rosso, P. Le Doussal, and K. J. Wiese, Phys. Rev. B **75**, 220201 (2007).
[58] Other choices of interest are, e.g., $g_k = \frac{1}{c(k^2+m^{4/\alpha})^{\alpha/2}}$ for $\alpha<2$ which models long-range elasticity.
[59] The bare correlator B is defined in the same way as in Refs. 11 and 13, but corresponds to $-\hat{f} \equiv B$ defined in Ref. 46.
[60] Corresponding to $B(z) = \left[B(0) - \frac{\gamma B_0}{\gamma-1}\right]\Theta(1-\gamma) + \frac{\gamma}{\gamma-1} B_0 \left(1 + \frac{z}{\gamma r_f^2}\right)^{1-\gamma}$ for $\gamma \neq 1$, and $B(z) = B(0) - B_0 \ln(1+z/r_f^2)$ for $\gamma=1$.
[61] In Refs. 11 and 13, model I was parametrized with $g \equiv B_0$ and $r_f \equiv 1$. The bare correlator of model II was taken in the form $B'(z) = -g\frac{1}{(a^2+z)^\gamma}$, corresponding to the reparametrization $ga^{-2\gamma} = B_0/r_f^2$, $a^2 = \gamma r_f^2$.
[62] For finite N, there is a range of values $\gamma > \gamma^*(N)$ for which model II renormalizes to the SR disorder class I, with $\gamma^*(N) \to \infty$ as $N \to \infty$.
[63] One should distinguish this "Larkin scale," which is a simple combination of dimensionful quantities meant only to provide an order of magnitude estimate, and a "Larkin mass" or a "Larkin length" which in some cases can be defined precisely from an observable, e.g., for $N=\infty$, an exact phase transition to a regime with many pure states occurs at a mass $m=m_c$ (see below).
[64] In the case of RSB (i.e., in the glass phase and within the GVM), there are some subtleties in this correspondence. One can define the intravalley connected average, given by $G_{aa} - G(1)$ (see below)—relevant for time scales in which no transitions between valleys occur—as well as the full connected correlation $G_{aa} - \int_0^1 d\mathsf{u}\, G(\mathsf{u})$.
[65] In the limit of large UV cutoff, $\Lambda \gg m_c(T)$, corresponding to the weak-collective pinning regime. Note that the UV cutoff needs to be retained only in the T dependence of $m_c(T)$ via $\hat{T}$ [cf. Eq. (19)].
[66] According to Eq. (19), in dimensions $d>2$, the temperature scales as $T \sim \hat{T}\Lambda^{-(d-2)}$ with $\hat{T} \leqslant O(1)$ at the transition and in the glassy regime. Thus, in the weak-collective pinning regime where $\Lambda \gg \mu_c = 1$, one always has $\mathsf{u}_c \sim T \sim \Lambda^{-(d-2)} \ll 1$. In long-range models $d<2$ with $\gamma < \gamma_c$, one finds that on the transition line the fluctuation dissipation ratio $\mathsf{u}_c = (1+\gamma)(2-d)/(4-d) \leqslant (1+\gamma_c(d))(2-d)/(4-d) = 1$ is always smaller than 1.
[67] The definition of $\hat{V}[v]$ can alternatively be interpreted as the free energy of the elastic manifold (with elastic properties described by g_k), where the quenched disorder has been displaced by $-v(x)$.
[68] As usual, formulas for discrete sums are obtained replacing $\int_x \equiv \Sigma_x$, $\int_k \equiv L^{-d}\Sigma_k$ and, for a uniform $v_x = v$, one has $v_k = L^d v\, \delta_{k,0}$.
[69] More accurately, the integral in the third line can be obtained as the limit of $(G(\mathsf{u}_1) - G(n))1^n_{(\mathsf{u}_1)} + \Sigma_{i=2}^{K-1}[G(\mathsf{u}_i) - G(\mathsf{u}_{i-1})]1^n_{(\mathsf{u}_i)} + [G(1) - G(\mathsf{u}_{K-1})]1^m_{(\mathsf{u}_K)}$ [with $G(1) = G(\mathsf{u}_K)$] of a K-step RSB as $K \to \infty$.
[70] The order $1 \leqslant \mathsf{u}_K \leqslant \ldots \leqslant \mathsf{u}_1 \leqslant n$ being reversed when the analytical continuation to $n<1$ is performed.
[71] J.-P. Bouchaud, M. Mézard, and G. Parisi, Phys. Rev. E **52**, 3656 (1995).
[72] B. Duplantier, J. Phys. A **14**, 283 (1981).
[73] The term $-q_{\ell-1}$ naturally arises in the construction (Ref. 69) for a complete Parisi matrix [see also Eq. (65)]. Here, it arises from the extra term $-q_{\ell-1}$ in the definition of g_ℓ, which involves an incomplete Parisi matrix (the replica sum is interrupted at u_ℓ).

[74] When comparing Eq. (115) with Eq. (113), note that $G^c_{T=0}=0$ because of Eq. (77).

[75] Note that the function $T^3 r_1[\hat{v}]$ in Eq. (134) differs from $T^3 \hat{r}_1[\hat{v}]$ in the systematic expansion (115) by a trivial quadratic term $-2T^3 dq(\mathsf{u}_c)/dT|_{T=0} \propto T^3 \hat{v}^2 = T v^2$.

[76] Independently for each of the N components $u_k^{i\alpha}$. This is left implicit here in order not to burden the notations.

[77] Equivalently, one can write $W_\alpha = \exp(-\beta F_\alpha)$ with a tail $P(F) \sim \exp(\mathsf{u}_c \beta F)$ for large negative F.

[78] We make the natural assumption that $B''(x)$ is monotonously decreasing with x.

[79] We correct a misprint of the one-step solution given in Ref. 46, which suggested that $\mathsf{u}(T\to 0) \sim T^{(2-d)/(4-d)}$.

[80] R. Monasson, Phys. Rev. Lett. **75**, 2847 (1995).

[81] The replicon instability and the clustering instability are defined and discussed in detail in Ref. 92, cf. Eqs. (A3.3), (A3.7), and (A3.8) and Eqs. (5.11), (A3.16), and (A3.17), respectively.

[82] However, $\mathsf{u}_c^{\mathrm{th}}$ will exceed 1 at small m and T close enough to $T_c(m_*)$.

[83] Even though distinct, they may occur at the same value of parameters in the case of the marginal one-step solution.

[84] A. J. Bray and M. A. Moore, J. Phys. C **12**, L441 (1979).

[85] L. F. Cugliandolo, T. Giamarchi, and P. Le Doussal, Phys. Rev. Lett. **96**, 217203 (2006).

[86] T. Giamarchi and P. Le Doussal, Phys. Rev. B **53**, 15206 (1996).

[87] G. Schehr, Phys. Rev. B **71**, 184204 (2005).

[88] M. Mueller and L. B. Ioffe, arXiv:0711.2668 (unpublished).

[89] M. Müller and L. B. Ioffe, Phys. Rev. Lett. **93**, 256403 (2004).

[90] S. Pankov, Phys. Rev. Lett. **96**, 197204 (2006).

[91] M. Müller and S. Pankov, Phys. Rev. B **75**, 144201 (2007).

[92] A. Crisanti and H.-J. Sommers, Z. Phys. B: Condens. Matter **87**, 341 (1992).

[93] O. Rivoire, G. Biroli, O. C. Martin, and M. Mézard, Eur. Phys. J. B **37**, 55 (2004).

[94] A. Montanari, G. Parisi, and F. Ricci-Tersenghi, J. Phys. A **37**, 2073 (2004).

[95] F. Krzakala, A. Pagnani, and M. Weigt, Phys. Rev. E **70**, 046705 (2004).

[96] L. Zdeborová and F. Krzakala, Phys. Rev. E **76**, 031131 (2007).

[97] In the case of lattice glasses, one finds the same regions of stability for u_c as here: The one-step solution is unstable to replicon fluctuations for $\mathsf{u}_c < \mathsf{u}^{\mathrm{th}}$, while it is unstable to the clustering instability for $\mathsf{u}_c > \mathsf{u}^{\mathrm{cp}}$.

[98] A. Crisanti and L. Leuzzi, Phys. Rev. B **76**, 184417 (2007).

[99] L. F. Cugliandolo and P. Le Doussal, Phys. Rev. E **53**, 1525 (1996).

[100] As in Sec. III C 3, it does not exactly coincide with the expansion in powers of T since some extra (weak) T dependence is hidden in other parameters such as, e.g., Σ_1. However, as before, the series can easily be rearranged later.

[101] Agreement with Eqs. (147) and (149) can be checked for the marginal one-step case using $\theta=0$, $\hat{\mathsf{u}}_c = A$ from Eq. (23), and $m^2 + \Sigma_1 = m_c^2$.

[102] Note that $(\tilde{u}^a - \tilde{u}^b)^2 = [\tilde{u}\tilde{u}]^{aa} - 2[\tilde{u}\tilde{u}]^{ab} + [\tilde{u}\tilde{u}]^{bb}$.

[103] Note that the condition is on $\tilde{v}$ *and not* on v since the saddle-point equations are expressed in terms of $\tilde{v}$. In other words, the condition is $v^{\pi(a)} = v^a + o(\sqrt{N})$.

[104] One may also consider higher bare cumulants $S^{(p)}$. While both the saddle-point equation in the regime $v \sim 1$ and the self-consistent equation for the correlator are changed, the essential results about the connection between the FRG regime $v^2 \sim N$ and the RSB regime $v \sim 1$ remain the same: One can derive a closed self-consistency equation for the renormalized force correlator $\tilde{B}'$ (involving the bare cumulants $S^{(p)}$), from which the exact FRG equation can be derived; in the glass phase, RSB introduces an anomaly in the self-consistency and the FRG equation; the identity $\tilde{B}'(0) = -T\sigma(0)/2$ matching FRG and RSB regimes holds everywhere in the phase diagram; and the force correlator exhibits a cusp at the origin, if and only if the saddle-point solution is marginally stable with respect to clustering fluctuations.

[105] For $\tilde{B}$, but this should be the same as for $\hat{B}$.

[106] A. V. Lopatin and L. B. Ioffe, Phys. Rev. B **66**, 174202 (2002).

[107] In one-step systems, the complexity usually jumps to a finite value at the transition, which is then assumed to remain constant throughout the glass phase under conditions of a rapid quench, because the trapping threshold states become stable and do not bifurcate. In the present case, the situation is similar, except that the complexity vanishes at the transition.

[108] To one loop a nonzero temperature generally produces an additional term $\sim T\nabla_u^2 R(u)$ in the FRG flow for $R(u)$. Upon proper rescaling of $R(u)$, so that a $T=0$ fixed point exists, its coefficient generally scales as $\sim T m^\theta$ and temperature is said to be irrelevant if $\theta < 0$, relevant if $\theta > 0$, or marginal if $\theta = 0$.

[109] The x dependence in the limit is delicate, since Eq. (282) is only correct asymptotically as $m \to 0$ if $\gamma > \gamma_c$, but not for $\gamma = \gamma_c$. This is because, for $\gamma = \gamma_c$, one cannot neglect the last term in the argument of B' in Eq. (271), while it is negligible for $\gamma > \gamma_c$ as $m \to 0$.

[110] Such as a suitable norm, e.g., $\int_x v_x^2$, remains of order 1.

[111] If the function is even, $1/|y|$ behavior is allowed.

[112] Although it is not excluded that another version of FRG could be built from it—in spirit, close to Polchinsky RG; see discussion in Ref. 13.

[113] This result is smaller than the one given in Ref. 47 by a factor of $\sqrt{2\pi}$.

[114] In Ref. 46, the result $\hat{\mathsf{u}}_c^{\mathrm{eq}} = 1/T_c(m=0)$ is given. This results, however, from a rather unrealistic assumption on the behavior of $B(x)$ at small x.

[115] H. Yoshino and T. Rizzo, arXiv:cond-mat/0608293, Phys. Rev. B (to be published).